

**INVESTIGATION OF PERSEA AMERICANA OIL AS
AN ALTERNATIVE TRANSFORMER INSULATION
OIL**

BENARD MUMO MAKAA

**MASTER OF SCIENCE
(Electrical Engineering)**

**JOMO KENYATTA UNIVERSITY OF
AGRICULTURE AND TECHNOLOGY**

2020

**Investigation of Persea americana oil as an alternative transformer
insulation oil**

Benard Mumo Makaa

**A thesis submitted in partial fulfillment of the requirements for the
degree of Master of Science in Electrical Engineering in the Jomo
Kenyatta University of Agriculture and Technology**

2020

DECLARATION

This thesis is my original work and has not been presented for a degree in any other university.

Signature..... Date.....

Benard Mumo Makaa

This thesis has been submitted for examination with our approval as the university supervisors:

Signature..... Date.....

DR. George K. Irungu, PhD

JKUAT, Kenya

Signature..... Date.....

Prof. David K. Murage, PhD

JKUAT, Kenya

DEDICATION

This work is dedicated to my grandmother Redemphta Mutete.

ACKNOWLEDGEMENT

Thank you, Almighty God, for blessing me with the resources to complete this research.

Thank you Dr. George Irungu and Prof. David Murage for your invaluable support, advice, time and very timely feedback. I remain indebted to you.

Thank you, Higher Education Loans Board, for the partial scholarship that came handy in financing my MSc studies.

Thank you JKUAT, School of Electrical, Electronic and Information Engineering staff and colleagues for input and help towards this work.

Thank you Vibhusha, Chandrakesh and other staff at Sigma Test and Research Centre for facilitating my work at the centre.

Thank you Eng. Edwin Odour and Eng. Jasper Odour and other staff at Edson Engineers for your support and encouragement.

Thank you, my colleagues, at the School of Electrical and Electronic Engineering at Technical University of Kenya for your support and advice.

And finally, thank you to my family and friends for your invaluable support.

TABLE OF CONTENTS

DECLARATION	ii
DEDICATION	iii
ACKNOWLEDGEMENT	iv
LIST OF FIGURES	xi
LIST OF TABLES	x
LIST OF APPENDICES.....	xiii
LIST OF ABBREVIATIONS.....	xiv
ABSTRACT	xvi
CHAPTER ONE	1
INTRODUCTION	1
1.1 Background Information	1
1.2 Problem Statement	3
1.3 Justification.....	3
1.4 Research Objectives	4
1.4.1 Main Objective.....	4
1.4.2 Specific Objectives.....	4
1.5 Research Scope	5
1.6 Contribution of the Thesis	5
1.7 List of Publications	5
1.8 Thesis outline.....	6
CHAPTER TWO	7
LITERATURE REVIEW.....	7
2.1 Transformer Liquid Insulation Overview.....	7
2.2 Natural Ester Insulating Oils	10
2.2.1 Degradation of NE insulating oils.....	13

2.3 Electrical Properties of Natural Oils	15
2.3.1 Dielectric Strength.....	15
2.3.2 Dielectric Dissipation Factor and Relative Permittivity.....	19
iii. Relative permittivity of the mixed liquids.....	21
2.3.4 Specific Resistivity.....	21
2.4 Physical-Chemical Properties of Natural Oils.....	22
2.4.1 Water content	22
2.4.2 Viscosity	23
2.4.3 Acidity Number Test	24
2.4.4 Density Test	25
2.4.5 Visual Examination	25
2.4.6 Interfacial Tension.....	26
2.5 Thermal Properties of Natural Oils.....	28
2.5.1 Flash Point	28
2.5.2 Pour Point Temperature.....	28
2.6 Laboratory Ageing System.....	28
2.7 Oxidation Stability	33
2.8 <i>Persea Americana</i> Oil	33
2.8.1 <i>Persea Americana</i> Production	33
2.8.2 Types of PAO.....	36
2.8.3 PAO Extraction	36
2.9 Summary of Research Gaps and Related works.....	38
CHAPTER THREE	40
METHODOLOGY	40
3.1 Overview.	40
3.1.1 Standards.....	40

3.1.2 Laboratory Ageing System	40
3.2 Electrical Properties	41
3.2.1 Breakdown Voltage (BDV)	41
3.2.2 Dielectric Dissipation Factor	46
3.2.3 Specific Resistivity	47
3.3 Chemical Properties	49
3.3.1 Neutralization Number	49
3.3.2 Corrosion Test.....	50
3.3.3 Oxidation Stability	51
3.4 Thermal Properties	51
3.4.1 Flash Point	51
3.4.2 Pour Point	52
3.5 Physical Properties.....	53
3.5.1 Water Content	54
3.5.2 Density.....	55
3.5.3 Visual examination.....	56
3.5.4 Viscosity Test.....	56
3.5.5 Interfacial Tension (IFT)	58
3.6 Accelerated Ageing.....	59
CHAPTER FOUR.....	61
RESULTS AND DISCUSSIONS.....	61
4.1 Overview	61
4.2 Electrical Properties	61
4.2.1 Breakdown Voltage (BDV)	61
4.2.2 Dielectric Dissipation Factor	73
4.2.2 Specific Resistance.....	74

4.3 Physical Properties	75
4.3.1 Appearance	75
4.3.2 Water Content	77
4.3.3 Density.....	78
4.3.4 Viscosity	79
4.3.5 Interfacial Tension (IFT)	80
4.4 Chemical Properties	81
4.4.1 Neutralization Value.....	81
4.5 Thermal Properties	82
4.5.1 Flash Point	82
4.5.2 Pour Point	84
4.6 Oxidation Stability	86
4.6.1 Neutralization Value after oxidation	86
4.6.2 Total sludge after oxidation	87
4.7 Accelerated Ageing Studies.....	87
4.7.1 Appearance	87
4.7.2 Specific Resistivity.....	89
4.7.3 Dielectric dissipation factor (TAN Delta)	89
4.7.4 Total Acidity	90
4.7.5 Total Sludge, % by mass	91
CHAPTER FIVE	93
CONCLUSIONS AND RECOMMENDATIONS	93
5.1 Conclusion	93
5.2 Limitations.....	94
5.3 Recommendations and Further Research	94
REFERENCES	96

APPENDICES.....106

LIST OF TABLES

Table 2.1: Typical physicochemical properties of different insulating liquids.	9
Table 2.2: Fatty acids composition of different vegetable oil.	11
Table 2.3: Test parameters for transformer accelerated ageing evaluation.....	29
Table: 2.4: Average Fatty Acid Composition (as Percentage of Total Fatty Acids).35	
Table 3.1: Technical Specifications of the motorized oil test.	44
Table 4.1: Weibull Parameters of the Breakdown Test	62
Table 4.2: Breakdown Probabilities from Weibull Distribution for PAO, MIO and Mixtures.	67
Table 4.3: Hypothesis test of conformity to normal distribution of AC BDV.	71
Table 4.4: Tan-Delta for PAO and MIO	74
Table 4.5: Resistivity for PAO and MIO	75
Table 4.6: Appearance of the oil samples for PAO and MIO.	76
Table 4.7: Water Content for PAO and MIO.	77
Table 4.8: Density Measurements for PAO and MIO.	78
Table 4.11: Neutralization value measurements for PAO and MIO.....	81
Table 4.12: Flash Point results for RPAO, EVPAO and MIO.	82
Table 4.14: Neutralization Value after oxidation for PAO and MIO.	86
Table 4.15: Total sludge after oxidation for RPAO, EVPAO and MIO.	87
Table 4.16: Appearance of samples after ageing for PAO and MIO.....	87
Table 4.17: Specific Resistivity results after accelerated ageing	89
Table 4.18: Dielectric dissipation factor results after accelerated ageing.....	90
Table 4.19: Total Acidity results after accelerated ageing for RPAO, EVPAO and MIO.....	90
Table AI: Test limits for new insulating mineral oil as per IEEE Std C57.106-2015	106
Table AII: Test limits for new Natural Ester Insulating Liquid as per IEEE Std C57.147-2018.....	107
Table AIII: Indian Standard-IS335-1993	108
Table AIV: Breakdown Voltage Raw Data	109

LIST OF FIGURES

Figure 2.1: Molecular structure of a natural ester.	10
Figure 2.2: Natural Ester development and use.	12
Figure 2.5: Breakdown Voltage Illustration in Liquid Dielectrics.....	16
Figure 2.6: The mechanism of oil degradation.....	30
Figure 2.7: Avocado fruit.....	34
Figure 3.1: Example of test cell and electrode arrangement in IEC 60156.	42
Figure 3.2: The BDV Test Cell.	43
Figure 3.4: Tan-delta set up.....	46
Figure 3.5: Simple vector diagram for dissipation factor measurement.....	47
Figure 3.6: Specific resistance set up.....	48
Figure 3.7: Test Cell for carrying specific resistance test.....	48
Figure 3.8: Acidity measurement set up.	49
Figure 3.9: ASTM D130 Test Method Colour Code.....	50
Figure 3.10: Oxidation stability measurement set up.	51
Figure 3.11: Flash Point measurement set up.	52
Figure 3.12: Pour Point measurement set up.....	53
Figure 3.13: Water content determination set up.	55
Figure 3.14: Density Measurement Apparatus.....	56
Figure 3.15: Glass capillary kinematic viscometer for measuring viscosity.	57
Figure 3.16: Viscosity Measurement Setup Experiment.	58
Figure 3.17: Interfacial tension set up.	59
Figure 3.18: Ageing Oven.....	60
Figure 4.1: Weibull BDV Plot for MIO.....	62
Figure 4.2: Weibull BDV Plot for RPAO.....	63
Figure 4.3: Weibull BDV Plot for EVPAO.	63
Figure 4.4: Weibull BDV Plot for 1:1 Mixture of MIO & RPAO.	64
Figure 4.5: Weibull BDV Plot for 1:1 Mixture of MIO & EVPAO.....	64
Figure 4.6: AC Breakdown voltage scattering of PAO, MIO and the Oil Mixtures. .	68
Figure 4.8: EVPAO BDV Histogram.....	69
Figure.4.9: MIO BDV Histogram.	70
Figure 4.10: 50% RPAO+50% MIO BDV Histogram.	70

Figure 4.11: BDV Histogram for EVPAO/MIO ratio 1:1.	71
Figure 4.12: Skewness and kurtosis of normal distribution of AC BDV of tested oils.	72
Figure 4.13: Mean of AC breakdown voltage of tested oils.	73
Figure 4.14: Appearance PAO and MIO.	76
Figure 4.15: Oil appearance after ageing.	88

LIST OF APPENDICES

Appendix I: Test Limits for New Insulating Mineral Oil as per IEEE Std C57.106-2015.	106
Appendix II: Test limits for New Natural Ester Insulating Liquid as per IEEE Std C57.147-2018	107
Appendix III: Indian Standard (IS335-1993)	108
Appendix IV: Breakdown Voltage (kV).....	109
Appendix V: Density	109
Appendix VI: Kinematic Viscosity, cSt	110
Appendix VII: Interfacial Tension	112
Appendix VIII: Neutralization Value.....	112
Appendix IX: Specific Resistivity, ohm-cm	113
Appendix X: Water content, ppm.....	115
Appendix XI: RPAO Oxidation stability.....	116
Appendix XII: RPAO Ageing Characteristics after accelerated ageing.....	116
Appendix XIII: EVPAO Oxidation stability	117
Appendix XIV: EVPAO Ageing Characteristics after accelerated ageing.....	118
Appendix XV: MIO Oxidation stability	119
Appendix XVI: MIO Ageing Characteristics after accelerated ageing.....	119

LIST OF ABBREVIATIONS

ANSI	American National Standards Institute
ASTM	American Society for Testing and Materials
BS	British Standard
BDV	Breakdown Voltage
DDF	Dielectric Dissipation Factor
EPA	Environmental Protection Agency
EVPAO	Extra Virgin Persea Americana Oil
HV	High Voltage
HO	High Oleic
FTIR	Fourier Transform Infrared Spectroscopy
IFT	Interfacial Tension
IEC	International Electrotechnical Commission
IEEE	Institute of Electrical and Electronic Engineers
IS	Indian Standards
KOH	Potassium Hydroxide
MIO	Mineral Insulating Oil
MUFA	Monounsaturated Fatty Acids
NE	Natural Esters
OSHA	Occupational Safety and Health Act
NN	Neutralization Number
PAO	Persea Americana oil
PCB	Polychlorinated biphenyl

PFAE	Palm Fatty Acid Ester
PD	Partial Discharges
PUFA	Polyunsaturated Fatty Acids
RPAO	Refined Persea Americana Oil
SFA	Saturated Fatty Acids

ABSTRACT

Mineral insulating oils have traditionally been used as insulating liquids in oil filled electrical equipment such as transformers since 1900's. They serve as coolants and dielectrics. These oils are however environmentally toxic and inflammable. They require costly fire protection schemes and deluge systems. Increasing awareness of fire safety and environmental protection has also led to a corresponding increasing trend of substituting mineral insulating oil with natural, environmentally friendly, plant-based oils (natural esters). The increase in power rating of transformers also calls for high temperature performance insulating oils. It has been noted that plant based dielectric fluids are better than mineral insulation oils in many technical aspects. Plant based insulating oils are non-toxic, and possess higher fire points and excellent biodegradability characteristics. Thus, in order to reduce the hazardous environmental impact and to improve the fire safety of transformers, there is an increasing need for plant based insulating liquids as transformer insulating oils. This thesis presents results of series of experiments that were performed to investigate the electrical, thermal, physical and chemical properties of food grade *Persea americana* oil (PAO). For comparison, the corresponding properties of mineral insulation oil (MIO) in the same experimental conditions were also measured and compared with those of PAO. In this investigation, two different types of *Persea americana* oil samples consisting of extra virgin and refined PAO were tested. The results obtained show that the average electrical, thermal, physical and chemical properties of PAO meet the IEC and IEEE specifications for new natural liquid insulation oils. This confirms that *Persea americana* oil can be used as an alternative transformer liquid insulation.

CHAPTER ONE

INTRODUCTION

1.1 Background Information

The demand for power transformers is increasing globally because of greater power requirements in developing countries and upgrading of ageing power equipment. Thus, there is a huge need for power transformers with improved environmental and disaster prevention performance (Gnanasekaran & Chavidi, 2018). Naphthenic mineral insulation oil with excellent cooling capabilities and high insulating performance is conventionally used for oil-immersed transformers. Mineral insulation oil (dielectric liquid) facilitates insulation protection in high voltage (HV) electrical equipment as well as enabling thermal stability of the HV systems because of their thermos-conduction properties (Jing, et al., 2014).

However, mineral insulation oil is extracted from petroleum, which is a non-renewable and limited resource. The already known petroleum stocks are estimated to become used up in less than 50 years going by the current consumption rate (Oommen, 2002). Worldwide estimates show that almost 30–40 million tons of mineral insulating oils are in use.

Mineral insulation oils are easily inflammable, are poorly degradable and can contaminate soil and watercourses, if spill over takes place. Fire protection problems associated with the installation of mineral insulation oil-based high voltage power equipment include fire safety, firewalls, and deluge systems.

Stringent environmental protection regulations also compel manufacturers and operators of HV equipment to use biodegradable plant-based liquids with low toxic levels. Decrease of the footprint of modern pulsed-power and HV electrical equipment has resulted in demand for insulating liquids with improved dielectric features because of the resultant higher levels of electrical stress (Jing, et al., 2014).

To address all of the above concerns, natural plant-based fluids derived from agricultural products are now serving as their replacement. The plant-based oils are

natural products and are renewable sources with plenty of supply and are “green products” that can replace mineral-based insulation oils, since their most attractive feature is high biodegradability (95–100%) and higher flash point (about 368°C) instead of about 150°C for most mineral-based insulating oils (Al-Eshaikh & Qureshi, 2012). It is a matter of fact that working temperature of the insulation oil, and hence deterioration rate of the power transformers increases with respect to working time and working stress. Mineral insulating oil has low temperature performance and this reduces the lifetime of the transformer insulation paper and, therefore, the lifespan of the power transformer. Combining together the fire safety and biodegradability can typically eliminate the traditional and conventional requirement for firewalls and expensive deluge systems. Several references (Oommen, 2002) (Hemmer, Badan & Schwab, 2002) (Amanullah, 2005) (Hosier, Rogers, Vaughan & Swindler, 2010) (Martin & Wang, 2008) demonstrate examples of use of vegetable-based oils for their dielectric application in power distribution transformers.

These factors have drawn the attention of power industry and researchers work on alternative dielectric fluids. Efforts have been put on development of natural plant based dielectric fluids for power transformers. Many researchers have investigated several other fluids for transformer insulation oil like vegetable oils, coconut oil, and palm oil which are commercially available in market.

In response to demand for natural fluids, manufacturers and processors of liquid insulation oils are hugely and actively involved in investing in development of new plant-based insulation oils for applications in the pulsed –power and power industries.

Natural, plant-based oils are considered as potential substitutes for traditional, non-renewable mineral insulation oils. Their properties are however not yet fully known and possible sources have not been explored fully.

Materials applied as dielectric fluids, should meet suggested minimum health and typical environment related requirements such as (McShane, 2001).

Such requirements are:

- a) Be essentially nontoxic.
- b) Be biodegradable.
- c) Produce by-products with acceptable low risk thermal degradation.
- d) Be recyclable, recondition-able, and readily disposable.
- e) Not be listed as a hazardous material by the EPA or OSHA.
- f) Be derivable from renewable resources.

Thus, to meet requirements of high fire point and environment protection, research on plant-based dielectric fluids is a high priority topic at several research centers worldwide.

For this investigation, food grade *Persea americana* oil was evaluated to look into the possibility of adapting it as a replacement for mineral-based insulating oil.

1.2 Problem Statement

Mineral insulating oil has been the standard insulating and cooling liquid for oil-immersed transformers, but there are many concerns and risks associated with its use such as inflammability, poor moisture tolerance, sulfidation corrosion, depletion of resources and environmental pollution when mineral insulation oil spills onto soil and water. Thus, there is need for alternatives which do not have these shortcomings.

1.3 Justification

Natural, plant based dielectric fluids are a viable natural alternative providing environmental, safety and performance benefits over and above traditional mineral insulation oils. Formulated from natural plant-based seed oils and food grade additives, these dielectric fluids are bio-based sustainable, renewable and recyclable providing sustainable environmental protection.

These fluids offer strong benefits for transformers in environmentally sensitive locations. In the event of an oil release, natural dielectric fluids quickly and thoroughly biodegrade in the environment and contain no harmful petroleum, halogens, silicones or Polychlorinated biphenyl (PCB) materials.

By investigating the electrical, thermal, physical and chemical properties of *Persea americana* oil and comparing with existing requirements for transformer insulation oils, conclusions were drawn as to the viability of *Persea americana* as an alternative transformer insulation oil. This research may also spur new interest in farming of *Persea americana* and related oil extra extraction industries because of the newly created demand. In addition, adoption of *Persea americana* as an alternative oil will reduce use of environmentally hazardous, mineral insulation oil. *Persea americana* oil is also high oleic (HO) and is less acidic, properties necessary for natural, plant-based oils used as transformer liquid insulation. To add to the corpus of this growing interest in plant-based oils, it is appropriate to investigate plants oils, which have a huge potential for applications as transformer insulation oils. *Persea americana* oil is also edible and widely available hence will not be prone to vandalism.

1.4 Research Objectives

1.4.1 Main Objective

The main objective of this study was to investigate the electrical, thermal, physical and chemical properties of *Persea americana* oil in order to find its potential application as a dielectric insulating fluid in electrical equipment.

1.4.2 Specific Objectives

The specific objectives of this study are:

1. To investigate the electrical properties of *Persea americana* oil such the dielectric strength, resistivity and dissipation factor($\tan\delta$)
2. To investigate the chemical properties (acidity and corrosion) of *Persea americana* oil.
3. To investigate the thermal properties (flash point and pour point). of *Persea americana* oil.
4. To investigate the physical properties of *Persea americana* oil such as viscosity, water content and colour.
5. To compare the electrical, chemical, thermal and physical properties of PAO & MIO.

1.5 Research Scope

- a) The work was limited to the investigation of the electrical, thermal, physical and chemical properties of *Persea americana* oil.
- b) The results were compared with those of mineral insulation oil and recommendations made based on the comparisons.
- c) Short-term and long-term performances of the *Persea americana* oil are investigated under open beaker accelerated ageing.

1.6 Contribution of the Thesis

The key contribution of this research is establishing through experimental investigation and analysis of the electrical, physical, chemical and thermal properties of *Persea americana* oil that PAO properties satisfy the IEEE Standard C57.147 (2018) in general. The accelerated ageing results also conform to IEEE and IS.335.1993 requirements. Therefore, PAO has been established as a potential replacement for mineral insulation oil.

1.7 List of Publications

1. Makaa, B.M; Irungu, G.K; Murage, D.K, 2019 “Electrical and Physicochemical Properties of Persea Americana Oil as an Alternative Transformer Insulation Oil.” Proceedings of IEEE SAUPEC/RobMech/PRASA 2019 Conference ,29 - 31 January 2019, Central University of Technology, Free State, Bloemfontein, South Africa. ISBN: 978-1-7281-0368-6 pp.247-253.
2. Makaa, B., Irungu, G., & Murage, D. ,2019. “Comparison of Statistical Breakdown Voltages in Persea Americana Oil and Mineral Insulation Oil and their Mixtures.” *European International Journal of Science and Technology*, Vol.6. No 2, ISBN: 2304-9693, March 2019, pp.27-36.

3. Makaa, B.M; Irungu, G.K; Murage, D.K,2019: “Investigation of Persea Americana Oil as an Alternative Transformer Insulation Oil.” Proceedings of IEEE 37th Electrical Insulation Conference (EIC), June 16-19, 2019, Hyatt Regency Calgary, Calgary, AB, Canada.ISBN:978-1-5386-7624-0 pp.197-200.
4. Makaa, B. M; Irungu, G.K; Murage, D.K,2019: “Study on the Ageing Characteristics of Persea Americana Oil as an Alternative Transformer Insulation oil”. Proceedings of 2019. IEEE, 37th Electrical Insulation Conference (EIC) held on June 16-19, 2019, at Hyatt Regency Calgary in Calgary, AB, Canada. ISSN: 978-1-5386-7624-0 pp.287-290.

1.8 Thesis outline

The thesis is organized into five chapters.

Chapter 1 gives a short introduction of the problem being solved, the background information and the proposed approach as well as the contributions of the research.

Chapter 2 deals with literature review. A brief overview of the main topics of this research are presented. An overview of mineral insulation oil, plant based (natural esters) insulation oil, and *Persea americana* oil is presented.

Chapter 3 handles methodology and describes in details the equipment and techniques that were used to carry out the experimental investigation of the electrical, physical, thermal and chemical properties of both *Persea americana* oil and mineral insulation oil.

Chapter 4 presents the results obtained from the experimental analysis of the PAO and MIO properties. Properties of PAO and MIO are compared based on IEEE standards.

Chapter 5 concludes the work performed in the study based on results obtained and also highlights the possible limitations. Moreover, further research work that can be carried out to is also suggested. This chapter is followed by the reference materials and appendices that have been used in the development of the thesis.

CHAPTER TWO

LITERATURE REVIEW

2.1 Transformer Liquid Insulation Overview

A transformer is an expensive, indispensable and strategically important piece of equipment of any electric power system. It is one of the most strategic components in an electric high voltage power network, since it ensures the safe operation of the power grid. The insulation system is the most imperative part of a transformer because the lifetime and reliable operation of the transformer are almost solely determined by the condition of its insulation system. There are three main types of transformers namely, oil filled, dry type and gas insulated. However, almost all the electrical load bearing transformers in power delivery systems around the world are oil filled (Rouse, 1998). Dry transformers are only in common use at voltage levels below 66 kV.

Liquid-cooled transformers have intrinsically highly efficient. For this reason, new developments in this field majorly focus on improving the safety and environmental properties of fire-resistant insulation fluids (high fire points) (Schäfer, Höhle & Schmeid, 2014). It is worth noting that a transformer oil is not only an insulator but is also a coolant.

As highlighted in the introduction of this thesis, mineral insulation oil shortcomings include low moisture tolerance, poor environmental performance, high flammability and presence of corrosive Sulphur. The key solution to all these problems is in use of plant based liquid insulation oils (natural esters). These oils are readily biodegradable, are fire safe, have excellent moisture tolerance and are free from corrosive Sulphur compounds. Plant based insulation oils have also been shown to extend the life of transformer cellulose insulation and therefore bringing more benefits to power utility operators.

Natural and synthetic esters are the currently used ester-based insulating liquids in the transformer liquid insulation industry. They are readily biodegradable, less toxic and less flammable K class fluids. An ester is a reaction product from the combination of an acid and an alcohol. They come in many forms and are used for a vast array of

applications. As mentioned above, the ester-based insulation fluids used in transformers can be split into two groups, synthetic and natural. For the synthetic esters, the raw materials are carefully selected so as to give a complete product that is tailored to a given specific application. For synthetic esters, the base oils can be altered significantly.

For natural esters (NE), the raw materials are directly derived from natural plant sources such as seed oils which may include soya bean, rapeseed oil or sunflower oil. The oils are chosen to produce the best possible fit to the specific application. However, their properties cannot be altered significantly as it is the case with synthetic esters. NE achieve a balance of external environmental properties and desirable transformer oil features not found in any other liquid insulation oils (Gnanasekaran & Chavidi, 2018). NE oils also have excellent green credentials. With their high flash and fire points, the fire hazard is significantly reduced. They are biodegradable and have low or no toxicity, so spillages have practically no impact on the environment. In addition, plant-based insulation oils also extend the service life of the solid composite cellulose materials used in transformer as part of the solid insulation. Technically speaking, plant-based oils bring further benefits in that, they have high water solubility, that is 20 to 30 times higher than that of mineral insulation oils at the ambient temperature before saturation. Thus, as cellulose based solid insulation is highly hygroscopic, a related merit is that the plant-based oil draws the moisture out and absorbs it. This keeps the solid insulation material dry and extends its life span considerably (Cigre working group, 2010). Vegetable oils also conduct heat more effectively thanks to their higher thermal conductivity.

NEs are widely used in distribution level transformers (Cigre working group, 2010) (Rafiq, Zhou, Ma, Wang & Li, 2015) and there is a growing trend to use NEs in high voltage and high-power transformers (ABB Brochure, 2011) (Rongsheng, Tornkvist, Chandramouli & Pettersson, 2009) (Moore, Wangard, Rapp, Woods & Del Vecchio, 2015). FR3 and BIOTEMP are two commercially available NE based insulating liquids. Synthetic esters (MIDEL 7131) are generally used in both traction and distribution level transformers and less common in power transformers due to their

high cost. All insulating liquids must meet certain specifications to use as an insulant and coolant in transformers. They should primarily have high electrical strength, good thermal conductivity, low viscosity, high fire point, low pour point, excellent chemical stability and the ability to absorb gases that may evolve in certain intense conditions (Heathcote, 2007). Moreover, better compatibility with cellulose insulation materials is of the utmost importance.

IEC Std. 60296 and ASTM Std. D 3487 cover the technical specifications for mineral insulating oils used in power and distribution electrical apparatus including transformers. The technical specifications and methods of handling NE based insulating liquids used in similar type of apparatus are detailed in ASTM Std. D 6871-03 (2008) and IEEE Std. C57.147 (2018). Table 2.1(Milledge, 2011) compares the typical properties of four different types of commercially available insulating liquids.

Table 2.1: Typical physicochemical properties of different insulating liquids.

Properties	Units	Test method	Typical Mineral oil	BIOTEM P	FR3	MIDEL 7131synthetic ester
Fire Point	°C	ASTM D 92	180	360	362	322
Flash Point	°C	ASTM D 92	160	325	326	275
Specific Gravity	g/ml	ASTM D 1298 @20°C	0.88	0.914	<0.92	0.97
Kinematic Viscosity	cSt	ASTM D 445 @ 40°C	12	42	34	29
Relative Permittivity			2.2	3.2	3.2	3.2
Oxidation Stability	% per mass	Sludge after 72 hrs	<0.1	0.01	solid	none
Neutralization number (Acidity)	mg KOH/g	ASTM D 974 IEC 61099 9.11	-	0.03 <0.03	0.02 -	<0.015 <0.03
Bio-degradability	%	CEC L-33-A-93 EEC Standard 79/831	- 83	99 -	>99 -	30 -

2.2 Natural Ester Insulating Oils

As highlighted before, the use of plant-based oils (natural esters) in transformers achieves an equilibrium of desirable external environmental properties and transformer insulation oil properties not found in other transformer insulation fluids. An attractive source of NE is edible seed oils. Used mainly in foodstuffs, these agricultural commodity oils are widely available and, unlike mineral insulation oil, are derived from renewable resources.

NE based insulating oils are commonly produced from soy, sunflower and rapeseeds mainly due to availability, low cost and having characteristics allowing them to be used as a coolant (heat transfer fluid) and insulant in transformers (Cigre working group, 2010). During manufacturing of the insulating oil, a special bleaching technique is applied to ensure low electrical conductivity of the resulting oil, a desired property for insulating oil. Finally processed oil is degassed and dehumidified to extract dissolved oxygen and moisture respectively. According to IEEE Guide for acceptance and maintenance of NE fluids in transformers, NEs are compatible and miscible in all proportions with conventional mineral insulating oil (MIO), but MIO causes the lowering of the fire and flash points of the resulting oil mixture (IEEE Standard. C57.147 ,2018). Concentration of mineral insulation oil in excess of 7 % causes the reduction of fire point of NE to below 300 °C. NE molecules are called triglycerides whose molecular structure has three fatty acid molecules chemically linked to a glycerol molecule as shown in Figure 2.1(Tenbohlen & Koch, 2010).

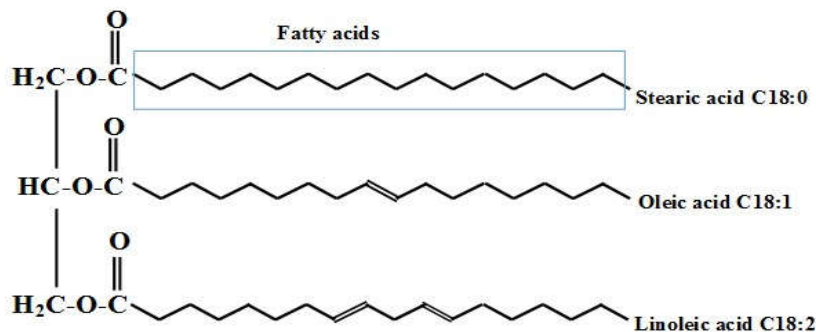


Figure 2.1: Molecular structure of a natural ester.

Constituents of all types of NE are almost the same. On the other hand, as listed in Table 2.2(Oommen, 2002) (Milledge, 2011) (Tenbohlen & Koch, 2010), fatty acid composition of vegetable oils extracted from different sources are dissimilar to some extent.

Table 2.2: Fatty acids composition of different vegetable oil.

Type of oil	Palmitic C16:0 +Stearic acid C18:0 (%)	Oleic acid C18:1(%)	Linoleic C18:2(%)	Linolenic C18:3(%)
HO sunflower	5	86	6	0.1
HO Soy	3-5	75-85	2-5	2-5
HO rapeseed	4-6	75-85	6-10	3
Typical sunflower	10	19	65	-
Typical soy	15	24	54	7

Vegetable oils with high % content of oleic fatty acids have been observed to have better insulation and cooling properties. In general, saturated, mono-unsaturated and polyunsaturated fatty acids with two or more carbon double bonds are available in NEs. The number of carbon atoms in saturated and mono-unsaturated fatty acids (oleic) are typically in the range between 8 to 22 and 10 to 22 respectively (Oommen, 2002) (Ciuriuc, Vihacencu, Dumitran & Notingher,2012). Di and tri-unsaturated fatty acids namely linoleic and linolenic mostly have 18 carbon atoms. Physicochemical properties of NEs such as viscosity, pour point and oxidation stability are solely determined by their fatty acids composition. Saturated fatty acid is a chemically stable compound. However, an increase of saturated fatty acid content in the oil causes an increase in the viscosity and to freeze oil to solid below room temperature.

On the other hand, increase of polyunsaturated fatty acids composition in oil results in lowering both pour point and viscosity. However, polyunsaturated fatty acids are highly susceptible to oxidation. The relative oxidation susceptibility of saturated: mono: di: tri: unsaturated C-18 (18 carbon atoms) fatty acids is roughly 1:10:100:200

(Oommen, 2002). Therefore, an increase in unsaturated fatty acids composition significantly reduces the chemical stability of oil.

Low pour point, low viscosity and high oxidation stability are desirable properties of insulating liquid in transformers. Therefore, high oleic (HO) vegetable oils are chosen in manufacturing insulating oil to ensure low pour point, low viscosity and desirable oxidation stability of the resulting oil. Due to ester groups in their molecules structure, NE based insulating oils are more hygroscopic than typical mineral insulation oil and their moisture solubility is about 1000 ppm at 25 °C. Moreover, they possess higher kinematic viscosity than mineral oil as listed in Table 2.1. NE insulating oils are generally more oxidation susceptible than conventional mineral oil. Therefore, in addition to 2, 6-di-tert-butyl-para-cresol, complex phenols and amines are also included as the oxidation inhibitors in NE based insulating oils (IEEE Standard. C57.147 ,2018). Though, oxidation inhibitors can provide enough oxidation stability, NE based insulating oils are recommended to only be used in hermetically sealed type transformers. The progression of natural esters as insulating liquids for electrical equipment could be described as still early in their utilization. Figure 2.2 shows historical progress of natural esters utilization (Fox & Stachowiak, 2007).

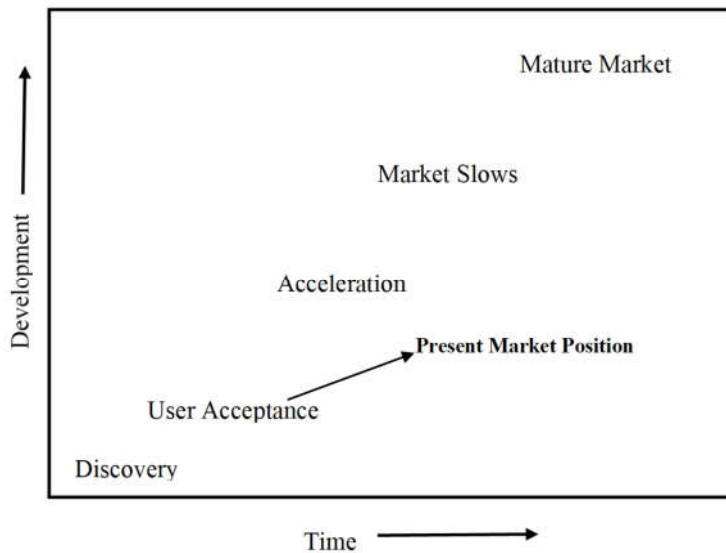


Figure 2.2: Natural Ester development and use.

2.2.1 Degradation of NE insulating oils

Oxidation is the major degradation mechanism of NEs and it is also a radical chain reaction similar to the mineral oil oxidation. Metals such as tin, iron and copper act as effective catalysts in oxidation of NE whereas lead shows very little impact. Since the strength of a hydrogen-carbon bond next to carbon-carbon double bond sites in fatty acid groups is weak, free radicals are easily formed in NEs by eliminating a hydrogen atom from the methylene group next to a double bond (Tenbohlen & Koch, 2010) (Fox & Stachowiak, 2007). It has been reported in the literature (Fox & Stachowiak, 2007) that vegetable oils containing polyunsaturated fatty acids auto oxidize even at room temperature but mono-unsaturated fatty acids (oleic acids) oxidize only at high temperature. Thus, it is clear that the degree of unsaturation is the major factor which determines the oxidation stability of NEs. As shown in Figure 2.3 (Fox & Stachowiak, 2007) (Wilhelm, Tulio & Almeida,2011), reaction among free radical, oxygen and oil molecules result in formation of triglyceride hydroperoxides and another radical propagating oxidative reaction (Ciuriuc, Vihacencu, Dumitran & Notingher,2012) (Fox & Stachowiak, 2007).

Triglyceride hydroperoxides break down to form more radicals leading to a chain reaction in a way similar to mineral oil oxidation. A myriad of non-volatile and volatile compounds including smaller oxygen containing by-products such as alcohols, aldehydes (octanal and nonanal with some heptanal), ketones (2, 4-heptadienal) and high molecular acids are also produced by decomposition of triglyceride hydro peroxides (Cigre working group, 2010) (Fox & Stachowiak, 2007) (Wilhelm, Tulio & Almeida,2011). At the last stage of oxidation, secondary non-volatile substances of oxidation are subjected to cyclisation and polymerization processes leading to a formation of high molecular weight compounds including gel and lacquer (Fox & Stachowiak, 2007). Concurrently the viscosity of NEs measurably increases and it degrades the cooling capability of oil.

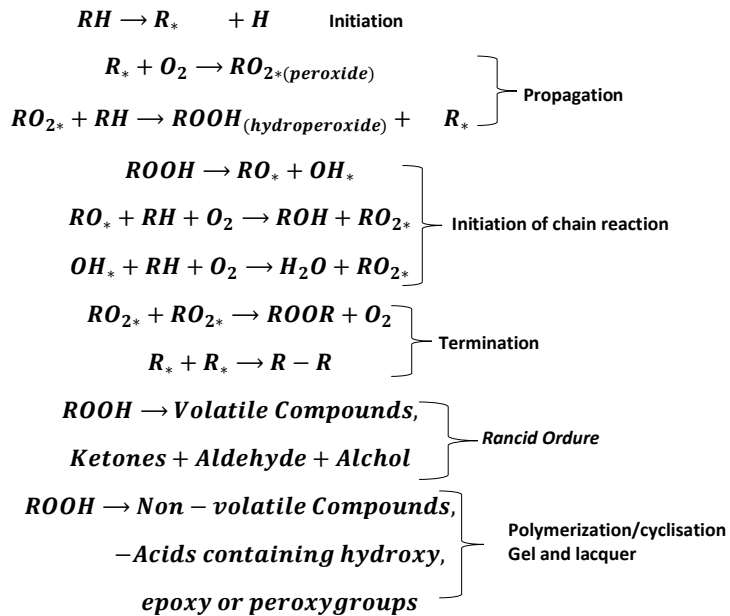


Figure 2.3: Major steps of NE self-oxidation (R denotes hydrocarbon unit).

In the case of NEs, hydrolysis is another degradation reaction, which concurrently occurs with oxidation. Because free fatty acid molecules themselves accelerate the hydrolysis reaction, this is called an autocatalytic reaction (Tenbohlen & Koch, 2010). There are three major steps in the hydrolysis reaction in NEs, which are also reversible as shown in Figure 2.4 (Rooney & Weatherley, 2001). In general, hydrolytic degradation largely increases the acidity of NEs over time. Acidity reduces resistivity of the oil and this adversely affects the insulation and cooling properties of the oil.

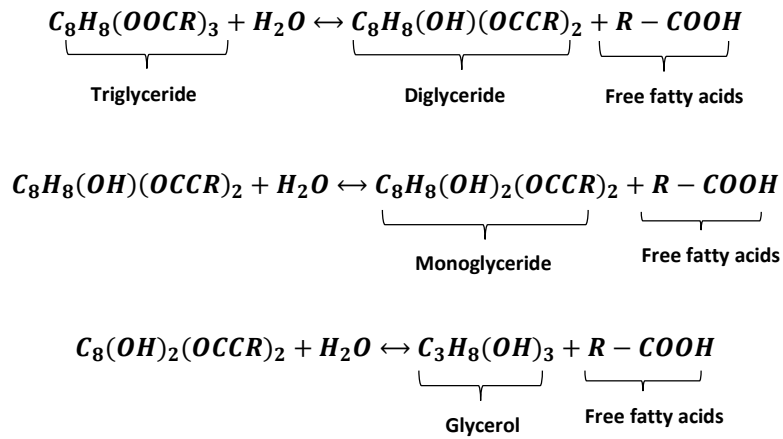


Figure 2.4: Major steps of NE hydrolysis degradation.

2.3 Electrical Properties of Natural Oils

The electrical properties of natural oils include: dielectric strength, dissipation factor and specific resistance.

2.3.1 Dielectric Strength

Dielectric strength determines the feasibility of oil as insulating material for the use in high voltage equipment. It helps determine the ability held for a material to withstand the electric field stress without breakdown.

It is determined by the strength of bonding between oil molecules, impurities, water and gas content.

Breakdown Voltage (BDV) at power frequency is the most commonly used parameter to assess the quality of insulating oils (IEC 60897 Standard, 1987). Breakdown voltage indicates the presence of contaminants such as water, cellulosic fibre, dirt and conductive particles in the liquid insulation. The presence of a significant concentration of contaminants results in a lower BDV. BDV is affected by the ambient air conditions, the electrodes geometry (shape and gap), and the type of applied voltage (i.e. alternating voltage, direct voltage and impulse voltage). IEC standard electrode will be used in this study.

The measurement of dielectric strength is performed as per IEC 60156 for measuring AC breakdown voltage and IEC 60897 for measuring lightning impulse breakdown voltage (IEC 60156 Standard, 2018) (IEC 60897 Standard ,1987).

According to IEC 60156, in the measuring of AC breakdown voltage, the test voltage must have a frequency in range of 45 – 65 Hz. This is called the power-frequency voltage. The voltage wave approximates a sinusoid with both half cycles closely alike. It should also have a ratio peak to rms values equal to the square root of 2 within $\pm 5\%$ (IEEE Standard 4, 2013). The generation of alternating high voltage is generally done by using a transformer or a resonant circuit. The varying leakage current should not affect the voltage in the test circuit. Hence this voltage should be stable enough. Breakdown voltage is also dependent on the relative water content. Increasing the relative water content reduces the value of the breakdown voltage.

2.4.1.1 Breakdown Voltage Mechanism in Liquid Dielectrics

Schottky effect explains the conduction and breakdown processes in liquid dielectrics. Due to impurities disassociation, the conduction of oil at low electric field (say, 1kV/cm) is largely ionic. This increases linearly with the applied field as shown in Figure 2.5. Breakdown occurs at higher electric field (say, 100 kV/cm) as a result of the rapid saturation of the conduction current.

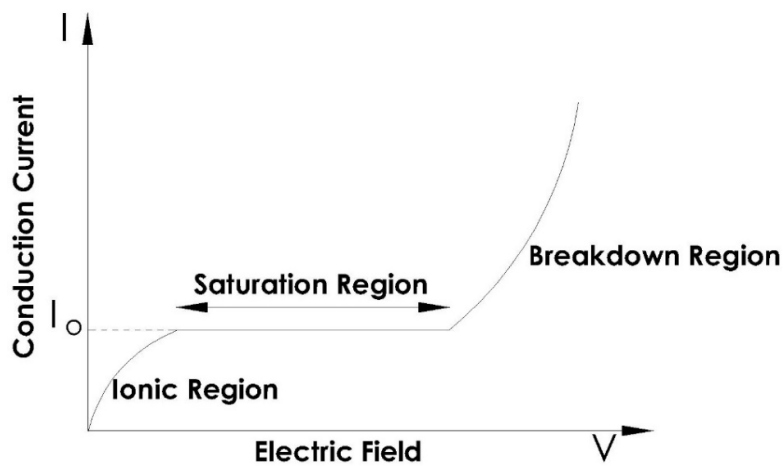


Figure 2.5: Breakdown Voltage Illustration in Liquid Dielectrics.

Theories that have been put forward to explain the breakdown voltage phenomenon in liquid dielectrics include:

- (I). Stressed oil volume theory.
- (II). Suspended particle theory.
- (III). Cavitations and bubble theory.

(I) Stressed oil volume theory.

As per this theory, the breakdown strength is a function of the largest possible impurity or weak link. Thus, the weakest region in the liquid dielectric, that is, the region that is stressed to the maximum and the oil volume in that region, defines the breakdown strength. The gas content in the oil, the oil viscosity and impurities also influence the breakdown strength of the liquid dielectric. These have been observed to reduce the breakdown strength of the liquid dielectric.

(II) Suspended particle theory.

Liquid dielectric contains solid impurities. These can either be fibers or dispersed solid particles. The permittivity of the liquid dielectrics (ϵ_1) is different from that of the solids (ϵ_2). Upon application of high voltage across two electrodes immersed into the liquid, the particles get polarized in the electric field \mathbf{E} applied between electrodes.

Let us assume that these solid particles are spheres of radius r . They get polarized in an electric field E and experience a force given by (2.2).

$$F = r^3 \frac{\epsilon_1 - \epsilon_2}{\epsilon_1 + 2\epsilon_2} E \cdot \frac{dE}{dx} \quad (2.2)$$

If $\epsilon_2 > \epsilon_1$, the force, F is directed towards areas of maximum stress. This may occur in case of presence of solid particles (for example, paper) in the liquid dielectric.

If $\epsilon_2 < \epsilon_1$, the force will be in the direction of areas of lower stress. This occurs in the case of presence of only gas bubbles. If the voltage is applied continuously and the duration is long enough, the force, F , drives the particles towards the areas of maximum stress. Supposing that the particles present are in large numbers, they then

become aligned because of F and thus form a stable chain that bridges the electrode gap thereby resulting to a breakdown between the electrodes.

A local field enhancement arises due to the presence of only a single particle between the electrodes and this also depends on its shape.

Local breakdown occurs near the particle if the field exceeds the breakdown strength of the liquid dielectric. This then results to the gas bubbles formation that may lead to the breakdown of the liquid.

(III) Cavitations and bubble theory.

According to this theory, the most common factor responsible for breakdown of liquid dielectrics is the formation of bubbles and cavities in liquid dielectrics.

The electric field in a gas bubble immersed in the liquid of permittivity ϵ_2 is given by 2.3.

$$E_b = \frac{3E_o}{\epsilon_2 + 2} \quad (2.3)$$

where E_o , is the field in the liquid in absence of the bubble. Discharge takes place when the field E_b , equals the gaseous ionization field, and this leads to liquid decomposition and therefore breakdown.

The bubble breakdown strength is accurately given by equation 2.4;

$$E_b = \frac{1}{\epsilon_2 + \epsilon_1} \left\{ \frac{2\pi\sigma(2\epsilon_2 + \epsilon_1)}{r} \left[\frac{\pi}{4} \sqrt{\frac{V_b}{2rE_o} - 1} \right] \right\}^{1/2} \quad (2.4)$$

where ϵ_1 and ϵ_2 are the permittivity of the bubble and the liquid respectively, r , the initial radius of the bubble, V_b , the voltage drops in the bubble, and σ is the surface tension of the liquid. As illustrated in the equation, the breakdown strength depends upon the hydrostatic pressure above the bubble and the liquid temperature. The theory does not

consider the production of the initial bubble and the results obtained via this theory do not agree well with experimental results.

Possible processes responsible for formation of the vapour bubbles as per this theory include.

- Dissociation of liquid molecules by electron collisions also results to gaseous products.
- There are also gas pockets that are formed at the electrodes' surfaces.
- Between the space charges, there are electrostatic repulsive forces that are sufficient and enough to overcome the surface tension.
- Corona type discharge from sharp points that initiates liquid vaporization. This vaporization is also caused by the irregularities on the electrode surfaces.

2.3.2 Dielectric Dissipation Factor and Relative Permittivity

i. Dielectric Dissipation Factor

DDF is also known as loss factor or tan delta ($\tan\delta$) or loss tangent of the transformer oil. Dissipation factor is the power loss factor in a liquid insulating material that it converted into heat when we use an alternating field. A low dissipation factor indicates that AC dielectric losses are low. Dissipation factor can be very useful for quality control and as an indicator in the changing of oil due to contaminants and ageing.

DDF is a dimensionless parameter measured at power frequency, which has been known as an effective method to assess the overall condition of transformer insulation over decades (Koch, Krueger & Puetter, 2009) (IEC Std. 61099, 2010) (IEC Std. 61203,1992). In general, the dissipation factor or power factor of insulating oils in good conditions have decimal values below 0.3(Max) for MIO and 4.0(Max) for natural oils at 100⁰ C.

ii. Relative Permittivity

The liquid insulation enables isolation of electrical components that are at high potential to parts of equipment connected to ground.

The liquid insulation is used alone or in combination with solid insulation. The more desirable relative permittivity value is the lowest possible one enabling to get the smallest possible capacitance of insulation, but oil must always meet the chemical and heat transfer properties.

The measurement of relative permittivity and dissipation factor is based on the standard ASTM D924-03a. (ASTM D 924 – 03a, 2003).

Frequency variation of the capacitance of the oil samples can be written as shown in 2.5.

$$C = C' - jC'' = C_0[\varepsilon' - j\varepsilon''] = C_0\varepsilon \quad (2.5)$$

The permittivity is given by (2.6)

$$\varepsilon = \varepsilon' - \varepsilon'' = [\varepsilon_\infty + \chi'(\omega)] - j \left[\frac{\sigma}{\omega\varepsilon_0} + \chi''(\omega) \right] \quad (2.6)$$

where σ and χ are the conductivity and the susceptibility respectively, C is the capacitance of the oil, and w is the frequency. Usually the change in susceptibility with respect to frequency is very small in oil and thus, the relative permittivity ε' can directly be obtained from ε' at 1 kHz i.e. ∞

Equation (2.7) describes how the loss tangent is calculated.

$$\tan\delta = \frac{C''(f)}{C'(f)} = \frac{\varepsilon''(f)}{\varepsilon'(f)} = \frac{\sigma}{2\pi f \varepsilon_0 \varepsilon_\infty} \quad (2.7)$$

Where in this context, ε_0 is permittivity of free space, $\varepsilon'(f)$ is the real components of the permittivity of the material as a function of angular frequency, $\varepsilon''(f)$ is loss due to polarization as a function of angular frequency and σ is the DC conductivity.

The conductivity can be obtained at -1 gradient of the log-log plot of $\tan\delta$ vs frequency.

The conductivity is temperature dependent and follows Arrhenius law as shown in equation 2.8.

$$\sigma = \sigma_0 e^{\left[\frac{E_a}{kT}\right]} \quad (2.8)$$

where K is the Boltzmann constant ($K = 1.38 \text{ E-}23 \text{ J/K}$), E_a is the activation energy in eV and T is the temperature in Kelvin. The activation energy for each sample, E_{dc} can be calculated from the results obtained from measurements conducted at two different temperature levels as shown in (2.9).

$$E_{dc} = \frac{T_1 T_2 \left[\frac{\sigma_{T_1}}{\sigma_{T_2}} \right]}{[T_1 - T_2]} \quad (2.9)$$

iii. Relative permittivity of the mixed liquids

The mixed liquids can be considered as two different dielectric layers. The indices 1 and 2 represent the mineral insulation oil and the plant-based liquid respectively, the thickness d_1 and d_2 of each depends on the percentage of each liquid.

The equivalent relative permittivity of the mixture having a thickness d is given by equation 2.10.

$$\epsilon_{re} = \frac{\epsilon_{r1} \frac{d}{d_1}}{1 + \frac{\epsilon_{r1} d_2}{\epsilon_{r2} d_1}} \quad (2.10)$$

The equivalent dissipation factor of the mixed insulating liquids, treated as two different layers is shown in equation 2.11.

$$\tan \delta_e = \frac{\epsilon_{r1} d_2 \tan \delta_2 + \epsilon_{r2} d_1 \tan \delta_1}{\epsilon_{r1} d_2 + \epsilon_{r2} d_1} \quad (2.11)$$

2.3.4 Specific Resistivity

Specific resistivity is the ratio of the direct current potential gradient in volts per centimeter (V/cm) paralleling the current flow within the sample to the current density in amperes per square centimeter (A/cm^2) at a given time under prescribed conditions. It is expressed in ohm-centimeter and is numerically equal to the resistance between opposite faces of a centimeter cube of the given liquid.

Resistivity Mechanism in Liquid Dielectrics.

Surface resistivity, volume resistivity and charge decay time are major characteristics of electrostatic properties of materials. Volume resistivity (in ohm-cm), is the resistivity of material measured on opposite ends of a material which is 1 cm thick. Surface resistivity (in ohm) is defined as the resistance between two electrodes placed along the same surface of the specimen under test. Liquid dielectrics are generally nonconductive. So, their resistivity is normally very high. Since electricity is conducted by movement of ions, then this implies there is little to no presence of free ions in the liquid dielectrics. Water is conductive in presence of dissolved salts and thus an amount of water content in the liquid dielectrics decreases the resistivity. Resistivity is an intrinsic property of a material, independent of its shape or size. Conductors have large free charge densities or ions whereas insulators like liquid dielectrics have most of the charges bound to atoms and thus not free to move.

2.4 Physical-Chemical Properties of Natural Oils

The physical-chemical properties of natural oils include: water content, density, viscosity, acidity, appearance and interfacial tension.

2.4.1 Water content

The water content of oil is one of the important parameters in the transformer insulation system. Water content influences the BDV of oil. The BDV of mineral insulation oil decreased approximately by 25 percent when the water content increased from 5 ppm to 20 ppm (IEEE Standard C57.106, 2015). However, the percentage of decrease is not directly applicable in ester oil. The presence of moisture in oil does not only reduce the dielectric strength of insulation; it also accelerates the insulation ageing process. Water particles can electrically bridge the electrodes gap and this may lead to a total breakdown of oil.

According to IEEE standard C.57.147, the maximum water content for ester oil is 200 ppm for apparatus having less than 69 kV of operating voltage, 150 ppm (for >69 kV <230 kV) and 100 ppm (for >230 kV) (IEEE Standard. C57.147 ,2018). Meanwhile IEEE C57.106 requires water content for mineral oil to be 25 ppm for equipment

having less than 69 kV of operating voltage, and 20 ppm (69-230 kV) and 10 ppm (>345 kV) (Dung, Hoidalén, Linhjell, Lundgaard & Unge, 2012).

2.4.2 Viscosity

In an operating transformer, current flows through windings, which have a certain resistance value. This causes power losses that are converted into heat energy.

Hot spots in certain parts of the transformer will cause ununiformed heat in the oil volume. Maximum heat in certain parts of the transformer is called the "Hot Spot Temperature" (HST).

The viscosity of oil within the range of normal operating temperature is important because it influences the cooling performance of oil. The oil that has a low viscosity will have a good natural and forced convection. This ability is needed to transfer heat from HST to the cooler part in transformer. IEEE C57.637-2015 and ASTM D3487-00 recommend a limit (maximum) kinematic viscosity for mineral oil of 12cSt at 40°C, meanwhile IEEE standard C.57.147 advises 50cSt at 40°C for natural ester oil (IEEE Standard. C57.147 ,2018).

The viscosity of insulating oil is usually measured by the time of flow of a given quantity of oil under controlled condition.

The dependence of viscosity on temperature can be determined using the Arrhenius relation for a thermally activated process, given by (2.12).

$$\mu(T) = A \exp\left(\frac{E_a}{KT}\right) \quad (2.12)$$

where A is given by (2.13)

$$A = \left(\frac{Nk}{V}\right) \exp(-\Delta S) \quad (2.13)$$

The dynamic viscosity, μ is in Pa. s, E_a is the activation energy for viscosity in eV, N is the number of molecules in moles, V is the molar volume of the liquid in m^3 and ΔS , the conductor entropy, can be used to determine the response of the viscosity of oil to temperature change.

With an assumption that the fluids are Newtonian, the kinematic viscosity can be calculated from (2.14)

$$v = \frac{\pi r^4 g l t}{8 L V} = k(t_2 - t_1) \quad (2.14)$$

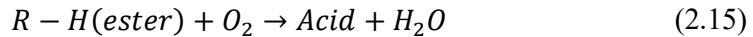
Where v is the Kinematic viscosity ($m^2 s^{-1}$), r is the capillary radius (m), l is the mean hydrostatic head (m), g is the acceleration due to gravity ($m s^{-2}$) (ms^{-2}), L is the capillary length (m), V is the flow volume of the fluid (m^3), t is the flow time through the tube, $t = t_2 - t_1$, (s) and k is the capillary constant in ($m^2 s^{-2}$) (Abeysundara, Weerakoon, Lucas, Gunatunga & Obadage, 2001).

2.4.3 Acidity Number Test

Acidity is the quantity of KOH (mg) necessary to neutralize the acid present in a gram of liquid insulation oil. It is also called the neutralization number test. It is the measure of the acidic constituent's contaminants that are in the oil. Internal sources (such as oil decomposition or oxidation) as well as external causes (such as atmospheric contamination) are the main causes of acidity in insulation oils. Acids can cause corrosion inside the transformer when water is present and this can destroy the transformer's insulating system. Acidity has also been found to accelerate the oxidation process in the insulation oil. The oxidation products and the acid in turn affect the dielectric properties of the oil. We can thus measure the ageing rate of the oil by measuring the acidity. They are directly proportional.

The acid number test of transformer insulation oil is important because the oil will be applied in an equipment made of metal. Measurement of acid number is attributable to the oxidation that occurs.

Plant based oils have naturally higher acid numbers than mineral insulating oils, even when new. The acid number helps determine when oil ought to be replaced. IEEE standard C.57.147 recommends that the maximum acidity number of natural ester oil is 0.06 mg KOH/g (IEEE Standard. C57.147 ,2018).The acid in ester may arise as a result of oxidation which releases acid and water according to (2.15)



Hydrolysis reaction of natural ester in the mixture releases fatty acid and glycerol which in turn also contributes to the increase of acidity of the mixture.

2.4.4 Density Test

In conjunction with other properties, density is a fundamental property that is used to characterize both the light and heavy fractions of oil. It is crucial to determine the density or relative density of oils as it is necessary in the conversion of the measured volumes at the standard temperature of 15°C. This measuring is carried out by following ASTM D4052-18 standard. (ASTM D4052-18, 2018). Density measurements based on use of the Archimedes principle take into account the gravity and buoyancy force acting on the plunger (calibrated glass weights) with a defined volume (V_{pl}). In order to calculate the density, it is important to know the mass (or weight) of the plunger calibrated (calibrated glass weight) in air (m_A) and immersed in the liquid (m_L). The density of the liquid can be calculated according to (2.16).

$$\sigma = \frac{m_A - m_L}{V_{pl}} \quad (2.16)$$

where the density σ is using the unit $g\ cm^{-3}$. It is necessary to know the weight of air in the plunger and its weight after immersion in a liquid.

2.4.5 Visual Examination

Colour of oil is a visual parameter, which reflects the degree of degradation and possible contamination of oil during ageing. Numerical value based on international colour standards (ASTM D1500,2007) is usually used in expressing colour changes of

oil. The colour number of oil before ageing and after ageing is estimated to ascertain the oil condition.

2.4.6 Interfacial Tension

Interfacial tension (IFT) between the water and oil interface is the measure of attractive force between the molecules of water and oil. Interfacial tension is useful for determining oil decay products and the presence of polar contaminants. New oil usually exhibits high interfacial tension.

The SI unit is milli-Newtons per meter (mN/m). This is equivalent to dynes per centimeter (dyne/cm). IFT is the force of attraction between the molecules at the interface of two fluids. At the liquid-air interface, the force is called surface tension. IFT is responsible for many liquid behaviors such as interfacial behaviour of vapor-liquid and liquid-liquid.

2.4.6.1 Interfacial Tension Mechanism in Liquid Dielectrics.

When the cohesive forces between molecules cause the surface of a liquid to contract to the smallest area, this is called, surface tension. When it occurs between molecules of different fluids, it is called, interfacial tension. Molecules on the surface are pulled inward by cohesive forces and this reduces the surface area. Molecules inside the liquid normally experience zero net force as they are surrounded on all sides.

As mentioned above, the surface forces affect liquid phase equilibria. Unbalanced molecular attractive forces (cohesion) and repulsive forces (adhesion) cause tension at the interface of the liquid phases. Interfacial Tension (IFT) is the improvement in intermolecular attractive forces of one fluid facing another and the dimension is normally in force per unit length.

According to Laplace's law, there is a linear relationship between two phases and the radius of the interface curvature. The law has been used to study both interfaces between different liquids and a liquid and its own vapour (surface tension) as shown below in (2.17).

$$\Delta P = \frac{\sigma}{r} \quad (2.17)$$

Where σ is the surface tension, r is the radius of curvature, and ΔP is the pressure difference between the inside and outside of the interface. Experimental techniques used to measure IFT include the capillary rise and du Nouy ring technique. In du Nouy ring technique, the IFT can be obtained as shown in (2.18).

$$\sigma = \delta \times \frac{g_c}{2\pi d} \quad (2.18)$$

Where σ is the IFT in dynes per centimeter, g_c is the gravitational constant (980cm/s^2), d is the ring diameter in cm, and δ is grams-force measured with analytic balance.

In the capillary rise technique, the height of the liquid rise in a capillary can be obtained as shown in (2.19).

$$h = \frac{2\sigma \times \cos\theta}{r\rho g_c} \quad (2.19)$$

Where ρ is the density of the denser liquid in g/cc , r is the capillary radius in cm, and $\cos\theta$ is the cosine of the angle between capillary wall and the surface tension inside the capillary.

IFT measurements are also a function of temperature of the experiment. IFT drops with increased temperature.

Air/oil and oil/water IFT is normally used to calculate a spreading coefficient and this gives an indication of the proclivity for the oil to spread. This is defined by (2.20).

$$\text{Spreading coefficient} = S_{WA}:S_{OA}:S_{WO} \quad (2.20)$$

S_{WA} is water/air interfacial tension, S_{OA} is oil/air IFT, and S_{WO} is water/oil IFT. Unlike density and viscosity, which show systematic variations with temperature and degree of evaporation, IFT of liquid dielectrics show no such correlations. IFT is responsible for many liquid behaviors such as interfacial behaviour of vapor-liquid and liquid-liquid.

2.5 Thermal Properties of Natural Oils

The thermal properties of natural oils include: flash point and pour point.

2.5.1 Flash Point

The flash point of a sample is the lowest temperature at which its vapour will form a flammable mixture with air under atmospheric pressure.

Nonflammable and flame-retardant properties are important for power transformers to prevent disasters (Gnanasekaran & Chavidi, 2018).

2.5.2 Pour Point Temperature

The pour point temperature of a sample is the lowest temperature at which the flow of the test sample is observed under standard test conditions.

2.6 Laboratory Ageing System

Accelerated ageing is carried out to predict the reliability of insulating material when in operation over a specified period of time. Ideal ageing test should include electrical, thermal and mechanical stresses which are actually responsible for ageing in transformers during operation. But thermal stress dominates the ageing factors (McShane, 2001) and so the simulated ageing test is based on accelerated thermal ageing to induce the ageing mechanisms within a short period of time. Ageing behaviour data on ester-based oil is still very scarce and also, laboratory simulation of a replica of insulation system in transformers still poses a challenge to researchers. Since abundant data on ageing behaviour of mineral oil-based insulating fluid is available, a comparative study of accelerated aged mineral oil and natural ester insulating oil is often used to extract information on the ageing behaviour of natural ester-based insulating fluid (Abdelmalik, 2012). As per IEEE standards, when a new insulation system is developed, it is recommended to test the system following IEEE C57.100 standard. Table 2.3 shows condensed data summary of the Standard Test Procedure for Thermal Evaluation of Oil-Immersed Distribution Transformers Life Test (IEEE C57.100, 1986). It shows the test parameters for transformer accelerated ageing evaluation.

Table 2.3: Test parameters for transformer accelerated ageing evaluation.

Test Cell	A	B	C
Target Hottest-Spot Temperature (°C)			
	167	175	183
Required Standard Expected Life (as per ANSI/IEEE C57.91-1981)			
Hours	1302	721	407
Years Equivalent	≈21	≈21	≈21
Standard Test Method Required Life (as per ANSI/IEEE C57.100-1986)			
Hours	6510	3604	2036
Years Equivalent	≈105	≈105	≈105

The ageing process is illustrated in Figure 2.6 below (Endah, 2010). It shows the influence of electrical and thermal pressure on the insulation material (Endah, 2010). Thermal and electrical pressure act on the insulation oil in a transformer that is in operation. This contributes to the ageing of the insulation and the transformer oil loses its viability. The combination of the available oxygen from dissolved air and hot cellulose and the electrical and thermal pressures decomposes the transformer oil and the oil becomes oxidized. This process leads to formation of sludge (precipitates), which is the main cause of overheating and damage to the solid insulation (Endah, 2010).

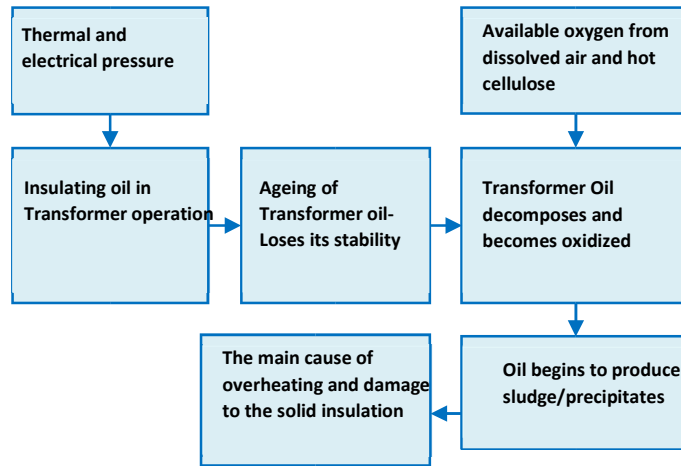


Figure 2.6: The mechanism of oil degradation.

Arrhenius equation is used to determine the rate of a chemical reaction as shown in 2.21(IEEE Std C57.91, 2011).

$$k = A \times e^{-\left(\frac{E}{RT}\right)} \quad (2.21)$$

Where

k=Reaction rate constant.

E=Activation energy of the reaction, (assumed constant), (calories/mol) or (J/mol] or (eV)

R=Boltzmann's constant ((1.987 calories / mol / K or 8.314 J / mol /K)

T = absolute temperature [Kelvin = 273 + 0C]

A = frequency factor (assumed constant)

The lifetime of the insulating material (t) to be tested is assumed to be inversely proportional to the rate of a chemical reaction, as given by 2.22 and 2.23(IEEE Std C57.91, 2011).

$$\ln k = \ln A - \left(\frac{E}{RT}\right) \quad (2.22)$$

$$\ln\left(\frac{t}{A}\right) = -\frac{E}{RT} \quad (2.23)$$

$$\frac{t}{A} = e^{-\frac{E}{RT}}$$

$$\text{And } t = Ae^{\left(\frac{B}{T}\right)}, \text{ where } B = \frac{-E}{R}$$

The lifetime of isolation, t,

where,

t = time / period for isolation [h]

T = absolute temperature of the insulation material [Kelvin]

A and B = constants experiment based materials reacting, reaction conditions, and the system of units

IEEE C57.91-2011 "IEEE Guide for Loading Mineral-Oil-Immersed Transformers and Step-Voltage Regulators", (IEEE Std C57.91, 2011) gives several thermal parameters that are used to build the model of the operating temperature of the transformer, one which is the hotspot temperature. This applies to distribution transformer windings submerged in oil. Evidence accumulated through experiments indicate that the relation of insulation deterioration to time and temperature follows and adaptation of the Arrhenius reaction rate theory shown in the form of equation 2.24. Per unit of time for insulation can be determined as given by 2.24(IEEE Std C57.91, 2011).

$$\text{Per unit of time} = Ae^{\left(\frac{B}{\theta_H+273}\right)} \quad (2.24)$$

$$\text{Per unit of time} = 980 \times 10^{-18} e^{\left(\frac{15000}{\theta_H+273}\right)} \quad (2.25)$$

where θ_H is the highest winding hotspot temperature ($^{\circ}\text{C}$).

Ageing Acceleration Factor (F_{AA}) and Equivalent Acceleration Factor (F_{EQA}) for hotspot temperature conditions change following the actual transformer load fluctuations during operation 24 hours cycle.

$$F_{AA} = e^{\left(\frac{15000}{383} - \frac{15000}{\theta_H + 273}\right)} \quad (2.26)$$

$$F_{EQA} = \frac{\sum_{n=1}^N F_{AA,n} \Delta t_n}{\sum_{n=1}^N \Delta t_n} \quad (2.27)$$

Where F_{EQA} = accelerated ageing factor equivalent

n = index of time interval, t .

N = total number of time intervals

Δt_n = interval of time [hours]

$F_{AA,n}$ is ageing acceleration factor for the temperature which exists during the time interval Δt_n

The percentage decrease in the lifetime of isolation within the total time (h) can be determined as given by (2.28).

$$\% \text{ decrease in the lifetime} = \frac{F_{EQA} \times t \times 100}{\text{Lifetime normal isolator}} \quad (2.28)$$

Where

F_{EQA} = accelerated ageing factor equivalent

t = total operating time period for 1 day [h]

Lifetime normal isolator = 20.55 years or 180,000 hours

As per (Husnayain & Garniwa, 2015), the normal lifetime isolation of 48,180 hours (or 5.5 years) is achieved under open beaker ageing system adopted in this thesis.

Previous studies of transformer oil insulation ageing show the influence of the three main agents, that is, moisture, temperature, oxygen on the degree of ageing. These are also called ageing factors. The presence of oxygen accelerates the ageing process by as much as 2.5 to 10 times (Fofana, Borsi, Gockenbach & Farzaneh, 2007).

2.7 Oxidation Stability

Oxidation studies are carried out as per ASTM D2440 –13. These tests are used to assess the amount of acid and sludge products formed in the transformer insulation oil when the oil is tested under standard conditions. Good oxidation stability ensures that the service life of the oil is maximized. This is achieved by minimizing the sludge and acid formation in the oil. The test does not model the whole insulation system (oil, paper, enamel, wire) and hence there is not proven correlation between performance in this test and performance in service. Oxidation stability is measured by the propensity of oils to form sludge and acid products during oxidation.

2.8 *Persea Americana* Oil

Persea americana oil is one of the main and major raw material for vegetable oil. It is a food grade oil that is processed from the *Persea americana* fruit pulp. As an edible oil, it can be used as an ingredient in many other dishes as well as a cooking oil. The oil is also used in cosmetics and also for lubrication (Mooz, Gaino, Shimano, Amancio, & Spoto, 2012).

2.8.1 *Persea Americana* Production

Persea americana (Avocado) tree is one of the most productive plants per unit of cultivated area. Avocado trees are very productive and can bear fruit all year round. At maximum production, a single mature tree can produce 70 to 100 kg of fruits per year or 1,000 fruits a year (Daily Nation ,2018).

Mexico is by far the world's largest avocado growing country, supplying 45 percent of the international avocado market (Mooz, Gaino, Shimano, Amancio, & Spoto, 2012).

Kenya is Africa's largest avocado producer country in Africa (followed by South Africa) and the sixth in the world. Kenya produces an estimated 200,000 metric tons (MT) of avocado annually, 70% of which is grown by small-scale farmers. Avocado can virtually grow well in most parts of the country apart from the coastal region due to salinity (Daily Nation ,2018).

Since Kenya is in subtropical climates and *Persea americana* does well in such climates, it is an ideal location for such kind of farming. Kenya's avocado season is mainly in March to September. The Fuerte variety is mainly available from March while the Hass variety is available from May.

The popular and main variety of *Persea americana* grown in Kenya is a local variety called "Kienyeji". Second in popularity is the Fuerte variety followed by the Hass variety. The least popular variety is the Pinkerton cultivar avocado [29].

Persea americana fruits have different chemical compositions, mostly in terms of the lipid levels in the pulp. It has been established that fruits with high levels of lipids are a crucial raw material for oil extraction [29]. *Persea americana* oil is low acidic, and this is useful in increasing the smoke point. Moreover, the more refined an oil is, the higher the smoke point (Daily Nation ,2018).

Avocado oil is one of few edible oils not derived from seeds; it is pressed from the fleshy pulp surrounding the avocado pit as shown in Figure 2.7.

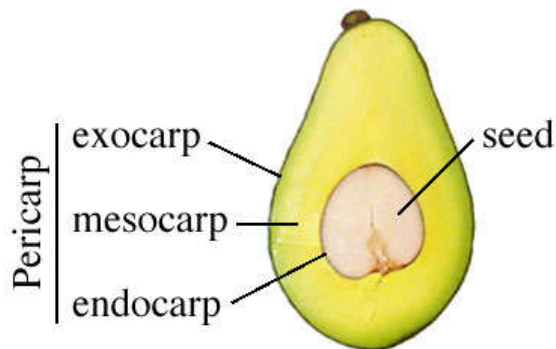


Figure 2.7: Avocado fruit.

The flesh of an avocado can contain up to 30% oil (based on fresh weight), but there is very little in the seed ($\approx 2\%$) or the skin ($\approx 7\%$). The *Persea americana* pulp has been used to produce oils that act as a substitute for olive oil. Olive oil has similarities with *Persea americana* oil in that both oils are extracted from the respective fruit pulp. They

also share some physicochemical properties such as fatty acid composition, especially the oleic acid (Tango, Carvalho, Soares, 2004) (Daily Nation ,2018).

Average fatty acid composition of the two main avocado varieties is shown in Table 2.4(Kadam & Salunkhe, 1995).

Table 2.4: Average Fatty Acid Composition (as Percentage of Total Fatty Acids)

Fatty acid	Fuerte		Hass	
	Mature pulp	Seed	Mature pulp	Seed
Saturated				
Myristic	0.05	0.9	0.07	0.7
Palmitic	12.2	19.4	10.7	21.0
Stearic	0.52	0.64	0.25	0.54
Arachidic	0.16	0.21	0.19	0.21
Monounsaturated				
Palmitoleic	4.6	3.7	6.4	3.6
Oleic	72.8	26.2	70.5	29.2
Polyunsaturated				
Linoleic	8.6	41.6	11.4	36.8
Linolenic	0.79	6.4	0.49	7.2
Arachidonic	0.28	0.95	0.0	0.75
Total saturated fatty acids (SFA)	12.93	21.15	11.21	22.45
Total unsaturated fatty acids (UFA)	87.07	78.85	88.79	77.55
UFA/SFA	6.73	3.73	7.92	3.45

The major fatty acid of avocado is always oleic, followed by palmitic and linoleic acids (Kadam & Salunkhe, 1995). Of the two varieties, Fuerte is better owing to the presence of higher percentage content of the oleic fatty acid. PAO compares well with the HO sunflower, HO Soy, HO sunflower as has observed in Table 2.2.

Persea americana presents several advantages that recommend both its production and usage. It can be cultivated in marginal soils. It can also do well in environments where

annual rainfall levels are much lower than those necessary for other plant-based oils such as rapeseed oil, palm oil, sunflower, soybeans oil, corn oil and others. *Persea americana* oil also has high presence of oleic fatty acids which are an essential property for any plant-based insulation oils.

2.8.2 Types of PAO

i. Refined Persea Americana Oil (RPAO)

Persea americana is one of few edible oils not derived from seeds; it is pressed from the fleshy pulp surrounding the avocado pit (Morton, 1987). A refined oil is one that has been bleached or deodorized after its extraction. Mechanically refined oil is treated to remove flaws from the oil such as chlorophylls and carotenoids. *Persea americana* can be mechanically refined because of its high smoke point (Wong, Jackman & Woolf, 2010).

ii. Extra Virgin Persea Americana Oil (EVPAO)

Extra virgin *Persea americana* oil is unrefined. It's mainly considered unrefined because it is not treated by chemicals nor altered by temperature. Cold pressed *Persea americana* oil is emerald green in colour when extracted. The reason for this is due to the fact that there are high levels of carotenoids and chlorophylls in the extracted oil. Chlorophyll can act as a sensitizer for photo-oxidation to occur. It does not contribute to oil stability though.

2.8.3 PAO Extraction

Persea americana oil extraction is done in the following stages: First is fruit washing then followed by de-stoning and de-skinning. The third stage involves mash preparation followed by thermal conditioning, oil extraction and finally purification (Wong, Jackman & Woolf, 2010).

a) **Fruit Washing**

The *Persea americana* fruit is washed in two stages. To remove the dust from the surface, they are immersed in water. They are then washed for the second time by using a water jet system to remove any remaining dirt from the outer skin(exocarp).

b) **De-stoning and De-skinning**

To separate the skin (90% of it) and pips from the pulp, the fruit is taken to a de-stoning machine. The degree of the skin removal depends on the quality being sought. The amount of skin that is processed into the mash drastically affects the composition and color of the *Persea americana* oil.

c) **Mash Preparation**

The pulp is pumped into rotating disc crusher which revolves at 1400 rotations per minute. The resulting mash is then conveyed at the center and sprayed towards the periphery by a toothed disc.

d) **Thermal Conditioning and Kneading**

The *Persea americana* mash obtained from the previous stage is then directed into kneading machinery where it is stirred continuously and slowly. This is done at a monitored temperature. This process causes small oil drops to be released. These then merge into bigger drops that are easily separated by centrifugal extraction.

e) **Oil Extraction and Purification**

In the centrifuge system, the mash is separated in oil, solid and vegetation water. To separate the oil from solid and liquid phases, a decanter centrifuge is used. The cold pressed *Persea americana* oil flowing from the decanter has some degree of water and solids. To remove the water and solid residues, it is sent to a vertical centrifuge.

2.9 Summary of Research Gaps and Related works

Many studies have established and confirmed the disadvantages of using mineral insulation oil (MIO) in oil immersed transformers. It has been established that MIO is non-biodegradable, flammable, toxic, and non-renewable and has low flash point. And hence the need to find suitable alternatives that can overcome these MIO limitations.

Further, during the last several decades, study on various natural plant-based insulation oils has been carried out extensively. Collectively these studies have mainly investigated oils such as Palm oil, Soya based oils, Corn oil, Coconut oil and Sunflower based oils (Al-Eshaikh & Qureshi, 2012) (Abeyesundara, Weerakoon, Lucas, Gunatunga & Obadage, 2001) (Naranpanawe, Fernando, & Kalpage, 2013) (Kano, Iwabuchi, Yamada, Hikosaka & Koide, 2008) (Hikosaka, Hatta, Yamazaki & Kano, 2007).

Hosier et al. (2010) have investigated the potential of five different food grade vegetable oils to use as insulating liquid in high voltage equipment through an accelerated ageing experiment. The ageing extent of oil is characterized by measuring viscosity and DDF over the ageing time. The major difference between vegetable oils used in this study is the degree of unsaturation of their fatty acids composition.

The major finding of their study is that olive oil which contains a high percentage of mono-unsaturated fatty acid shows excellent resistance to ageing (comparable to FR3). On the other hand, oils with high poly-unsaturated fatty acids are more prone to oxidative degradation. They suggest that vegetable oils high in mono-unsaturated fat are suitable for electrical insulating purposes after they are carefully processed to offer low dielectric loss.

Kano et al. (2008) have carried out performance analysis of Coconut, Castor and Sesame oils and found out that castor oil and sesame oil had the potential to use as an alternative liquid insulation for transformers.

Research work has also been carried out on Palm oil. Its properties have been investigated and there are commercial companies producing ready grade palm

insulation oil such as Palm Fatty Acid Ester (PFAE). PFAE has 0.6 times less viscosity and 1.3 times higher dielectric constant than mineral oil (Naranpanawe, Fernando, & Kalpage, 2013) (Kanoh, Iwabuchi, Yamada, Hikosaka & Koide, 2008). Current researches now focus on specific qualities of palm oil such as Oxidative Stability of Palm Fatty Acid Ester (PFAE) as an Insulating Oil (Hikosaka, Hatta, Yamazaki & Kanoh, 2007). Research efforts to modify palm-based oils resulted in the successful development and commercialization of Palm Fatty Acid Ester (PFAE) oil by Lion Corporation of Japan while others like Refined, Bleached, Deodorized Palm Oil (RBDPO) and Red Palm Oil are at some advanced stage of research (Naranpanawe, Fernando, & Kalpage, 2013) (Kanoh, Iwabuchi, Yamada, Hikosaka & Koide, 2008) (Abdullahi, Bashi, Yunus, Mohibullah & Nurdin, 2004) (Sitinjak, Suhariadi & Imsak, 2003).

The main challenge in using plant-based oils as an effective alternative transformer insulation fluid is in synthesizing a fluid with high oxidative stability and a low pour point. Several research groups have shown that the modification of the molecular structure of vegetable oil at the C=C bond site could alter the physical-chemical properties of the oil (Sharma, Liu, Adhvaryu & Erhan, 2008) (Erhan, Adhvaryu & Liu, 2002). Thus, research on other natural esters as alternative transformer oils is timely. Previous research on Avocado oil has mainly focused on it as food and cosmetic product. No previous research has been done on *Persea americana* oil as an alternative transformer insulation oil.

The investigation of *Persea americana* oil for replacing mineral oil in liquid-filled power transformers is clearly new.

CHAPTER THREE

METHODOLOGY

3.1 Overview.

The objectives of this investigative research were achieved by carrying out various chemical, electrical, physical and thermal properties on *Persea americana* oil and comparing the results with those new mineral insulating oil. The equipment used and the accompanying procedures are discussed

The samples that were investigated included both food grade extra virgin and refined *Persea americana* oil. Both sample types of oils investigated were taken out of their containers as such and subjected to esterification process and experimentation. Open beaker accelerated ageing was also carried out on all samples.

The experiments were carried out at Sigma Test and Research Centre laboratory, in Mangolpuri, New Delhi, India. The room (lab) temperature was $27\pm 2^{\circ}\text{C}$ and relative humidity was $65\pm 5\%$.

3.1.1 Standards

In this investigation, the measurements of the physical, chemical, electrical and thermal properties were performed based on ASTM, IEEE, IS and IEC standards in accordance with the equipment available at Sigma Test and Research Centre laboratory, in Mangolpuri, New Delhi, India.

3.1.2 Laboratory Ageing System

Accelerated ageing was carried out to predict the reliability of insulating liquids when in operation over a specified period of time as required of new insulating oils. The ageing experiment was conducted in order to see how the properties of the insulating oil samples vary with respect to the ageing time (Abdelmalik, 2012). Open beaker method with a copper catalyst was employed and the samples were subjected to 115°C temperature for a period of 96 hours as per ASTM D1934-95(2012). As per (Husnayain & Garniwa, 2015), the normal lifetime isolation of 48,180 hours (or 5.5

years) is achieved under open beaker ageing system adopted in this thesis. The copper catalyst was added once and there was no stirring of the oil.

3.2 Electrical Properties

The electrical properties tested included: dielectric strength, dissipation factor and specific resistance or resistivity.

3.2.1 Breakdown Voltage (BDV)

The breakdown voltage of an insulating liquid is one of the most important electrical properties. It helps transformer designers ensure correct distances between live and ground conductors. This is necessary to protect the live part of transformers from the grounded part, and prevent the field in the system from increasing above the dielectric breakdown strength of the system.

IEC Std. 60156 and ASTM Std. D1816-12 prescribe the standard test procedure for analyzing breakdown voltage of insulating liquids having a petroleum origin. ASTM D1816 and IEC 60156 specify different types of electrodes, electrode gaps, voltage ramp rates, stir times between tests and sample sizes. Since plant based insulating oils possess a higher viscosity than typical mineral oil, IEEE Std. C57.147-2018 recommends longer rest time (about 15 minutes at room temperature) than the standard values provided in IEC and ASTM standards before analyzing the BDV to allow air bubbles to escape.

Figure 3.1 shows a commonly used test cell and electrode arrangement suggested in IEC 60156(IEC 60156 Standard, 2018) which was used in this research to measure the BDV of the insulating oils.

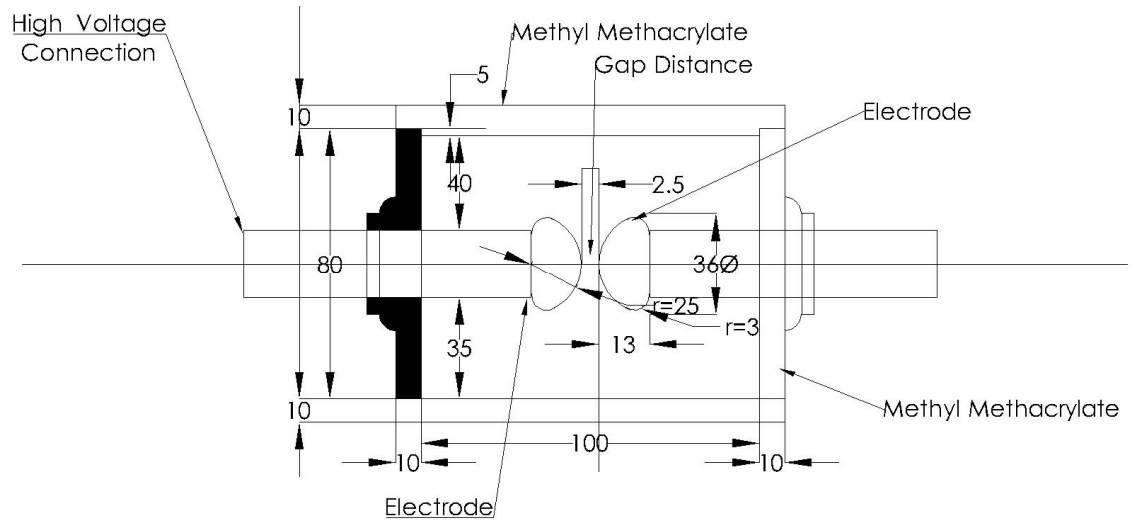


Figure 3.1: Example of test cell and electrode arrangement in IEC 60156.

Experiment Technique

A transparent test cell of Baur oil tester of 400 ml volume was used in breakdown voltage testing. A transparent material was used to ensure that there were no trapped air bubbles in the test cell before the start of the experiment. The electrode arrangement consists of two brass spheres of 12.5 mm diameter, separated by a distance of 2.50 ± 0.05 mm. In accordance to IEC 60156 Standard (IEC 60156 Standard, 2018), the test cell and electrodes were cleaned by using volatile solvent before testing. The sphere electrodes were polished by using abrasive cloth. Then, they were washed by hot tap water in temperature of 60°C-80°C.

The electrodes were assembled in the test cell as shown in Figure 3.2 and followed by drying process by using a hot air dryer.



Figure 3.2: The BDV Test Cell.

The oils samples were poured into the test cell slowly and allowed to stand for 30 minutes for RPAO, EVPAO, MIO and their mixtures, respectively, for the gases trapped in the oil to escape.

The tests were carried out using Motorized Oil Test Set (Figure 3.3) by RE India.



Figure 3.3: The BDV Motorized Oil Test Set.

The test unit has a High Voltage Transformer with epoxy encapsulated secondary coils. The high voltage transformer feeds High Tension (H.T) through electrodes to

the oil test in removable oil test cell with adjustable gap as per IEC 60156 Standard (IEC 60156 Standard, 2018). The H.T is varied by changing the primary voltage through a variac. The system uses a motorized variac for rise of voltage at a pre-set rate of rise of voltage generated. A double throw switch is provided with circuit off zero started and has a locking pre-set tripping arrangement. Technical specifications of the motorized oil test are shown in Table 3.1.

Table 3.1: Technical Specifications of the motorized oil test.

Parameter	Description
Make	Rectifiers & Electronics Pvt.Ltd(RE)
Rate of rise	2kV/sec
Volts Range	Input=230V. Output=0-100kV
Capacity	1kVA
Display	On LCD
Frequency	50Hz
Current	Input=4A. Output=10mA

The experimental results used in the analysis were the maximum AC voltage values. The voltage is automatically and continuously applied with the rate of rise 2 ± 0.2 kV/s until breakdown occurs. Ten tests were carried out as per IEC 60156 standard for each of the three samples and their respective mixtures. IEC 60156 requires six tests only.

The breakdown voltage tests of oil mixtures were also carried out to examine the insulation behavior of power transformers when re-filling with RPAO or EVPAO at a ratio of 50:50. Statistical analysis was carried out using the Microsoft Office Excel 2013, SPSS 23.0 and Weibull DR-21 software packages to show how the data is distributed to allow the calculation of the standard deviation of the breakdown voltage for each liquid.

BDV Statistical Analysis

The characterization of breakdown field strength of materials requires several measurements on 'identical' samples. The variation in the values of each breakdown

for the same sample is due to random distribution of the weakest paths. Probability density functions which include the Gaussian, Weibull, and Gumbel probability distribution functions can be used as analytical tools for the breakdown behaviour.

The Weibull statistics is based on extreme-value statistics and is most commonly used. It was reported to have wide applicability and is based on an extreme value distribution in which the system fails when the weakest link fails (Dissado & Fothergill, 1992). It also allows the analysis of small data set. The cumulative probability of failure for the two-parameter Weibull distribution is given by 3.1(Dissado & Fothergill, 1992).

$$F(v) = 1 - \exp\left\{-\left(\frac{v}{\alpha}\right)^\beta\right\} \quad (3.1)$$

where;

V is the breakdown voltage in volts, $F(v)$ is the cumulative failure probability at a voltage less than or equal to v . α , the scale parameter (characteristic BDV) is the value of v , at which the cumulative failure probability is 0.632 (that is $1-1/e$ where e is the exponential constant). β , is the shape parameter, which is a measure of the range of failure voltages.

Skewness and Kurtosis values can also be determined from the BDV data. From kurtosis and skewness values, one can determine whether a distribution frequency is normal. In a normal distribution, the kurtosis and skewness values are 0(zero). The kurtosis and skewness values indicate the deviation from normal. Two types of distributions have been established. A leptokurtic and platykurtic distribution (Dang, Beroual & Perrier, 2012). A leptokurtic distribution has a positive kurtosis and many scores in the tails (also called heavy tailed distribution) and is pointy. A platykurtic distribution has a negative kurtosis and is relatively thin (has light tails) and tends to flatter than normal. When the frequent scores are clustered at the lower end and the tail points the higher or more positive scores, it is referred to as a positive skewness. If the frequent scores are clustered at the higher end and the tail happens to point towards the more negative scores, it is referred to as a negative skewness.

3.2.2 Dielectric Dissipation Factor

It is also known as a loss factor or tan-delta. It is the power loss factor in a liquid insulating material that is converted into heat when an alternating field is used. It is a measure of imperfection of dielectric nature of oil. A low dissipation factor indicates that AC dielectric losses are low. Dissipation factor can be very useful as quality control and as an indicator in the changing of oil due to contaminants and ageing (Hussain & Karmakar, 2014). For a perfect dielectric when applied with a sinusoidal AC voltage, the current flowing through it should lead the voltage by 90 degrees. But it is not the case in reality. The angle by which it is short of 90 degrees is called the loss angle. The tan-delta measurements were carried out in accordance with ASTM D 924 – 03a (ASTM D 924 – 03a, 2003). The Tan-delta Model OTS-2K1, Sivanada (India) was used as shown in Figure 3.4.



Figure 3.4: Tan-delta set up.

Most field measurements are performed at rated voltage or at a maximum of 10 kV [59]. When an AC voltage is applied across an insulator, there is a current flowing through it. This current mainly has two components namely, capacitive and resistive current as shown in Figure 3.5 (IEEE Std. 62, 1995). Basically, DDF also known as $\tan\delta$ is the ratio of resistive current to capacitive current. The resistive current of an insulation system in good condition is much lower than the capacitive current.

Thereby, the source voltage is nearly 90 degrees lagging the source current which means DDF is very small. Any deterioration of the insulation causes an increase in the resistive current and gives rise to DDF. ASTM Std. D 924 and IEC Std. 60247 prescribe the standard procedure to obtain DDF of insulating oils in the commercial frequency range of 45-65 Hz and 40-62 Hz respectively.

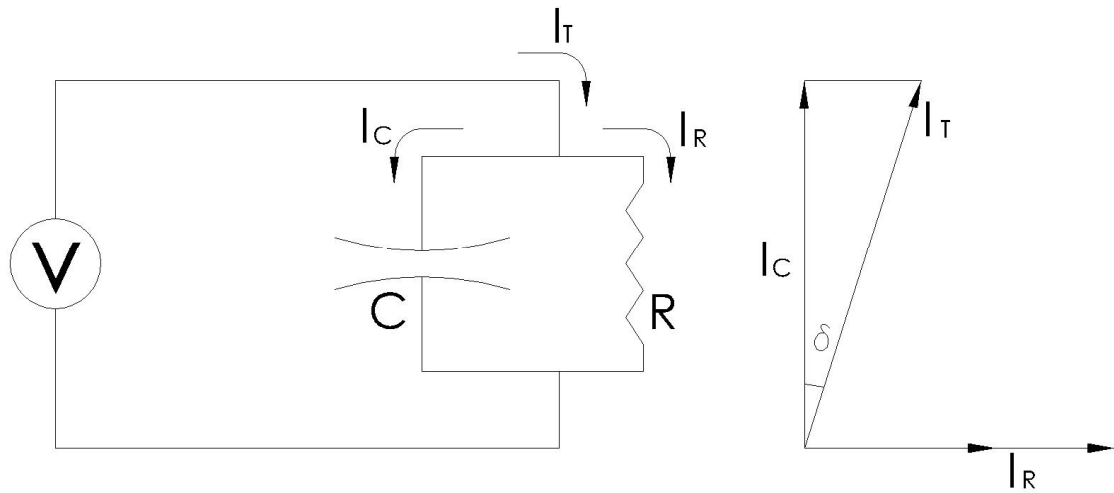


Figure 3.5: Simple vector diagram for dissipation factor measurement.

3.2.3 Specific Resistivity

Specific resistivity is the ratio of the direct current potential gradient in volts per centimeter (V/cm) paralleling the current flow within the sample to the current density in amperes per square centimeter (A/cm²) at a given time under prescribed conditions. This study was carried out in a stainless steel three terminal test cell of capacity 40ml as shown in Figure 3.6. The Specific Resistivity measurements were carried out at Sigma Test and Research Center (India) in accordance with ASTM D1169-64 (ASTM D1169-64, 2011). The Tan-delta Model OTS-2K1, Sivanada (India) was used as shown in figure 3.5. The test cell (Figure 3.7) was thoroughly cleaned and dried. The oil was poured in the test cell and an electric stress of 300V/mm was applied and tested at 90°C. The specific resistivity was calculated as per (3.2).

$$\text{Specific Resistivity} = \text{Instrument Reading} \times \text{Cell constant} \quad (3.2)$$

The cell constant is obtained from the test cell use (Figure 3.7) and the instrument reading is obtained from the Tan-delta Model OTS-2K1.

Resistivity measurements are carried out at 90⁰C for monitoring purpose. New oil is tested at both at room temperature (27⁰C) as well as 90⁰C. Useful information can be obtained by measuring resistivity at both ambient temperature and at 90⁰C.

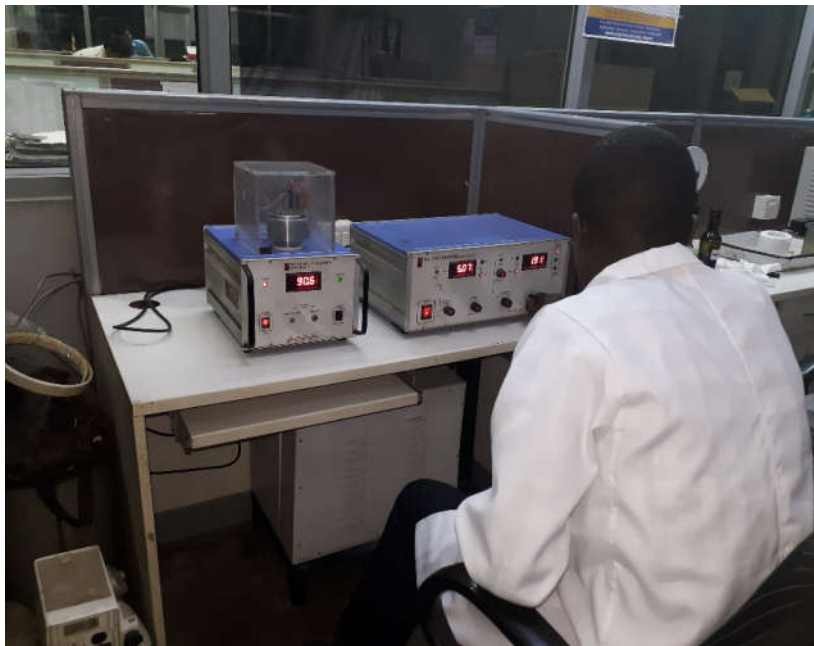


Figure 3.6: Specific resistance set up.



Figure 3.7: Test Cell for carrying specific resistance test.

3.3 Chemical Properties

The chemical properties tested include: neutralization number, corrosion and oxidation stability.

3.3.1 Neutralization Number

Acidity is the measure of free acids present in the liquid insulating oil and is expressed as milligrams of potassium hydroxide required to neutralize the total free acids in one gram of the oil. The acidic content of the plant-based oil samples is determined using colour indicator titration and is expressed in milligrams of potassium hydroxide per gram of the sample required to neutralize the sample. The acid number test of transformer oil is important because the oil will be applied in an equipment made of metal. Measurement of acid number could be attributed to the oxidation that occurs. Plant based oils have naturally higher acid numbers than petroleum oils, even when new. The acid number may be used to determine when oil should be replaced or reclaimed. IEEE standard C.57.147 recommends that the maximum acidity number of natural ester oil is 0.06 mgKOH/g (IEEE Standard. C57.147 ,2018). The tests were carried out in accordance with ASTM D974-14e2. Figure 3.8 shows the acidity measurement set up.



Figure 3.8: Acidity measurement set up.

3.3.2 Corrosion Test

The copper strip corrosion test is used to determine the relative degree of corrosivity of the oil product due to presence of active sulfur compounds.

To carry out the test, a polished copper coil was immersed in a 50mL of the respective samples at a raised temperature of 100⁰ C, for a period of 96 hours. At the end of this period, the copper strip was cleaned and thoroughly examined for trace of corrosion. Results are rated by comparing the stains on the copper strip to the ASTM color-match scale from 1a to 4c. As shown in Figure 3.9, for appearance of freshly polished copper strip with slight and barely noticeable discoloration, a rating of 1A is given. For a slight tarnish, 1B is given and the ratings proceed further down the scale as the corrosion staining severity of the test strip increases. 4C is the worst with the test strip appearing as severely corroded, blackened, and pitted.

The tests were carried out in accordance with ASTM D130(ASTM D130-12, 2012).

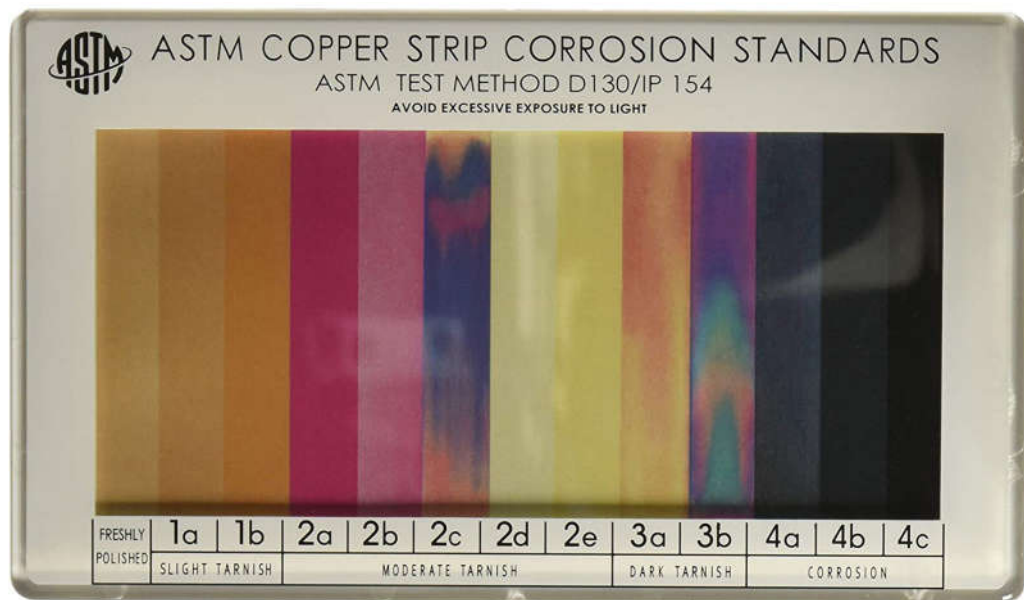


Figure 3.9:ASTM D130 Test Method Colour Code.

3.3.3 Oxidation Stability

Oxidation Stability is an important parameter for transformer insulation oils. Oxidation degradation of transformer oils is a well-known phenomenon because it is extremely difficult to banish oxygen entirely from an operating transformer.

Oxidation stability was carried out by bubbling a stream of air (oxygen) through the oil samples under test at a flow rate of 150ml/hr as per IEC61125 (2018). The samples were maintained for a period of 164 hours at a temperature of 70⁰C. The tests were carried out in accordance with ASTM D 2440 – 13(ASTM D 2440 – 13, 2013) as shown in Figure 3.10. After the end of 164 hours, Acidity and Sludge tests were carried out for all the samples. The total sludge value is the percentage by weight of insoluble matter formed when the oil is heated and oxidized under specified conditions.



Figure 3.10: Oxidation stability measurement set up.

3.4 Thermal Properties

The thermal properties tested included: flash point and pour point.

3.4.1 Flash Point

Flash Point of oil is the minimum temperature at which it gives enough vapours to form a flammable mixture with air under the test conditions.

The flash point of oil was measured using Pensky-Marten's Closed Cup Flash Point apparatus of Model 04115(Sivanada, India), as shown in Figure 3.11. All parts of the cup and its accessories were thoroughly cleaned and dried before starting the test. The cup was filled with sample to be tested to the level indicated by the filling mark. The lid was placed on the cup and set the latter on the stove. The locking device was properly engaged. A thermometer was inserted and the test flame was adjusted to a 4mm in diameter. The heat was supplied at a rate of 5^o to 6^oC/min. The flash point was recorded on the thermometer at the time of the test flame application, which causes a distinct flash in the interior of the cup. This test was carried out in accordance with ASTM D93 – 18(ASTM D93 – 18, 2018).



Figure 3.11: Flash Point measurement set up.

3.4.2 Pour Point

Pour is the lowest temperature expressed as a multiple of 3^oC at which the insulation oil is observed to flow when cooled and examined under standard and prescribed conditions as described by ASTM D97 (ASTM D97 – 05, 2005).

The tests were carried in High Precision bath with temperature range -80^oC-100^oC (Fluke Model 7381) as shown in Figure 3.12.

The oil sample was poured into two test jars (tubes) to the level mark 51mm. The test jars were then closed with a cork which was adjusted to fit tightly.

The test jars were then placed in the water bath. The specimen was cooled at a rate of 1.5°C per minute and the appearance and flow characteristic of the specimen was visually examined. The test jar was tilted at temperature intervals of 3°C to ascertain movement of the specimen in the jar. The lowest temperature at which movement of the test specimen was visually observed and recorded as the pour point of the sample. This was done by removing the test jars from the water bath jacket carefully and tilting them enough to ascertain whether there was a movement of the oil in the test jar. The temperature at which the oil ceased to flow was then noted and recorded down. This is the temperature at which the test jar shows no movement when it is held in a horizontal position for exactly 5 seconds.

This test was carried out in accordance with ASTM D97 (ASTM D97 – 05, 2005) and the pour point for the three samples was measured.

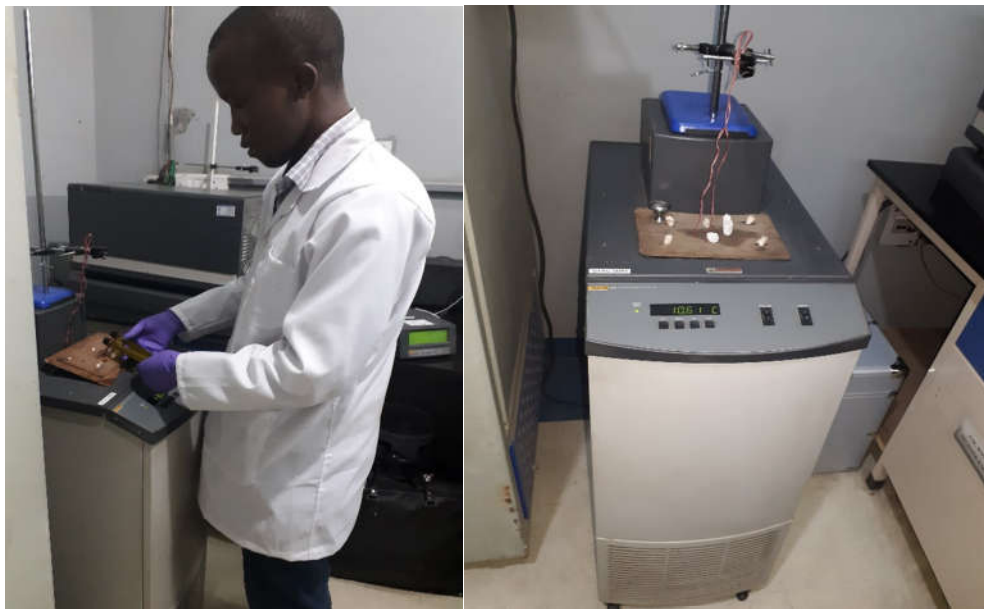


Figure 3.12: Pour Point measurement set up.

3.5 Physical Properties.

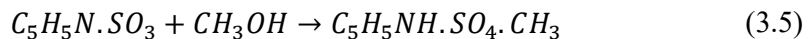
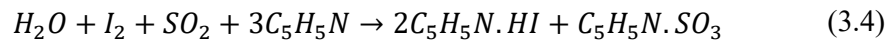
The Physical properties examined included: water content, density, appearance, viscosity, and interfacial tension.

3.5.1 Water Content

Water content has effect on the dielectric properties of insulating fluid. Excessive water content may deteriorate the breakdown characteristic of the insulating fluid. The automatic coulometric Karl Fischer instrument, Model VEEGO/MATIC 111 as shown in Figure 3.13 was used to determine the moisture content. The sample was mixed with a base solution of iodide ion and Sulphur (IV) oxide. Iodine is generated electrolytically and reacts with water. It is generated in proportion to the quantity of electricity according to Faraday's law, given by (3.3).



The reactions occurring in a Karl Fisher titration are known to be complex, but are essentially of water with iodine, Sulphur (IV) oxide, an organic base and an alcohol in an organic solvent. The original Karl Fischer reagent used pyridine and methanol, and the reactions may be expressed as (3.3) and (3.4).



Iodine generated by the electrolysis, as shown in reaction (3.2), reacts with the water in a similar way to the Karl Fischer reactions (3.3) and (3.4). A pair of platinum electrodes normally immersed in the anodic solutions detect the end point of the reaction. At this point, excess iodine depolarizes the dual platinum electrodes thereby producing a change in the current/voltage ration which then activates the end point indicator and then stops the current integrator. The reading is displayed in micrograms of water. This is after the current integrator integrates the current consumed during the electrolysis process and eventually calculating the water equivalent according to Faraday's law. This test was carried out using automatic coulometric Karl Fischer titration in accordance with ASTM D6304 - 16e1 (ASTM D6304 -16).



Figure 3.13: Water content determination set up.

3.5.2 Density

For the purpose of this method, density is the mass (weight in vacuum) of liquid per unit volume. In conjunction with other properties, density is a key property that is used to characterize both the light and heavy fractions of oil. It is crucial to determine the density or relative density of oils as it is necessary in the conversion of the measured volumes at the standard temperature of 15°C. The mass of the sample oil was determined using a digital balance and the volume was as indicated in the Borosil volumetric beaker used as shown in Figure 3.14. This test was carried out in accordance with ASTM D4052-18 Standard (ASTM D4052-18, 2018).

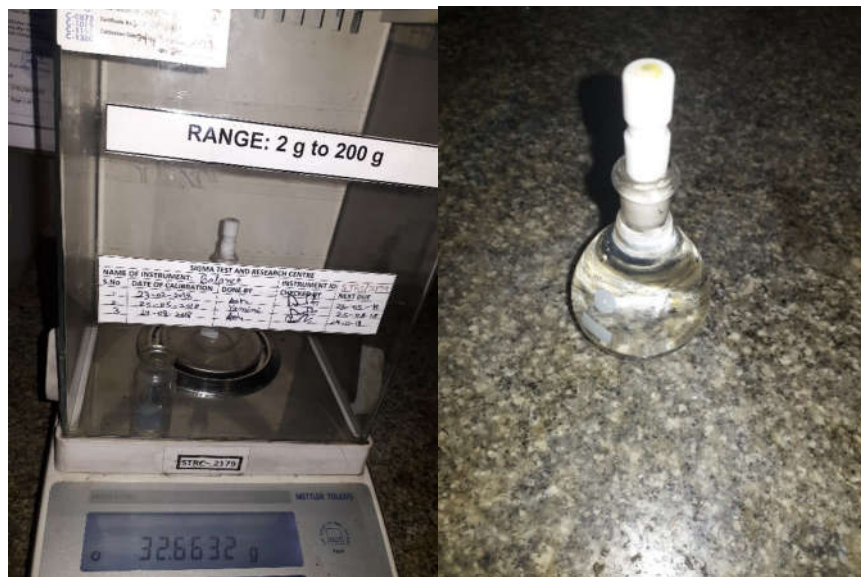


Figure 3.14: Density Measurement Apparatus.

3.5.3 Visual examination

The colour of oil is a visual parameter which reflects the degree of degradation and possible contamination of oil during use. To express the colour changes of the oil, a numeric value based on international colour standards, ASTM D1500 is used.

The oil samples were visually examined and their colours compared with the ASTM colour scale in accordance with ASTM D1500 (ASTM D1500, 2007).

3.5.4 Viscosity Test

Viscosity of oil is its resistance to flow. A study of the viscosity and flow properties of the natural oil is essential for its consideration as a potential choice as a bio-based insulating fluid. Viscosity of oil can be expressed in two ways-Dynamic viscosity and Kinematic viscosity. The definition of dynamic viscosity is given as the ratio between the applied shear stress and rate of shear of oil. Kinematic viscosity of the oil is its resistance of flow under gravity. Dynamic viscosity of oil can be computed by multiplying kinematic viscosity by its density. Unit of dynamic viscosity of oil is Poise and that of Kinematic viscosity is Stokes. There are various viscosity measurement techniques that have been developed over the years. The commonly used techniques for liquids with negligible non-Newtonian effect are capillary viscometers. These are

founded on the rationale that a specific volume of the liquid will flow through the capillary under gravity and the fact that the time required for this volume of the liquid to flow is directly proportional to the kinematic viscosity.

A suspended-level capillary viscometer was used to determine the kinematic viscosity. The viscometer is a U-shaped piece of glassware (Figure 3.15). It has an additional arm extending from the end of the capillary. This arm is to ensure that the pressure head is only dependent on a fixed height and not on the total volume of the liquid in the viscometer.



Figure 3.15: Glass capillary kinematic viscometer for measuring viscosity.

The sample was put into the viscometer's reservoir. A syringe was used to suck the sample through the capillary and the measuring bulb. It was then allowed to travel back through the measuring bulb. The time it takes the sample to travel back through the two calibrated marks was used along with the calibration constant to calculate the kinematic viscosity of the sample. Measurements were taken at both 27°C and 40°C.

For 40°C, the viscometer was immersed in a water bath equipped with a thermostatic temperature controller as illustrated in Figure 3.16. The controller controls the temperature of the system within accuracy of 0.5°C. The sample was introduced into

the reservoir of the viscometer. The temperature was set to 27°C and the system was allowed to attain thermal equilibrium. The measurement process was then repeated. Kinematic viscosity was calculated as per (3.5).

$$\text{Kinematic Viscosity} = \text{Viscometer Tube Factor} \times \text{Time} \quad (3.6)$$



Figure 3.16: Viscosity Measurement Setup Experiment.

The test was carried out with a U-Tube Viscometer and a Viscosity Bath, Model Welkins in accordance with ASTM D 445-17a. (ASTM D445 – 17a, 2017). The Viscometer Tube Factor is also known as the calibration constant and was read from the Viscometer Tube calibration data sheet.

3.5.5 Interfacial Tension (IFT)

Interfacial tension between the water and oil interface is the measure of attractive force between the molecules of water and oil. It is measured using platinum ring tensiometer. The interfacial tensiometer Model Petro-Diesel Insts (Chandernagore) was used to carry out the IFT study as shown in the Figure 3.17. A planar platinum ring is first placed in the interface of water and oil. A torsion wire is then used to lift it into the oil. The force required to lift the ring from the interface is proportional to interfacial tension. The test was carried out at Sigma Test and Research Center (India) in

accordance with ASTM D 971-12 (ASTM D 971: 2012, 2012). Three measurements were taken for each sample and the average result calculated.



Figure 3.17: Interfacial tension set up.

3.6 Accelerated Ageing

Accelerated ageing is carried out to predict the reliability of insulating material when in operation over a specified period of time. Ideal ageing test should include electrical, thermal and mechanical stresses which are actually responsible for ageing in transformers during operation. But thermal stress dominates the ageing factors and so the simulated ageing test was based on accelerated thermal ageing to induce the ageing mechanisms within a short period of time.

The ageing studies were carried out by applying accelerated thermal stress. This was carried out by the Open Beaker method with a copper catalyst.

The oil samples were put in 400ml capacity borosilicate beakers. Copper catalysts were then inserted in the oil's samples. The beakers were placed in a pre-heated oven and the temperatures maintained at 115°C for a period of 96 hours as shown in Figure 3.18 as per ASTM D1934 standard.

After the end of 96 hours, the aged oil samples were used for determination of resistivity (specific resistance), dielectric dissipation factor, total acidity and total sludge.

The tests were carried out in accordance with ASTM D1934 - 95(2012) (ASTM D1934 – 95,2012).



Figure 3.18: Ageing Oven.

CHAPTER FOUR

RESULTS AND DISCUSSIONS

4.1 Overview

This chapter presents the results obtained from the experimental study, their analysis and discussions.

A wide range of experiments were performed on the *Persea americana* food grade samples, RPAO and EVPAO. Similar experiments were also carried out on mineral insulation oil (MIO) for comparison purposes. Experimental data on the electrical, physical, thermal and chemical and properties of the samples are presented in this chapter. The properties of RPAO and EVPAO were compared with those of MIO.

4.2 Electrical Properties

The results and discussion for BDV, Dielectric Dissipation Factor (Tan Delta) and Specific Resistivity for samples tested are presented in this section.

4.2.1 Breakdown Voltage (BDV)

BDV is the single most important and popular test to gauge oil condition. Results obtained indicate RPAO has the highest BDV of 74 kV, followed by MIO with BDV of 65 kV and EVPAO with BDV of 36 kV. As per the illustrations in figure 2.6, high BDV implies that it takes a stronger electric field for the sample to undergo saturation. As it will be shown later, high moisture content greatly influenced the BDV for the given samples. The breakdown field data was fitted into the Weibull distribution function and the characteristic breakdown field of the samples, the shape parameter, and the confidence bounds of the distribution describing the samples were estimated. Figure 4.1 through Figure 4.7 show the Weibull plot of AC breakdown field data of RPAO, EVPAO, MIO and mixture of RPAO and EVPAO with MIO in 1:1 ratio respectively. The Weibull parameters of the oil samples are given in Table 4.1. The Weibull distribution of the natural oils (RPAO and EVPAO) was compared to that of mineral insulation oil (MIO). The characteristic breakdown strength of the samples

denoted as α , and the shape parameter, β , are tabulated with their respective 95% confidence intervals.

Table 4.1: Weibull Parameters of the Breakdown Test.

Sample	N	Characteristic Value, α (kV)	95% Conf. Bound for (kV)	Shape Parameter, β	95% Conf. Bound for β	Correlation Coefficient
RPAO	10	74	73.61 – 76.95	132	96.45 – 44.728	0.971
EVPAO	10	36	35.56 – 39.71	58	38.75 – 98.32	0.969
MIO	10	65	64.56 – 71.72	67	40.68 – 103.21	0.991
RPAO+MIO	10	67	66.54 – 70.70	116	70.62 – 179.19	0.946
EVPAO+MIO	10	26	26.17 – 30.12	46	30.45 – 77.26	0.962

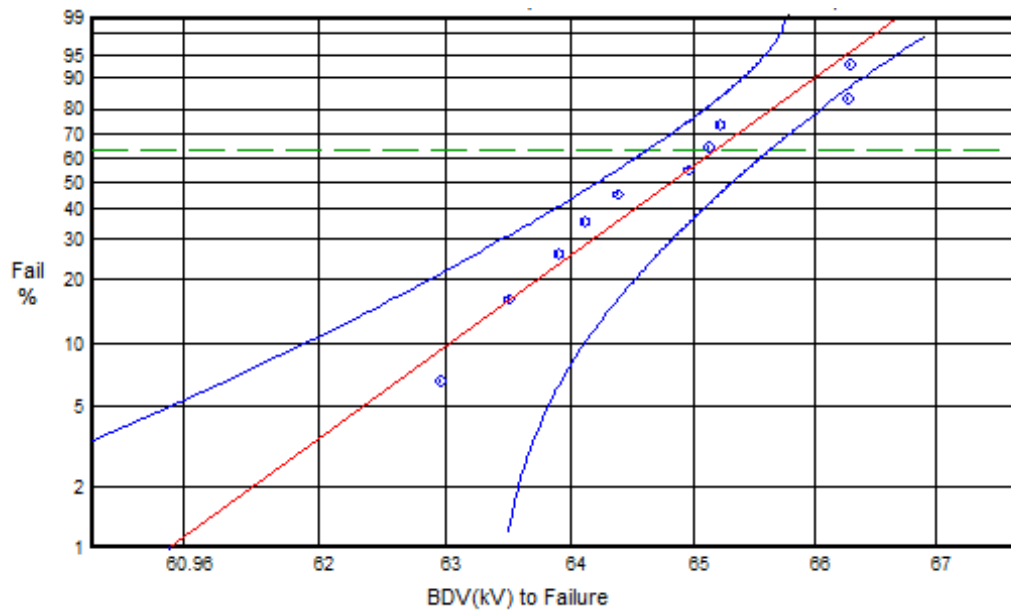


Figure 4.1: Weibull BDV Plot for MIO.

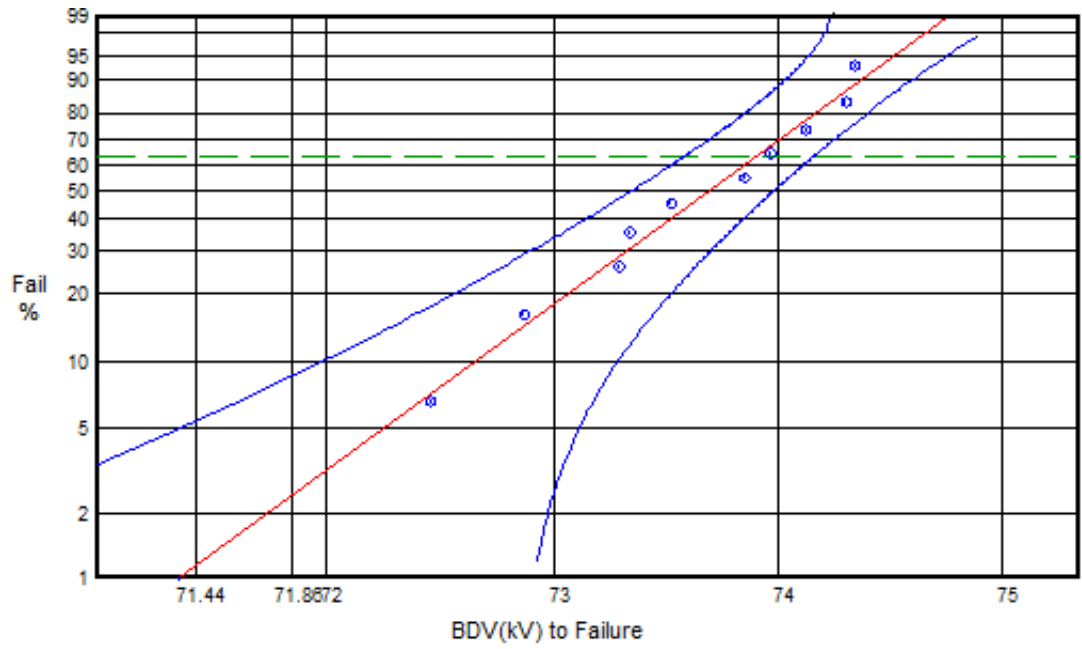


Figure 4.2: Weibull BDV Plot for RPAO.

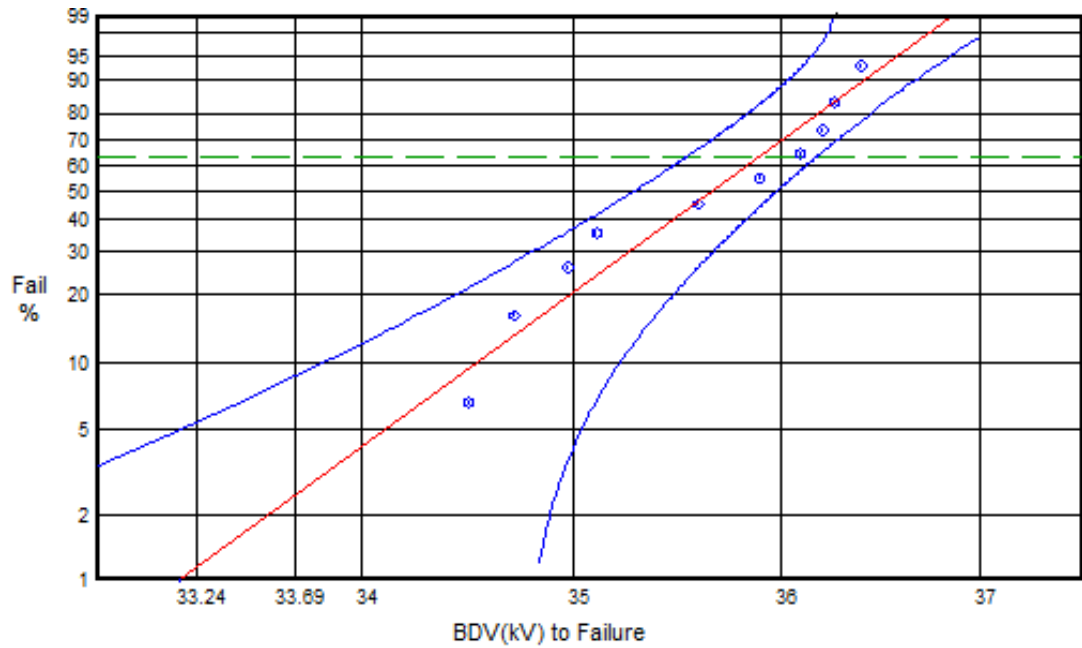


Figure 4.3: Weibull BDV Plot for EVP AO.

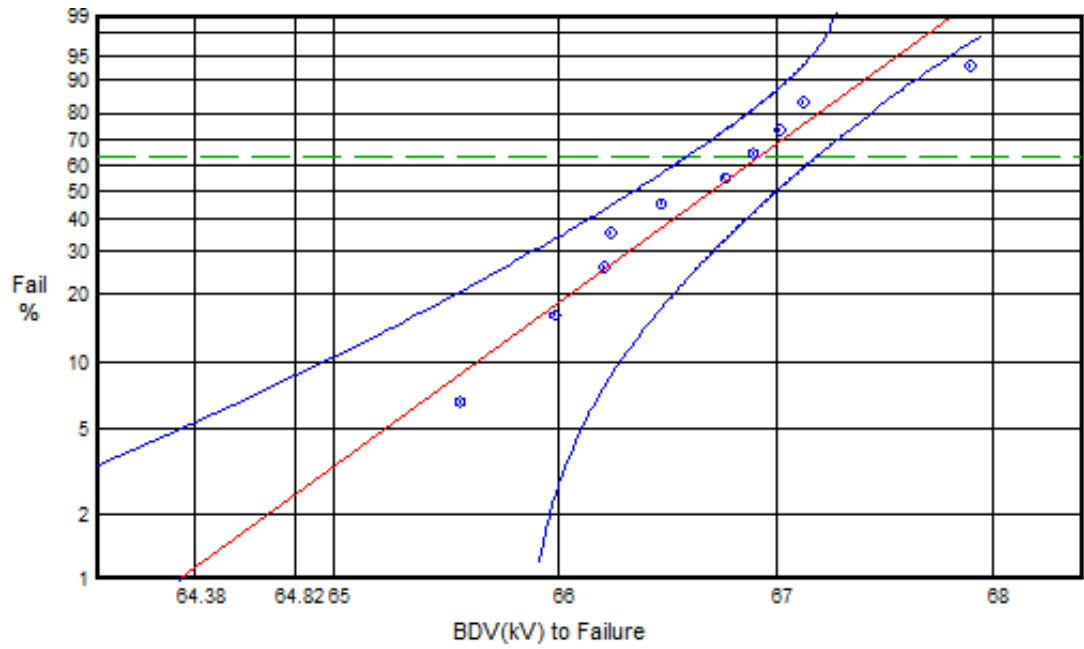


Figure 4.4: Weibull BDV Plot for 1:1 Mixture of MIO & RPAO.

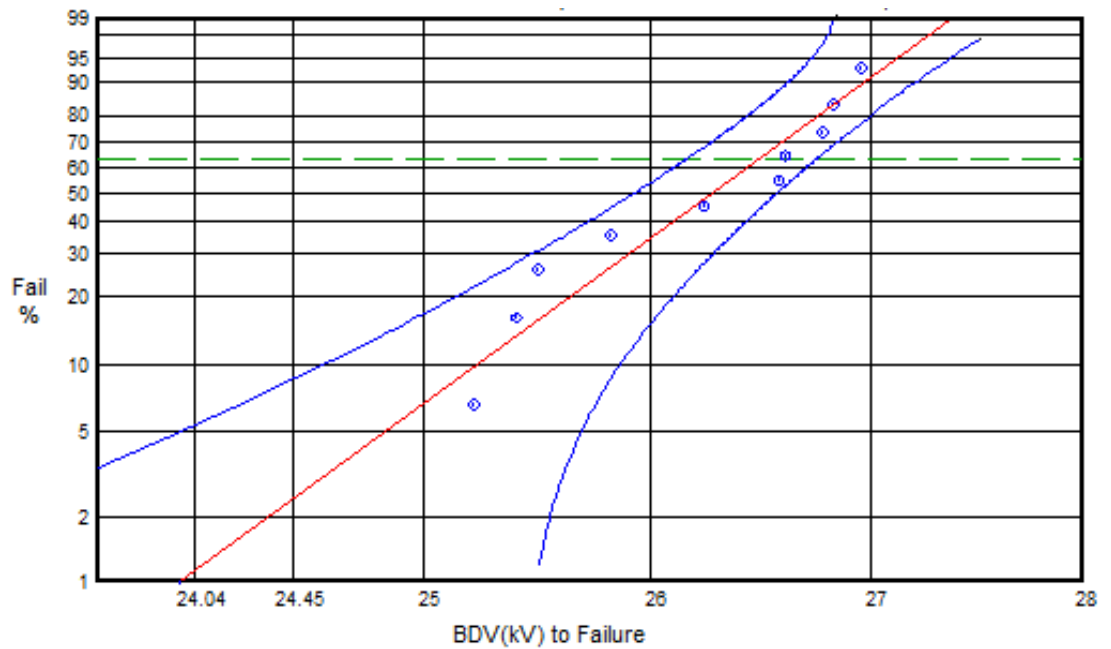


Figure 4.5: Weibull BDV Plot for 1:1 Mixture of MIO & EVPAO.

The correlation coefficients of the BDV data when fitted to the Weibull function are much greater than the critical correlation coefficient of $R^2=0.918$ for 10 breakdowns (IEC 62539, 2007). This demonstrates a strong linear relationship between the two variables. The statistical data shows a huge improvement in the characteristic breakdown strength of refined *Persea americana* oil (RPAO) when compared with Extra Virgin *Persea americana* Oil (EVPAO). This shows that the refining process improves the breakdown field strength. This attributed to reduced concentration of impurities observed. This low breakdown strength of EVPAO suggests that the impurities in the liquid may have aligned to at least partially form a bridge across the gap due to its attraction towards higher field region. This may have increased the field in the liquid within the gap, leading to breakdown after it reached critical value. The characteristic electric field strength of the RPAO under 2.5 mm gap is about 106% higher than EVPAO and 13% higher than MIO. The high values for the fitted shape parameter, β , of RPAO demonstrates that RPAO has a narrow distribution of breakdown field.

The characteristic electric field strength of the mixture RPAO+MIO under 2.5mm gap is about 2.7% higher than MIO. This demonstrates that mixing RPAO and MIO in 1:1 slightly improves the overall characteristic electric field. The characteristic electric field strength of the mixture EVPAO+MIO under 2.5mm gap is about 59% less than that of MIO. This demonstrates that mixing EVPAO and MIO in 1:1 hugely decreases the overall characteristic electric field.

The EVPAO sample contains particles as impurities, which are dispersed in the liquid. Application of a high electric field may have caused the particles to drift towards the region of strongest field. The strongest field is around the region of shortest distance for the sphere-sphere electrode gap. The particles in the field region may have resulted in flux concentration at the surface of the high voltage electrode. Other particles may also have been attracted towards the higher flux concentration and may have aligned to form a partial bridge across the gap.

This may have possibly led to an increase in the field in the liquid, therefore causing early breakdown. The partial bridge particles caused local field enhancement, which may have resulted in local breakdown near the particles when the field exceeds the dielectric strength of the liquid. This could result to formation of gas bubbles. Discharges may then occur when the electric field in the spherical gas bubbles becomes equal to the gaseous ionization field. The end result is the decomposition of the liquid and the eventual breakdown of the samples.

Over the full range of failure probability, the characteristic breakdown strength of the RPAO is significantly greater than that of the mineral insulation oil. High β values for RPAO and RPAO +MIO suggest low dispersion in the breakdown data of the samples. The dispersion of the breakdown data of EVPAO, MIO and EVPAO+MIO, as seen from the β , values is higher than that of RPAO and RPAO+MIO. The presented results are comparative studies within the experimental limit of the standard breakdown test cell. Large quantity of oil sample (enough to carry out about 100 tests) is required for a repeat measurement using standard breakdown test cell to be confident of the values.

When replacing mineral oil by RPAO, the mixing of RPAO and mineral oil cannot be avoided because the draining process will still leave oil remains in the spaces between windings and the bottom of the tank. Hence, it is necessary to examine the effect of the mixture percentage on breakdown voltage. The mixture of 50% RPAO and 50% MIO, 50% EVPAO and 50% MIO was investigated. Figures 4.4 and 4.5 show the breakdown voltage results of the oil mixture, RPAO and MIO, EVPAO and MIO, under AC voltages. It appears that the values of breakdown voltages are scattered around the mean (characteristic value average value) of the breakdown voltage.

It is observed that the mean of AC breakdown voltage of RPAO is higher than that of the oil mixtures (RPAO and MIO). The mean AC breakdown voltage of the oil mixtures (RPAO and MIO) is higher than that of MIO. This indicates that there is no problem in the event that RPAO is mixed with mineral oil in replacement process in installed transformer. The mean AC breakdown voltage of EVPAO and its mixture (EVAPAO and MIO) is the lowest one.

The breakdown voltage of RPAO is higher than that of EVPAO. The presence of significant impurities in EVPAO may have influence on the breakdown voltage. The shape parameter, which is related to the statistical consistency of the data, was high for breakdown data for RPAO and lowest for EVPAO. This is an indication of lower predicted breakdown field value for low probabilities (for example, 1% probability). The predicted 1% breakdown probability of EVPAO and MIO are below the values for RPAO as shown in Table 4.2. This suggests that the breakdown voltage for RPAO has lower probability of failure at lower applied fields compared with that of EVPAO and MIO samples.

Table 4.2: Breakdown Probabilities from Weibull Distribution for PAO, MIO and Mixtures.

Samples	$U_{1\%}(kV)$	$U_{50\%}(kV)$	<i>Characteristic Value, α (kV)</i>	<i>Shape Parameter, β</i>
RPAO	74.187	73.46	73.90	132.39
EVPAO	36.219	35.43	35.89	58.22
MIO	65.685	64.43	65.17	67.11
RPAO+MIO	65.69	64.43	66.91	116.26
EVPAO+MIO	24.94	24.23	26.49	46.26

It appears that the values of breakdown voltages are scattered around the mean of the average BDV. The average BDV of RPAO is slightly higher than that of MIO. The distribution frequency of AC breakdown voltage appears to obey a normal distribution as shown in Figures 4.7 to 4.11. To determine whether the distribution of the data obtained is normal, one applies Shapiro-Wilk (Shapiro & Wilk ,1965) tests to calculate W-value and P-value (Table 4.3). In this statistical analysis, normal distribution is considered with a significant level test of 5% ($\alpha = 0.05$). P-value is the probability of making mistake that the null hypothesis is rejected. If P-value is higher than the significant level ($\alpha =0.05$), one accepts null hypothesis that the sample data follows a statistical distribution. It appears from this table that all sample data tested are accepted.

Figure 4.6 shows the BDV results for RPAO, EVPAO, MIO and the mixtures.

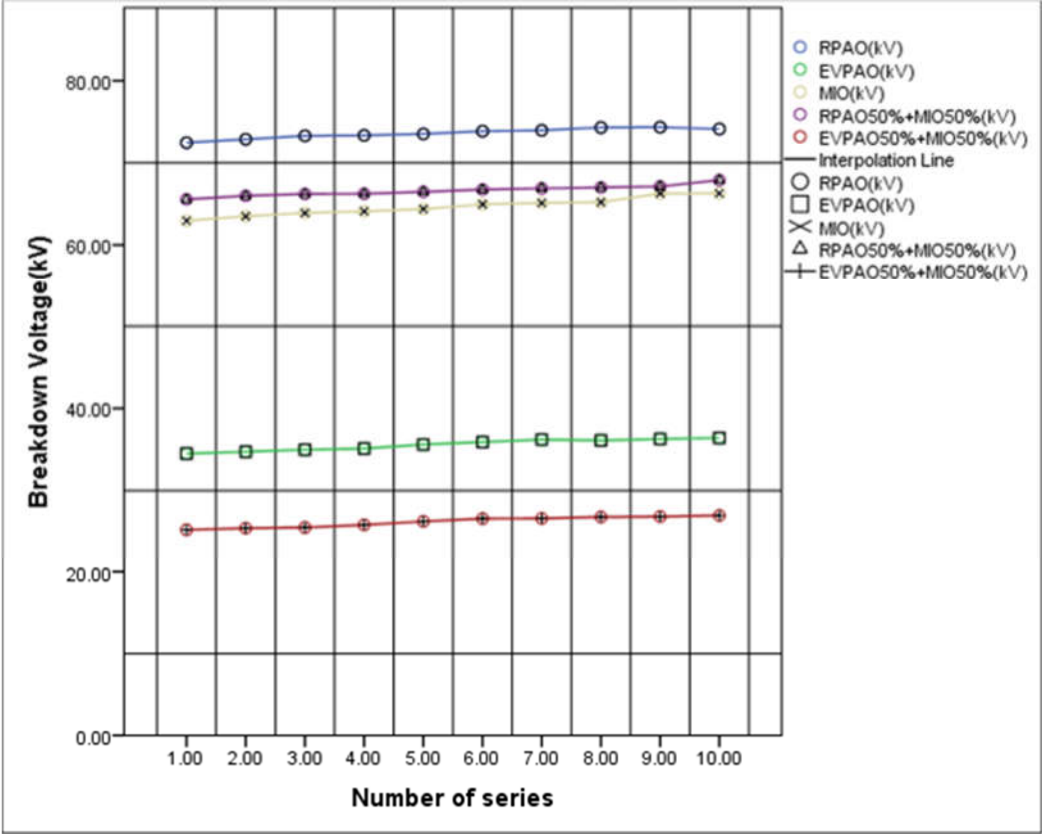


Figure 4.6: AC Breakdown voltage scattering of PAO, MIO and the Oil Mixtures.

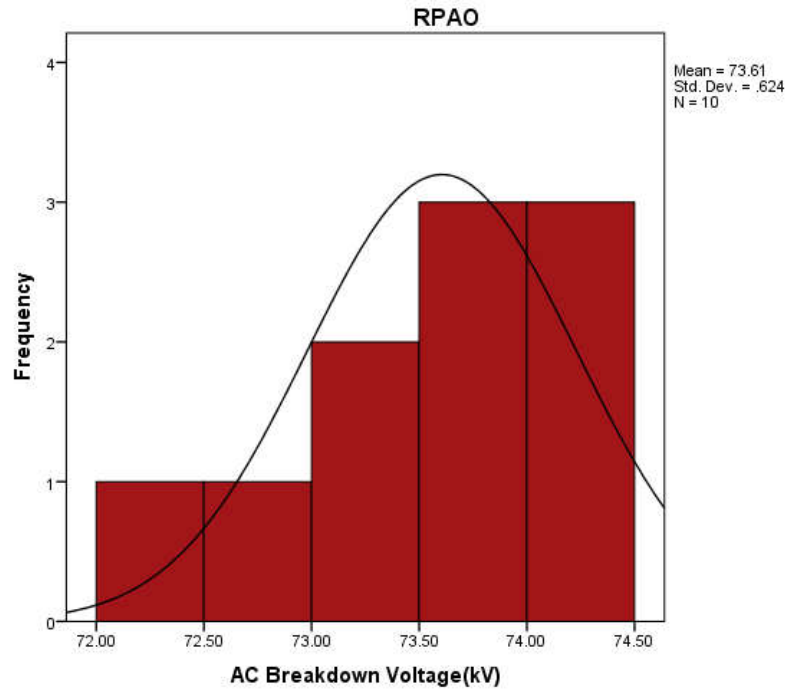


Figure 4.7: RPAO BDV Histogram.

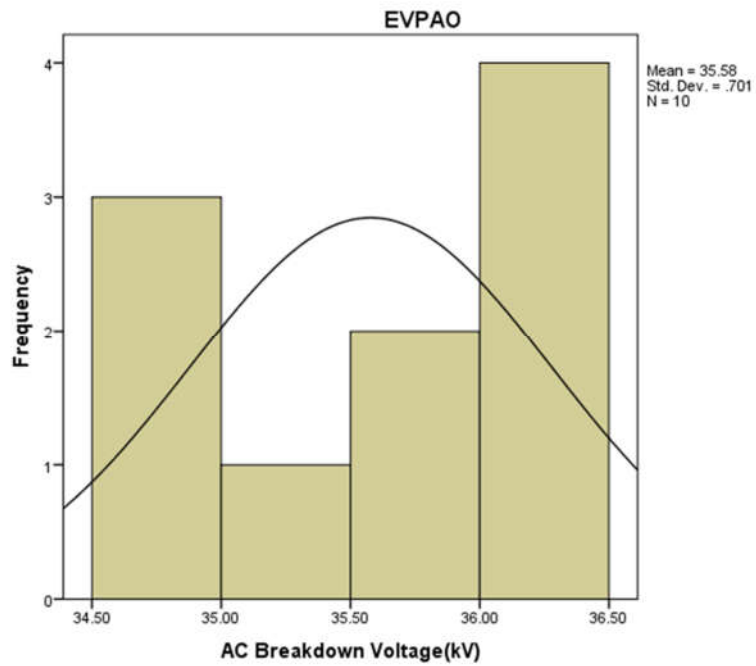


Figure 4.8: EVPAO BDV Histogram.

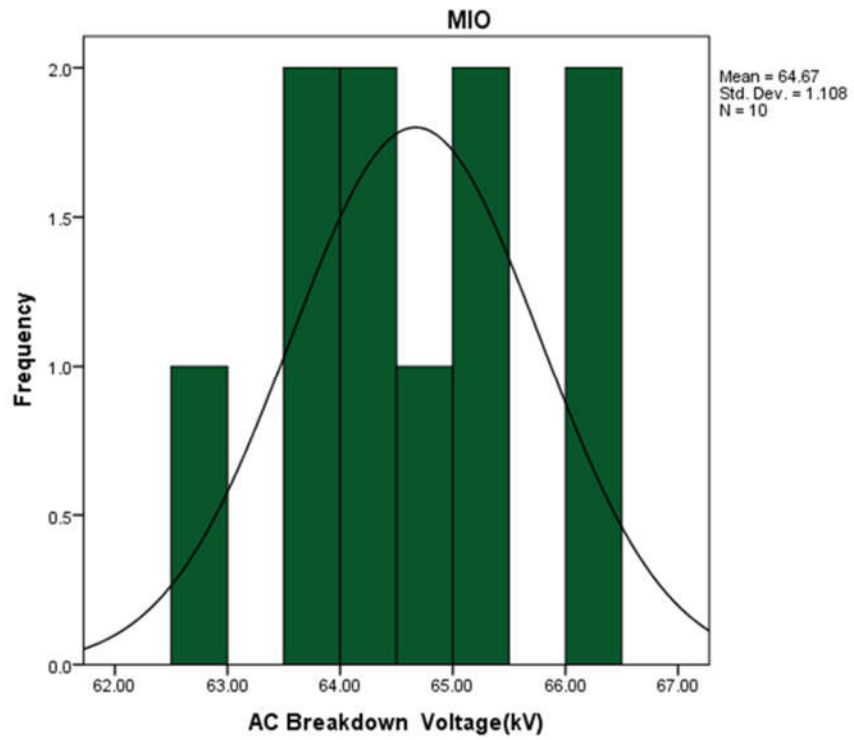


Figure.4.9: MIO BDV Histogram.

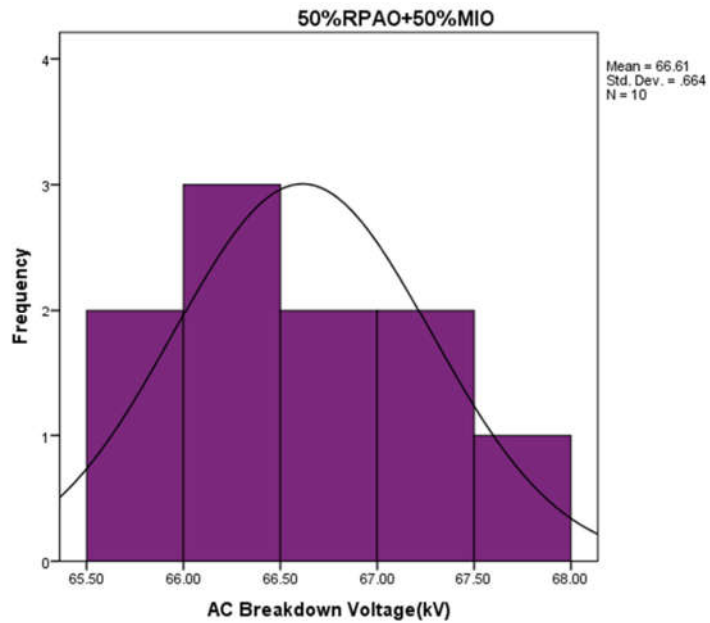


Figure 4.10:50% RPAO+50% MIO BDV Histogram.

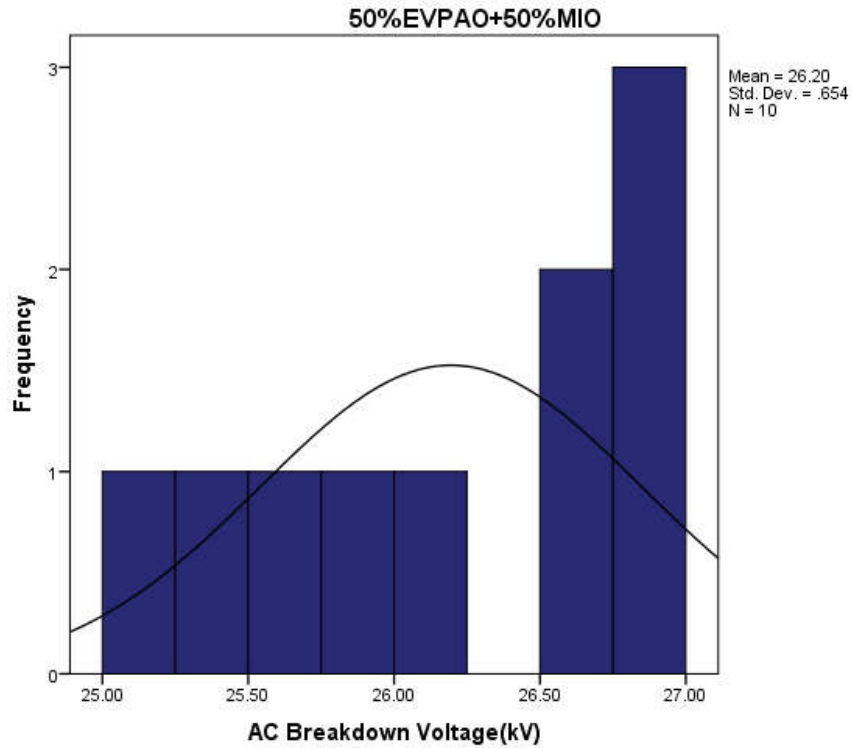


Figure 4.11: BDV Histogram for EVPAO/MIO ratio 1:1.

Table 4.3: Hypothesis test of conformity to normal distribution of AC BDV.

Sample	W	p-value	Conformity to Normal distribution
RPAO	0.942	0.574	accepted
EVPAO	0.905	0.248	accepted
MIO	0.956	0.740	accepted
50%RPAO+50%MIO	0.981	0.969	accepted
EVPAO50%+MIO50%	0.891	0.173	accepted

The skewness and kurtosis values obtained from the SPSS program are presented in Figure 4.12.

The skewness values of the breakdown voltage of MIO and RPAO50%+MIO50% are positive. This indicates a pile-up of scores to the left of distribution. The skewness values of RPAO, EVPAO and EVPAO50%+MIO50% are negative. This indicates that a pile-up of scores on the right side of the distribution.

Except for the oil mixture RPAO50%+MIO50%, the kurtosis values for all tested values are negative. This implies that all distributions are platykurtic, except for the distribution of oil mixtures RPAO50%+MIO50%.

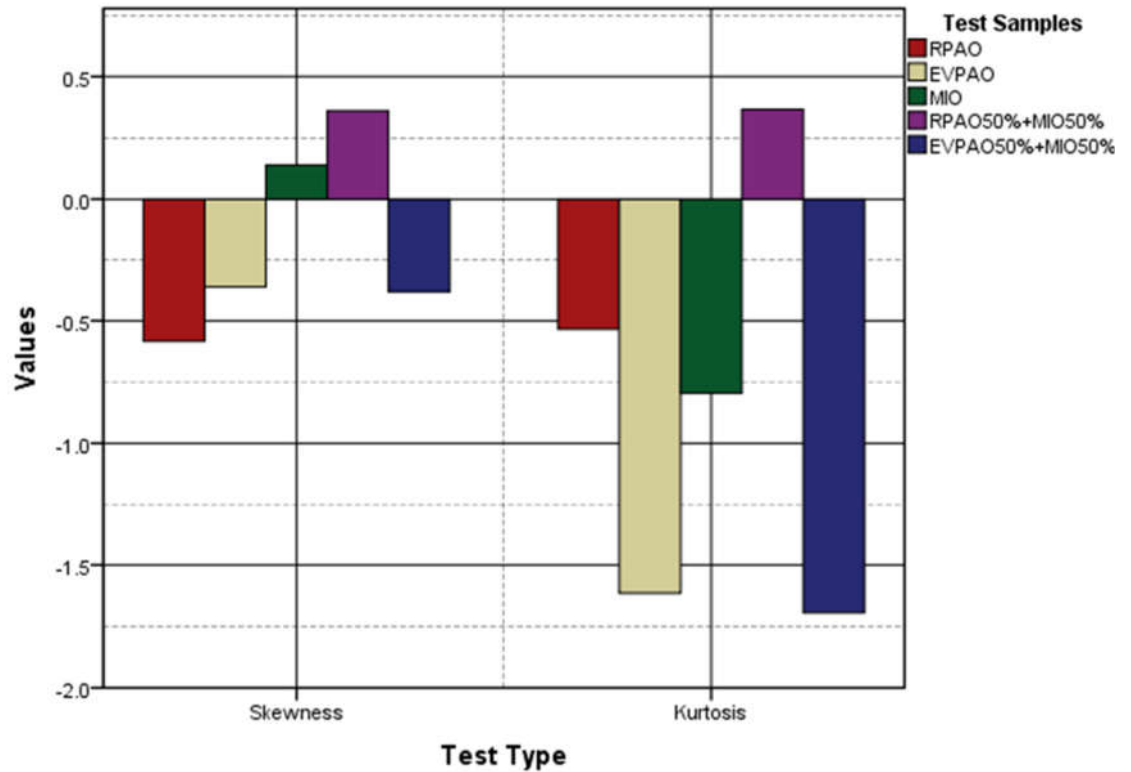


Figure 4.12: Skewness and kurtosis of normal distribution of AC BDV of tested oils.

Figure 4.13 shows the average value of all tested oils under AC voltage. It is observed that the AC mean breakdown voltage of RPAO is the highest of the all the samples tested. The AC mean breakdown voltage of the mixture EVPAO50%+MIO50% is the lowest. The AC mean breakdown voltage of the mixture RPAO50%+MIO50% is higher than that of MIO. This indicates that there is no problem in the event that RPAO (or PAO) is mixed with the MIO during the replacement process in an already installed transformer as mentioned earlier.

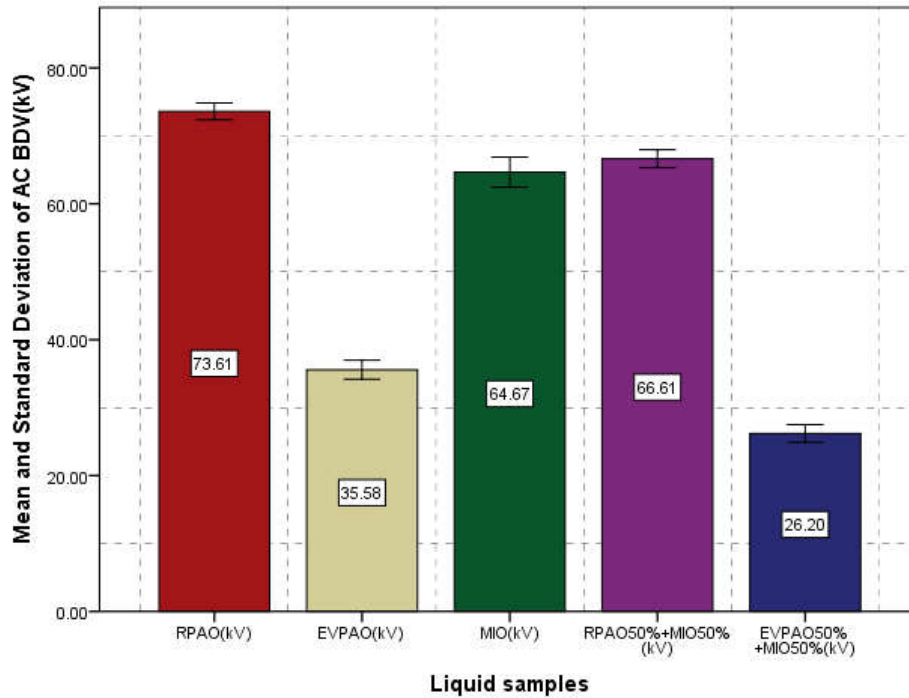


Figure 4.13: Mean of AC breakdown voltage of tested oils.

4.2.2 Dielectric Dissipation Factor

The tangent of the loss angle is called dielectric dissipation factor. A high tan-delta is an indication of presence of contaminants. Good oil should have 0.2(max) tan-delta as ASTM D 924-65 [41]. A high tan-delta is an indication of presence of contaminants such as soluble varnishes, resins, and particles such as chlorophyll (Ferguson, Lobeiras & Sabau, 2002) (Fosana, Wasserberg & Gockenbach, 2002).

There is generally a relationship between tan-delta and resistivity, both being affected by contaminants. A decrease in resistivity is accompanied by an increase in tan-delta. They are indirectly proportional to each other.

Table 4.4 shows the dissipation factor for various samples tested.

Table 4.4: Tan-Delta for PAO and MIO

Samples	Tan Delta, % (at 100°C & 40 Hz to 60 Hz)	IEEE C57.147-2018	IEEE.Std C57.106-2015	IS.335. (1993)
RPAO	0.33	4.0(%Max)	-	-
EVPAO	1.86	4.0(%Max)	-	-
MIO	0.26	-	0.30(%Max)	0.4(%Max)

The high tan-delta indicates that the oil samples were highly contaminated. RPAO and EVPAO met the IEEE C57.147-2018 requirements. MIO had the lowest tan-delta.

4.2.2 Specific Resistance

The specific resistance or resistivity of the insulation oil should be as high as possible. Presence of moisture, acidity and solid contaminants considerably reduces the oil resistivity (Kazmierski, Sobocki & Olech,1998) (Saha, Hilli, & Le, 1998). Resistivity of oil reduces considerably due to presence of moisture, acidity and solid contaminants (Kazmierski, Sobocki & Olech,1998) (Saha, Hilli, & Le, 1998). Contamination of oil can easily be indicated by changes in the value of resistivity. Thus, resistivity can be used to detect oil contamination in cases where acidity tests fail to indicate oil contamination. A satisfactory value at 90⁰C and unsatisfactory values at room temperature is an indication of the presence of water or degradation products precipitable in the cold but generally at a tolerable level. Getting unsatisfactory results at each temperature implies a great extent of contamination and the oil may not be restored to satisfactory levels by reconditioning. Table 4.5 shows the specific resistance for various samples tested:

Table 4.5: Resistivity for PAO and MIO.

Samples	Resistivity (at 27°C), ohm-cm	Resistivity (at 90°C), ohm-cm	IS.335. (1993) at 27°C, ohm-cm, (Min)	IS.335. (1993) at 90°C, ohm-cm, (Min)
RPAO	7.35x10 ¹²	2.56x10 ¹²	-	-
EVPAO	0.28x10 ¹²	0.51x10 ¹²	-	-
MIO	0.94x10 ¹²	0.48x10 ¹²	1500 x 10 ¹² (Min)	35 x 10 ¹² Min

RPAO has the highest resistivity as compared to all the other samples at both 27°C and 90°C. This indicates that it is less contaminated as compared to other samples shown.

4.3 Physical Properties

The results and discussion for Appearance, Water Content, Density, Viscosity, and Interfacial Tension for samples tested are presented in this section.

4.3.1 Appearance

The appearance and colour of RPAO, EVPAO and MIO were observed and tabulated in Table 4.6. The colour of RPAO was clear light yellow and transparent while that of EVPAO was emerald green with suspended sediments (Figure 4.16). The EVPAO color could be due to the high levels of chlorophylls that may be present in the oil sample.

Table 4.6: Appearance of the oil samples for PAO and MIO.

Samples	Appearance	IEEE	IS:335-1993
		C57.147-2018	
RPAO	Light yellow liquid, clear and translucent and free from suspended matter or sediments	Bright and clear	
EVPAO	Yellow liquid with suspended matter or sediments	Bright and clear	
MIO	Colourless, clear and transparent liquid and free from suspended matter or sediments	-	The oil shall be clear and transparent and free from suspended matter or sediments



(a)RPAO

(b) EVPAO

(c) MIO

Figure 4.14: Appearance PAO and MIO.

4.3.2 Water Content

The water content of RPAO, EVPAO and MIO was determined as shown in Table 4.7. The water present in oil is allowed at parts per million (ppm) levels. The accurate measurement of water content at such low levels requires sophisticated instruments such as the Automatic Karl Fischer Titration.

Table 4.7: Water Content for PAO and MIO.

Samples	Water Content, (ppm)	IEEE .C57.147 (ppm) (Max)	IEEE.C57.10 6(ppm) (Max)	IS.335. (1993) (ppm) (Max)
RPAO	136.05	200		-
EVPAO	924.71	200		-
MIO	88.77		35	50

High water content greatly influenced the BDV for the given samples. For example, RPAO had a water content of 136.05ppm while EVPAO had the water content of 924.71ppm. This is as shown in Table 4.7.

EVPAO had the highest water content owing to the manner in which it is processed from the *Persea americana* pulp (extra virgin). Extra virgin (cold pressed) oils retain all their flavour, aroma, and nutritional value. MIO had the lowest water content. To remove the water content, the oil samples can be dried in a vacuum.

Considering the fact that most of the transformers operate at temperatures ranging from 40⁰C to 90⁰C, the presence of water content plays an important role in the failure of the transformer. Water content is recognized to be a major cause of insulation failure.

The level of moisture content in transformer oil can affect the insulation properties of the oil. Knowledge of the initial water content will serve as a reference in the monitoring of the water while the oil is in service; since water is one of the by-products

of ageing deterioration. An increase in the water content of used insulating oil may be a marker for deterioration.

Transformer’s solid insulation is also affected by water presence. When a transformer is filled with the insulation oil, the moisture in the oil is absorbed by the paper. Since the paper is highly hygroscopic in nature, the insulation property is affected. High water content also increases the electrical conductivity, dissipation factor and reduces the electric strength. Thus, it eventually decreases the safety margin [78, 79]. (Koreh, Torkos, Bashir & Borossay, 1998) (Boubakeur, Mecheri & Boumerzoug, 1999)

4.3.3 Density

The density of the oil samples is as shown in Table 4.8.

Table 4.8: Density Measurements for PAO and MIO.

Samples	Density at 29.5°C, (g/cm ³)	IEEE C57.147, (g/cm ³) (Max)	IEEE.Std C57.106, (g/cm ³) (Max)	IS.335. (1993), (g/cm ³)(Max)
RPAO	0.903	0.96	-	-
EVPAO	0.903	0.96	-	-
MIO	0.825	-	0.91	0.89

RPAO and EVPAO have the same density as expected. MIO density meets the density specifications for new mineral insulation oils as per ASTM D4052-18 (ASTM D4052-18, 2018). MIO had the lowest density (0.825g/cm³) while RPAO and EVPAO had the highest (0.903 g/cm³). This implies that MIO is the lightest oil of the three. It can thus occupy less volume for the same mass as compared to other samples. Density also has influence on viscosity. The lower the density, the less the viscosity. MIO with density of 0.825g/cm³ has viscosity of 10.46cSt, while RPAO with density of 0.903 g/cm³ has viscosity of 45.66cSt at 27°C respectively.

In conjunction with other properties, density is a fundamental property that is used to characterize both the light and heavy fractions of oil. It is crucial to determine the density or relative density of oils as it is necessary in the conversion of the measured volumes at the standard temperature of 15°C.

4.3.4 Viscosity

The kinematic viscosity measured for the three samples is shown in Table 4.9.

Table 4.9: Kinematic viscosity results for RPAO, EVPAO and MIO.

Samples	Kinematic Viscosity, cSt at 27°C	Kinematic Viscosity, cSt at 40°C	IEEE C57.147 at 40°C, (cSt)(Max)	IS.335. (1993) at 40°C, (cSt)(Max)
RPAO	45.66	35.58	50	-
EVPAO	52.03	38.54	50	-
MIO	10.46	8.15	-	27

The variation in viscosity is apparent in all the three samples. Increase in temperature leads to a corresponding decrease in kinematic viscosity. Temperature increase leads to thermal or kinetic energy increase of each molecule and this eventually reduces the cohesive energy of the oil molecules. This in turn decreases the resistive force acting between layers of the natural oils travelling at different velocities. This increases the molecule's mobility, resulting in the viscosity reduction (Massey & Ward-Smith, 2006).

The high viscosity in both RPAO and EVPAO could be attributed to the presence of fatty acids and glycerol. The glycerol initially bonds together the fatty acids in the oil hence increasing the molecular mass of the oils. This should be expected since the saturated fatty acids dominate the composition of the natural oils.

Good oil should have less viscosity so that it offers less resistance to oil flow so that it does not affect the cooling of transformer adversely (Belanger, 1999). Viscosity is one of the main parameters in design calculations for heat transfer self-cooled transformers or even the forced convection in large transformer units (Rao, 1996). A low value of viscosity and a good heat transfer capability are needed to achieve high performance. Low viscosity also assists initial penetration of the oil into narrow ducts and promotes circulation through the windings to overcome local overheating, which would result from more lengthy residence of the oil at any hot spots. Equally important is the fact that viscosity of oil should increase as little as possible with decrease in temperatures. The heat exchange property can be measured using a liquid parameter known as Reynolds number. This parameter is used to determine whether oil has a turbulent or laminar flow. Reynolds number is related to dynamic viscosity with the expression:

$$Re = \frac{w \cdot d}{\mu} \quad (4.5)$$

Where μ is the dynamic viscosity, w is the oil velocity and d is diameter of the channel. A turbulent oil flow is reported to have more effective cooling effect than laminar flow (Massey & Ward-Smith, 2006). Turbulent flow has Reynolds number greater than 4000, while value below 2000 is regarded as laminar flow. From the expression in equation 4.5, a lower viscosity gives higher Reynolds number. Reynold number was not determined for the samples tested as the equipment used was unavailable.

4.3.5 Interfacial Tension (IFT)

The results of interfacial tension for the oil samples are shown in Table 4.10. As shown in Table 4.10, MIO had the lowest interfacial tension while RPAO had the highest interfacial tension.

Interfacial tension is useful in investigating the presence of oil decay products and polar contaminants. New oil usually exhibits high interfacial tension. Polar contaminants have high affinity towards water molecules as well as the oil molecules (Darveniza, Saha, Hill, Le, 1998). At the interface they extend across to the water, thus a vertical force is exerted reducing interfacial tension. The results as shown in Table 4.10 indicate that MIO had insignificant amounts of polar contaminants.

Table 4.10: Interfacial Tension (IFT) results for PAO and MIO.

Samples	Interfacial Tension (at 27°C), N/m.	IEEE C57.147	IEEE.Std C57.106(Min)	IS.335. (1993) (Min)
RPAO	0.048	-	-	
EVPAO	0.051	-	-	
MIO	0.046	-	0.04	0.04

4.4 Chemical Properties

The results for Neutralization Value test for the samples tested are presented in this section.

4.4.1 Neutralization Value

Acidity of a new oil is normally insignificant. Table 4.11 shows the acidity values for the three samples. Acidity of oil is harmful to transformer's solid insulation. The presence of acids can also induce rusting of iron in presence of moisture. MIO met the acidity specifications for new mineral insulation oils as per IEEE Std C57.106. The acidity of EVPAO appeared to be high. RPAO and MIO fulfilled the IEEE C.57.147 and IEEE STD C57.106 requirements respectively.

Table 4.11: Neutralization value measurements for PAO and MIO.

Samples	Total Acidity, mg KOH/g.	IEEE C57.147(Max)	IEEE Std C57.106(Max)	IS.335. (1993) (Max)
RPAO	0.073	0.	-	-
EVPAO	1.49	0.6	-	-
MIO	0.013	-	0.3	0.3

The presence of acids can lead to reaction with the bulk oil which may result in the formation of sludge and varnish deposits. The sludge in the worst case may result in

blocking of oil canals in the transformer. This may affect the efficiency of the cooling unit of the transformer, leading to overheating and eventual breakdown. High acid content in insulating oil has the consequence of increasing ionic dissociation leading to higher concentration of charge carriers and an increase in electrical conductivity. The fatty acids in natural oils have different characteristics compared with mineral oil. The acids react with the OH (hydroxyl) groups on the cellulose in transformers via transesterification (Rapp, McShane & Luksich, 2005). The esterification reaction chemically modifies and protects the Kraft paper from degradation due to age. The acidic content of insulating fluid increased with ageing since acidic products are among the by-products of ageing. The test can be used as a measure of quality control of freshly prepared oil for insulation and insulating oil in use.

4.5 Thermal Properties

The results and discussion for Flash Point and Pour Point for samples tested are presented in this section.

4.5.1 Flash Point

It is desirable that the oil should have very high flash point ($>140^{\circ}\text{C}$). Table 4.12 shows the flash points for oil samples tested.

Table 4.12: Flash Point results for RPAO, EVPAO and MIO.

Samples	Flash Point, °C	IEEE C57.147(°C) (Min)	IEEE C57.106(°C) (Min)	IS.335. (1993) (°C) (Min)
RPAO	310	275	-	-
EVPAO	142	275	-	-
MIO	156	-	-	140

Of the three samples, RPAO had the highest flashpoint and fulfils the IEEE.C57.147 requirements. EVPAO had the lowest flashpoint and did not meet the IEEE C57.147

standard. This is due to the presence of high amounts of moisture and contaminants compared to the other samples used.

4.4.1.1 Flash Point Mechanism in Liquid Dielectrics.

Liquid dielectrics have a specific vapor pressure. This is subject to Boyle's law and is a function of its temperature. The vapor increases with increase in temperature. The concentration of the vapor increases with vapor increase. Therefore, temperature determines the vapor concentration in the air. A certain concentration of the vapor is necessary to sustain the air combustion and is called, the lower flammable limit. As mentioned elsewhere, ASTM provides standard method of measuring the flashpoint. Generally, the experimentation involves a cup holding the liquid to be tested, a way to alter the liquid temperature and an arrangement (flame or electrical wire) to bring an ignition source into the proximity of the vaporizing surface. The cup is either open or closed.

A flash (brief flame) occurs when the liquid has given off sufficient vapours to be ignited. The liquid is then said to have reached its flash point.

Flash point is generally higher for liquids of higher specific gravity. RPAO, whose density is 0.903 g/cm^3 has a higher flash point (310°C) than that of MIO (156°C), whose density is 0.825g/cm^3 .

It is also known to depend on the barometric pressure, the apparatus and experimental procedure used. The open cup flash points are somewhat higher than the closed cup flash points for same substance. This is due to the fact that the closed cup situation is less conducive to the convective and diffusive dispersion of the vapours; therefore, a lean limit mixture is more readily formed in the closed space.

As a general rule for hydrocarbons, the simpler the molecule, the lower the flash point. Hence, higher flash point for RPAO implies that its molecules are more complex as compared to those of MIO. Flash point can also be influenced by presence of impurities. Low flash point for EVPAO implies that it had high concentration of impurities as compared to other samples. This can be confirmed from the sludge results

obtained for the samples. EVPAO has the highest sludge content as presented elsewhere in this thesis.

4.5.2 Pour Point

The pour point of a sample is the lowest temperature at which the flow of the test sample is observed under standard test conditions.

Table 4.13: Pour point results for RPAO, EVPAO and MIO.

Samples	Pour Point, °C	IEEE C57.147 Std, (°C) (Max)	IEEE C57.106 Std, (°C) (Max)	IS.335. (1993) Std, (°C) (Max)
RPAO	-7	-10	-	-
EVPAO	-4	-10	-	-
MIO	-31	-	-40	- 6

As mentioned elsewhere, the pour point is the temperature at which no flow of oil is visible. It represents a consistent temperature at which the liquid will pour very slowly.

Natural oils have lower pour point temperatures as compared to mineral insulation oils. Pour point depressant additives such as Polymethacrylate (PMA) and Sorbitan Tristearate can be added to the natural oils in case of use in regions that may have winter time. However, they can be used without the low temperature additives in tropical regions (like in Northern and Sub-Saharan Africa).

RPAO and MIO did not meet the IEEE.C57.147 and IEEE.C57.106 requirements respectively as shown in Table 4.13. This implies that PAO may not be used in areas that experience winter seasons, but as noted above, pour point depressant additives can be used.

Pour Point Mechanism in Liquid Dielectrics

As the liquid dielectric gets cooled, energy is released. The attractive forces now draw the molecules close together. The liquid molecules start aligning themselves up to a point where a solid is formed (if further cooling is carried out). If a liquid has a low pour point, this indicates that the attractive forces between its molecules are less strong and thus it will take more time and energy to bring the molecules close to one another. Particles in a solid state are tightly packed together, making it rigid and increasing its resistance to flow.

Light liquid dielectrics with low viscosities will have generally lower pour points. This can be observed from the results obtained. MIO which has density of 0.825g/cm^3 has the lowest pour point. RPAO and EVPAO both with density of 0.903g/cm^3 , have a pour point of -7°C and -4°C respectively. RPAO has a viscosity of 44.46 cSt. EVPAO with the highest viscosity also has the highest pour point (-4°C). MIO, with the lowest viscosity of 10.46cSt has the lowest pour point (-31°C).

Generally, heavy liquid dielectrics such as natural esters have high pour points when compared to mineral insulation oils. These plants based liquid dielectrics consist of fatty acid methyl ester (FAME), a carbon chain which has 14-16 carbon atoms. The congealing points of these fatty acid methyl esters are low. These low points lead to poor low temperature performance. This poor performance hugely influences their utilization in regions that experience winter. The low temperature property can however be improved by use of pour point depressants and branched chain esters. The stability of the liquid dielectric against aggregation is very much dependent on the electrostatic factor, which is governed by the presence of an electrical double layer on the surface of the dispersed particles. The oil soluble additives may create either negative or positive charges on the solid hydrocarbon particles, and this is related to the presence of the electrical double layer. Wax content and molecular weight distribution of the waxes are the primary factors in determining whether a liquid dielectric has high or low pour point.

4.6 Oxidation Stability

Oxidation studies were carried out as per ASTM D2440 –13. These tests were used to assess the amount of acid and sludge products formed in the transformer insulation oil when the oil is tested under standard conditions. The test is used as a control test for checking the consistency of oxidation stability of oil production (Rao, 1996). Oxidation stability is measured by the propensity of oils to form sludge and acid products during oxidation.

4.6.1 Neutralization Value after oxidation

The neutralization value after oxidation is as shown in Table 4.14 and Figure 4.24. RPAO and MIO met the IEEE.Std.C57.147 and IEEE.Std.C57.106 requirements respectively.

Table 4.14: Neutralization Value after oxidation for PAO and MIO.

Sample	Neutralization Value before oxidation, mgKOH/g	Neutralization Value after oxidation, mgKOH/g	IEEE Std. C57.147.20, Max. (mgKOH/g)	IEEE Std. C57.106, Max. (mgKOH/g)	IEEE Std. C57.106, Max. (mgKOH/g)
RPAO	0.073	0.062	0.06	-	-
EVPAO	1.49	0.934	0.06	-	-
MIO	0.013	0.087	-	0.3	0.4

Acidity for MIO increased while it seemed to decrease for both RPAO and EVPAO. This could be due to the basic nature of PAO. PAO, as a plant oil, is not acidic as other plant oils are. Thus, oxidation could only have produced neutral or alkaline solution that may have neutralized the trace acids that remain in the oil after it is processed, hence the reduction in acidity in the tests. The oxidative stability of RPAO and EVPAO can be improved by the addition of anti-oxidants as it has been the case for the existing commercial plant-based dielectrics such as Envirotemp FR3 or ABB BIOTEMP.

4.6.2 Total sludge after oxidation

The total sludge after oxidation is as shown in Table 4.15.

Table 4.15: Total sludge after oxidation for RPAO, EVPAO and MIO.

Samples	Total sludge after oxidation, % by mass	IS.335. (1993) Std
RPAO	0.035	-
EVPAO	0.039	-
MIO	0.047	0.1 (Max)

The total sludge after oxidation met the specified requirements for all the oil samples.

4.7 Accelerated Ageing Studies

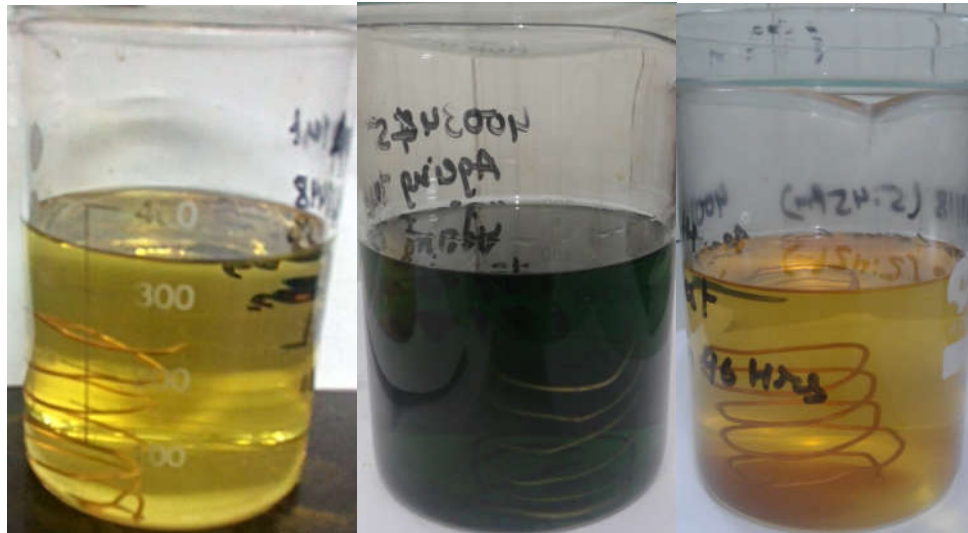
The accelerated ageing studies were carried out as per ASTM D1934-95(2012). Open beaker method with copper catalyst was employed. Tests carried were: Specific Resistivity, TAN Delta, Total Acidity and Total Sludge. These are the tests required for new insulation oil as per IS.335. (1993). At the time of writing this, there are no IEEE standards requirements on open beaker accelerated ageing for new insulation oils hence the use of IS.335. (1993).

4.7.1 Appearance

The appearance of the samples after ageing is as shown in Table 4.16 and Figure 4.15.

Table 4.16: Appearance of samples after ageing for PAO and MIO.

Sample	Appearance	IS.335. (1993)
RPAO	Light yellow liquid	-
EVPAO	Dark green liquid.	-
MIO	Light yellow liquid.	Bright and clear



(a) RPAO

(b) EVPAO

(c) MIO

Figure 4.15: Oil appearance after ageing.

EVPAO dark green colour implies that it was more contaminated by impurities than the rest of the other samples. This is also in direct relation to its water content.

EVPAO had moisture content of 924.71ppm before ageing while RPAO had 136.05ppm. During ageing, water breaks(dissociates) down into its constituent elements and these react with the fatty acids and other molecules present in the oils samples under test to form complex solid compounds. This is reflected by the colour changes. This chemical reaction is well is well described in Chapter 2 under Figure 2.3 and Figure 2.4. These colour changes can well be contrasted with the colours of the fresh oil samples shown in Figure 4.16.

4.7.2 Specific Resistivity

Table 4.17: Specific Resistivity results after accelerated ageing

Sample	Resistivity, ohm-cm, before ageing at 27°C	Resistivity, ohm-cm, before ageing at 90°C	Resistivity, ohm-cm, after ageing at 27°C	Resistivity, ohm-cm after ageing at 90°C
RPAO	7.35×10^{12}	2.56×10^{12}	2.40×10^{12}	0.66×10^{12}
EVPAO	0.28×10^{12}	0.51×10^{12}	0.76×10^{12}	0.29×10^{12}
MIO	0.94×10^{12}	0.48×10^{12}	0.65×10^{12}	0.16×10^{12}

Resistivity of oil varies greatly with temperature of oil. Presence of moisture, acidity and contaminants greatly reduce the oil resistivity. Therefore, during ageing, moisture and acidity increased in the samples since it was open beaker accelerated ageing. Open beaker ageing means the oil samples are exposed directly to air and moisture in the surroundings. Therefore, decreasing resistivity can be an indicator of presence of impurities in the liquid dielectric. It is also worth noting that in all cases, resistivity decreased with increased temperature. For example, for RPAO, resistivity at 27°C is 2.40×10^{12} while at 90°C is, 0.66×10^{12} after ageing. Increased thermal agitation increases the number of free charges available to conduct current.

Except for EVPAO, resistivity decreased after accelerated ageing as shown in Table 4.17 and for all the temperatures considered.

4.7.3 Dielectric dissipation factor (TAN Delta)

RPAO TAN delta increased from 0.33 to 1.35. EVPAO increased from 1.86 to 4.51 while MIO had increment from 0.26 to 0.82. EVPAO seemed to have the greatest TAN delta increment of all the samples as shown in table 4.18. This could be attributed to the presence of impurities and solid contaminants.

Table 4.18: Dielectric dissipation factor results after accelerated ageing

Sample	TAN Delta at 90°C before accelerated ageing	TAN Delta at 90°C after accelerated ageing.	IS.335. (1993), (%Max)	IEEE C.57.147, (%Max)
RPAO	0.33	1.35	-	4.0
EVPAO	1.86	4.51	-	4.0
MIO	0.26	0.82	0.20	-

4.7.4 Total Acidity

As shown in Table 4.19 the MIO acidity increased from 0.013mg KOH/g to 0.11mg KOH/g as expected while that for the RPAO and EVPAO seem to have decreased with the accelerated ageing (open beaker method with copper catalyst). The trace acids that remain after oil processing seem to have contributed to the initial high acidity. These may have reacted with air and moisture to form neutral compounds under thermal stress. PAO is also not acidic in nature and this may explain the decreased acidity after ageing. Acidity of oil is expected to slowly increase with ageing of transformer oil.

Table 4.19: Total Acidity results after accelerated ageing for RPAO, EVPAO and MIO.

Sample	Total Acidity, mg KOH/g before accelerated ageing	Total Acidity, mg KOH/g after accelerated ageing	IS.335. (1993), (Max) mgKOH/g
RPAO	0.073	0.033	-
EVPAO	1.49	0.44	-
MIO	0.013	0.11	0.05

The acidity of insulating fluid can be increased by thermal degradation of the fluid. This is because oxidation products are often acidic in nature. Two general types of

acids are formed during the ageing of insulation oils. They are low molecular weight acids (LMWA) and high molecular weight acids (HMWA). Presence of LMWAs lowers the flash point of the oil. Presence of HMWAs leads to reaction with the bulk oil which results in sludge and varnish deposits formation [86].

4.7.5 Total Sludge, % by mass

Table 4.20 Total Sludge after accelerated ageing for PAO and MIO.

Samples	Total sludge after oxidation, % by mass	IS.335. (1993), % by mass. (Max)
RPAO	0.046	-
EVPAO	0.069	-
MIO	0.036	0.05

As shown in Table 4.20, the total sludge, % by mass for RPAO and MIO samples seemed to meet the requirements by IS: 12177-1987 of 0.05% maximum for MIO.

Of the three samples tested, EVPAO had the highest sludge content at 0.069 while MIO had the lowest sludge content at 0.036. This implies that EVPAO may have been waxy and that its molecular weight was higher than that of MIO. The results also imply that there is a relationship between the pour point and the sludge content. For example, EVPAO had a pour point of -4°C while MIO had a pour point of -31°C . Low pour point is a predictor of low sludge content. Higher pour liquid dielectrics are waxy and thus tend to form substances that enhance sludge formation. It should be noted that presence of sludge in the liquid dielectric primarily interferes with its cooling and insulation mechanisms. All the samples tested had sludge content that satisfied the IS.335 (1993) standard except the EVPAO.

Summary of the results obtained is shown in Table 4.21(Makaa, Irungu & Murage, 2019).

Table 4.21. Summary of Test Results

Property	Test Method	RPAO	EVPAO	MIO
Appearance	ASTM D1500	Clear and transparent	With suspended sediments	Clear and transparent
Interfacial tension(mN/m)	ASTM D971	48	51	46
Relative Density at 15°C [g/cm ³]	ASTM D1298	0.903	0.903	0.825
Flash Point, °C	ASTM D93 - 18	310	142	156
Pour Point, °C	ASTM D97	-7	-4	-31
Viscosity Test @ 27 °C, cSt	ASTM D 445-17a	45.66	52.03	10.46
Viscosity Test @ 40 °C, cSt	ASTM D 445-17a	35.58	38.54	8.15
Water Content, (ppm)	ASTM D1533	136.05	924.71	30.88
Neutralization Number (NN) mg KOH/g	ASTM D974 - 14e2	0.073	1.49	0.013
Resistivity (at 27°C), ohm-cm)	ASTM D1169-64	7.35x10 ¹²	0.28x10 ¹²	0.94x10 ¹²
Resistivity (at 90°C), ohm-cm	ASTM D1169-64	2.56x10 ¹²	0.51x10 ¹²	0.48x10 ¹²
Breakdown Voltage (BDV)(kV)	ASTM D 1816 (a)/IEC 60156	74	36	65
Dielectric Dissipation Factor (DDF) at 100°	ASTM Std. D 924	0.33	1.86	0.26

CHAPTER FIVE

CONCLUSIONS AND RECOMMENDATIONS

5.1 Conclusion

The work presented in this thesis was an experimental research to investigate *Persea americana* oil as an alternative transformer insulation oil. The research objectives were achieved by carrying out a series of experiments on the electrical, physical, thermal and chemical properties of food grade *Persea americana* oil. The key contribution of this research is establishing through experimental investigation and analysis of the electrical, physical, chemical and thermal properties of *Persea americana* oil that PAO properties satisfy the IEEE Standard C57.147 (2018) in general.

The research shows that the average AC breakdown voltage (BDV) of RPAO is 74kV while the BDV of EVPAO is 36kV and that of MIO is 65kV. It was also observed that the average BDV of a mixture of RPAO and MIO is lower than that of RPAO but higher than that of MIO. The statistical analysis of the electrical breakdown data shows that the characteristic breakdown field of the RPAO is more consistent with a higher predictable breakdown field for low probability of breakdown failure. RPAO has higher resistivity than EVPAO and MIO.

The research also shows that Extra Virgin PAO, obtained from cold pressing has high viscosity and acidity as compared to RPAO. The performed corrosion test basing on ASTM D130 using copper strip shows that MIO, RPAO & EVPAO are non-corrosive and they have 1A ASTM class. The high temperature thermal results show that the RPAO & EVPAO possesses flash point that is above the specified minimum. RPAO flash point is the highest of all the samples tested. RPAO flash point is 310⁰C, EVPAO 142⁰C while MIO⁰C flash point is 156⁰C. The Pour point does not comply with the IEEE standard C.57.147-2018 of -10⁰C.

RPAO point is -7⁰C while pour point for EVPAO is -4⁰C. Additives can be used to decrease it. The oil can be used in temperate regions. The flash point (-310⁰C) meets value required by the standard.

The research also shows that ageing has a significant negative effect on the properties of the oil samples. Resistivity was found to decrease with ageing for RPAO and MIO. Dielectric dissipation factor increased after ageing for all samples. Acidity for MIO increased while it decreased for both RPAO and EVPAO. Sludge test results satisfied IS.335. (1993) requirements for all samples considered. The aged RPAO, EVPAO and MIO changed colours. RPAO and EVPAO acidities reduced with the accelerated ageing. The research shows that the physicochemical properties of RPAO such as visual examination, color and corrosivity are appropriate to the value required by C.57.147-2018 standard.

Based on the results of this research, it can be concluded that PAO could be a potential replacement for mineral insulation oil for electrical insulation, especially in power transformers(69kV). In conclusion, the set objectives of this research were achieved. The properties of PAO suggest that the PAO can be adopted as an alternative transformer insulation oil. PAO may now require a development stage for testing and adoption by electrical distribution companies.

5.2 Limitations

There was time limitation as the experiments were carried out at Sigma Research and Test Centre, in Delhi, India. Hence very long term accelerated ageing was not possible. The one employed was open beaker accelerated ageing at 115⁰C for 96 hours as allowed for new insulating liquids while oxidation tests were carried out after subjecting the oil samples to a temperature of 70⁰C for a period of 164 hours. As well, a single temperature accelerated ageing test was performed. Ageing test for the suitability of the oil in closed system was not performed due to time limit (may take about at least one year) and also due to lack of equipment to carry out the test. The presence of the impurities was suspected to affect flash point and thermo-oxidative stability of the PAO samples.

5.3 Recommendations and Further Research

The research work presented in this thesis focused on exploring the suitability of *Persea americana* oil as an alternative transformer insulation oil. This was

accomplished through performing various tests to investigate its properties. Though most of the properties were comparable to those of mineral insulation oil and the outcome look promising and therefore further work is needed to firmly establish its applicability.

Some of the areas that need consideration are;

- a) Effect of ageing on the PAO-paper insulation system. This is important so as to establish how PAO properties change in a practical composite transformer insulation system. This is because high or medium voltage insulation systems are usually a combination of solid /liquid. This can be carried out for considerable period of time, say 5 years or more.
- b) Creeping discharges characteristics over pressboard immersed in PAO under lightning impulse voltage. Study of the characteristics of creeping discharges over pressboard immersed in the PAO may be important for the design and optimization of the size of high-voltage equipment.
- c) Ageing test under a hermitically closed system to be carried out for the suitability of the oil in such systems. Study of the aged samples by dissolved gas analysis is also important.

REFERENCES

- ABB Brochure (2011). BIOTEMP® dielectric insulating fluid. Zürich: ABB.
- Abdelmalik A.A. 2012. *The Feasibility of Using a Vegetable Oil-Based Fluid as Electrical Insulating Oil*. Unpublished PhD Thesis, University of Leicester.
- Abeyesundara, D.C., Weerakoon, C., Lucas, J R, Gunatunga, K.A.I., Obadage, K.C. (2001). Coconut Oil as an Alternative to Transformer Oil. *ERU Symposium*. Moratuwa: University of Moratuwa.
- Abdullahi, U., Bashi, S., Yunus, R., Mohibullah, & Nurdin, H. (2004). The potentials of palm oil as a dielectric fluid. PECon 2004. *Proceedings of National Power and Energy Conference* (pp 224-228). Piscataway, NJ: IEEE.
- Al-Eshaikh, M. A. & Qureshi, M. I. (2012). Evaluation of Food Grade Corn Oil for Electrical Applications. *International Journal of Green Energy*, 9(5), pp 441-455, DOI: 10.1080/15435075.2011.641186.
- Amanullah, M. (2005). Analysis of electro-chemical characteristics of vegetable oils as an alternative source to mineral based dielectric fluid. *Fourteenth International Conference and Breakdown in Dielectric Liquid* (pp. 201–4). Coinara, Portugal: IEEE.
- Morton, J (1987). Avocado oil: *Persea Americana*. Retrieved 2018-10-18 from https://hort.purdue.edu/newcrop/morton/avocado_ars.html
- ASTM D1169-64 (2011). Standard Test Method for Specific Resistance (Resistivity) of Electrical Insulating Liquids. West Conshohocken: ASTM International.
- ASTM D130-12 (2012). Standard Test Method for Corrosiveness to Copper from Petroleum Products by Copper Strip Test. West Conshohocken: ASTM International.

ASTM D1500 (2007), Standard Test Method for ASTM Color of Petroleum Products (ASTM Color Scale). West Conshohocken: ASTM International.

ASTM D1934 – 95 (2012). Standard Test Method for Oxidative Ageing of Electrical Insulating Petroleum Oils by Open-Beaker Method. ASTM International.

ASTM D 2440 – 13 (2013). Standard Test Method for Oxidation Stability of Mineral Insulating Oil. West Conshohocken: ASTM International.

ASTM D4052-18(2018). Standard Test Method for Density and Relative Density of Liquids by Digital Density Meter. West Conshohocken: ASTM International.

ASTM D445 – 17a (2017). Standard Test Method for Kinematic Viscosity of Transparent and Opaque Liquids (and Calculation of Dynamic Viscosity). West Conshohocken: ASTM International.

ASTM D6304 –16(2016). Standard Test Method for Determination of Water in Petroleum Products, Lubricating Oils, and Additives by Coulometric Karl Fischer Titration. West Conshohocken: ASTM International.

ASTM D93 – 18(2018). Standard Test Method for Corrosiveness to Copper from Petroleum Products by Copper Strip Test. West Conshohocken: ASTM International.

ASTM D 924 – 03a (2003). Standard Test Method for Dissipation Factor (or Power Factor) and Relative Permittivity (Dielectric Constant) of Electrical Insulating Liquids. West Conshohocken: ASTM International.

ASTM D97 – 05(2005). Standard Test Method for Pour Point of Petroleum Products. West Conshohocken: ASTM International.

ASTM D 971(2012). Test method for interfacial tension of oil against water by the ring method. West Conshohocken: ASTM International.

Belanger, M., (1999). Transformer diagnosis: Part 1: A statistical justification for preventative maintenance. *Electricity Today*, 11(6) 5-8.

- Boubakeur, A., Boubakeur, M., Boumerzoug, M. (1999). Influence of continuous thermal ageing on the properties of XLPE used in medium voltage cables. *11th International Symposium on High Voltage Engineering, ISH'99* (pp280), London, United Kingdom.
- Cigre working group. (2010). A2.35, Experience in Service with New Insulating Liquids. Cigre Brochure 436.
- Ciuriuc, A.M., Vihacencu, S., Dumitran, L. M., & Notingher, P. V. (2012). Comparative study on power transformers vegetable and mineral oil ageing. *International Conference on Applied and Theoretical Electricity* (pp. 1-6). Craiova.
- Darveniza, M., Saha T. K., Hill, D. J. T. & Le, T. T. (1998). Investigations into effective methods for assessing the condition of insulation in aged power transformers. *Transactions on Power Delivery*, 13(4) , 1214-1223.doi: 10.1109/61.714487.
- Dang, V.H, Beroual, A. & Perrier C. (2012). Comparative study of statistical breakdown in mineral, synthetic and natural ester oils under AC voltage. *IEEE Trans. Dielectrics and Electrical Insulation*, 19(5), 1508-1513.
- Daily Nation. (2018). *What avocado export market wants from you?* Retrieved March 3, 2018 from <https://www.nation.co.ke/business/seedsforgold/What-avocado-export-market-wants-from-you/2301238-4172194-h78exr/index.html>
- Darma, S, I. S. (2008). Dielectric Properties of Mixtures between Mineral Oil and Natural Ester. *Proceedings of 2008 International Symposium on Electrical Insulating Materials*. Yokkaichi, Mie, Japan.
- Dissado L.A., & Fothergill, J.C. (1992). Electrical degradation and breakdown in polymers. *IEE*.

- Dung.N. V., Hoidalen. K., Linhjell.D., Lundgaard. E., and Unge. (2012). A study on positive streamer channels in Marcol Oil. *2012 Annual Report Conference on Electrical Insulation and Dielectric Phenomena (CEIDP)* (pp. 365–370).
- El-Refaie M.M.E., Salem, M.R., and Ahmed, W.A. (2009). Prediction of the Characteristics of Transformer Oil under Different Operation Conditions. *World Academy of Science, Engineering and Technology*, 53, pp 764-768.
- Endah, Y., (2010). *Analysis of Dielectric Properties Comparison between Mineral Oil and Synthetic Ester Oil*. Unpublished Master Thesis. Delft University of Technology.
- Erhan, S. Z., Adhvaryu A. & Liu, Z., (2002). Chemical Modified Vegetable Oil-Based Industrial Fluid. *US Patent US 6,583,302 B1*.
- Ferguson., Lobeiras, A., & Sabau, J. (2002) Suspended Particles in liquid insulation of ageing transformers”. *IEEE Electrical Insulation Magazine*, 18(4), 17-23.
- Fofana, I., Borsi, H., Gockenbach, E. and Farzaneh, M. (2007). Ageing of transformer insulating materials under selective conditions. *European. Transactions on. Electrical. Power*, 17, pp 450-470. doi:10.1002/etep.134.
- Fosana, I., Wasserberg, Borsi, V, H. & Gockenbach, E. (2002). Challenge of mixed insulating liquids for use in high-voltage transformers. *IEE Electrical insulation magazine*, 18(4), pp 5-16.
- Fox, N. J. & Stachowiak, G. W. (2007). Vegetable oil-based lubricants—A review of oxidation. *Tribology International*, 40, pp. 1035-1046.
- Gnanasekaran. D. & Chavidi V. P. (2018). *Vegetable Oil based Bio-lubricants and Transformer Fluids Applications in Power Plants* (1st ed). Singapore: Springer Singapore.
- Gnanasekaran. D. & Chavidi V. P. (2018). Properties of Vegetable Fluids: A Green Insulator for Power Sector. In *Vegetable Oil based Bio-lubricants and*

Transformer Fluids Applications in Power Plants (1st ed). Singapore: Springer Singapore. pp. 133–158.

Hemmer, M., Badan R., & Schwab, A. J. (2002). Electrical properties of rapeseed oil. *Annual Report CEIDP* (pp. 83–6). Lancurn, Mexico: CEIDP.

Heathcote. J. (2007). Basic Materials, in *J and P Transformer Book - A Practical Technology of the Power Transformer* (13th Ed). London: Elsevier.

Hikosaka, T., Hatta, Y., Koide, H., Yamazaki, A. & Kanoh, T. (2007). Basic characteristics of Environment-conscious Transformers Impregnated with Oil Palm Fatty Acid Ester (PFAE). *15th International Symposium on High Voltage Engineering, T8-13*.

Hosier, I. L., Rogers C., Vaughan, A. A., & Swindler S. G. (2010). Ageing behavior of vegetable oil blends. *Annual Report, Conference on Electrical Insulation and Dielectric Phenomena*, (pp. 1–4). West Lafayette, IN.

Husnayain, F., Latif, M. & Garniwa, I. (2015). Transformer oil lifetime prediction using the Arrhenius law based on physical and electrical characteristics. *2015 International Conference on Quality in Research (QiR)*, pp. 115-120. Lombok: 10.1109/QiR.2015.7374908.

Hussain, K. & Karmakar, S. (2014). Condition assessment of transformer oil using UV-Visible spectroscopy. *2014 Eighteenth National Power Systems Conference (NPSC)*, (pp. 1-5).

IEC 60156 Standard (2018). *Insulating Liquids – Determination of the Breakdown Voltage at Power Frequency – Test Method*. Geneva: International Electrotechnical Commission.

IEC 60897 Standard, (1987). *Method for the determination of the lightning impulse breakdown voltage of insulating liquids*. Geneva: International Electrotechnical Commission.

- IEC Std. 61099(2010). *Insulating liquids - Specifications for unused synthetic organic esters for electrical purposes*. Geneva: International Electrotechnical Commission.
- IEC Std. 61203(1992). *Synthetic organic esters for electrical purposes - Guide for maintenance of transformer esters in equipment"*. Geneva: International Electrotechnical Commission.
- IEC 62539(2007). *Guide for the statistical analysis of electrical insulation breakdown data*. Geneva: International Electrotechnical Commission.
- IEEE Standard 4, (2013). *IEEE Standard Techniques for High voltage Testing*. New Jersey: Institute of Electrical and Electronics Engineers.
- IEEE Standard C57.106(2015). *IEEE Guide for Acceptance and Maintenance of Insulating Oil in Equipment*. New Jersey: Institute of Electrical and Electronics Engineers.
- IEEE Standard. C57.147(2018). *IEEE Guide for Acceptance and Maintenance of Natural Ester Fluids in Transformers*. New Jersey: Institute of Electrical and Electronics Engineers.
- IEEE Std C57.91(2011). *IEEE Guide for Loading Mineral-Oil Immersed Transformers*. New Jersey: Institute of Electrical and Electronics Engineers.
- IEEE Std. 62-(1995). *IEEE Guide for Diagnostic Field Testing of Electric Power Apparatus -Part 1: Oil Filled Power Transformers, Regulators, and Reactors*. New Jersey: Institute of Electrical and Electronics Engineers.
- IEEE C57.100(1986). *IEEE Standard Test Procedure for Thermal Evaluation of Oil-Immersed Distribution Transformers*. New Jersey: Institute of Electrical and Electronics Engineers.
- Jing, Y., Timoshkin, I. V., Wilson, M. P., Given, M. J. Given, MacGregor S. J., & Wang, T. (2014). Dielectric properties of natural Ester, synthetic ester midel

7131 and mineral oil Diala D. *IEEE Transactions on Dielectrics and Electrical Insulation*, 21(2), pp. 644 - 652.

Kadam & Salunkhe (1995). Avocado in Handbook of Fruit Science and Technology. Production, Composition, Storage, and Processing, pp: 363-375. New York: Marcel Dekker, Inc,

Kanoh, T., Iwabuchi H., Hoshida., Yamada, J., Hikosaka, T., Hatta, A., Koide, H. (2008). Analyses of Electro-Chemical Characteristics of Palm Fatty Acid Esters as Insulating Oil. *IEEE Transactions on Dielectric Insulation*, pp.307-310.

Kazmierski, M., Sobocki, R., & Olech, W. (1998). Selected elements of life management of large transformers- A polish experience. *International Council on Large Electric Systems (CIGRE)*. Paris, France: CIGRE.

Koch, M., Krueger, M., & Puetter, M. (2009). Advanced insulation diagnostic by dielectric Spectroscopy. *Asia Pacific Technical conference*. Sydney, Australia.

Koreh, O., Torkos., Mahara, M. B & Borossay, J. (1998). Study of water clusters in insulating oils by Fourier transform infrared spectroscopy. *IEEE Transactions on Dielectrics and Electrical Insulation*, 5(6) 896-901.

Martin, D., and Wang, Z. D. (2008) Statistical analysis of the AC breakdown voltages of ester-based transformer oil. *IEEE Transactions on Dielectric and Electrical Insulation*, 15 (1),1044–50.

Makaa, B.M., Irungu, G.K & Murage D.K (2019). Electrical and Physicochemical Properties of Persea Americana Oil as an Alternative Transformer Insulation Oil. *IEEE SAUPEC/RobMech/PRASA 2019 Conference Proceedings*, (247-253). Bloemfontein, South Africa: IEEE.

Massey B., Ward-Smith J., (2006). *Mechanics of Fluids (8th Ed)*, Oxfordshire: Taylor and Francis.

- McShane, C.P, (2001). Relative Properties of the New Combustion-Resistant Vegetable-Oil-Based Dielectric Coolants for Distribution and Power Transformers. *IEEE Transactions on Industry Applications*, 37(4), 1132 – 1139.
- Milledge. M. P. T. (2011). Introduction to BIOTEMP. The superior, biodegradable, high fire point, dielectric insulating fluid. *ABB seminar presentation*. Canberra: ABB.
- Moore, S. P., Wangard, W., Rapp, K. J., Woods, D. L., & Del Vecchio R. M. (2015). Cold Start of a 240-MVA Generator Step-Up Transformer Filled with Natural Ester Fluid. *IEEE Transactions on Power Delivery*, 30,256-263.
- Mooz, E. D, Gaino, N.M, Shimano, M.Y.H., Amancio. D, Spoto, M.H.F. (2012). *Physical and chemical characterization of the pulp of different varieties of avocado targeting oil extraction potential*. Retrieved March 18,2019 from <http://dx.doi.org/10.1590/S0101-20612012005000055>.
- Naranpanawe, W.M.L.B., Fernando, M.A.R.M., Kumara, J.R.S.S., Naramapanawa, E.M.S.N.& Kalpage, C.S. (2013). Performance Analysis of Natural Esters as Transformer Liquid Insulation – Coconut, Castor and Sesame oils .*2013 IEEE 8th International Conference on Industrial and Information Systems*. Colombo: IEEE.
- Oommen, T. V. (2002). Vegetable oils for liquid-filled transformers. *IEEE Electrical Insulation Magazine* 18 (1),6–11.
- Rafiq, M., Zhou Y., Ma, K., Wang, W., Li, C., & Wang, Q., (2015). Use of vegetable oils as transformer oils – a review. *Renewable and Sustainable Energy Reviews*, 52, 308–324.
- Rao, T.O.B. (1996). Relevance of transformer oil testing to its field performance. *ITMA Journal*, 15-37.

- Rapp K.J., McShane C.P., & Luksich, J., (2005). Interaction Mechanisms of Natural Ester Dielectric Fluid and Kraft Paper. *Proceedings of 15th IEEE International Conference on Dielectric Liquids (ICDL)*, Coimbra: IEEE.
- Rooney, D. & Weatherley, L. R. (2001). The effect of reaction conditions upon lipase catalyzed hydrolysis of high oleate sunflower oil in a stirred liquid–liquid reactor. *Journal of Process Biochemistry*, 36, 947-953.
- Rongsheng, L., Tornkvist, C., Chandramouli ,V., Girlanda ,O., & Pettersson ,L. A. A.(2009). Ester fluids as alternative for mineral oil: The difference in streamer velocity and LI breakdown voltage. *IEEE conference on Electrical Insulation and Dielectric Phenomena*, ,543-548. Virginia Beach. IEEE.
- Rouse, T. O. (1998). Mineral insulating oil in transformers. *IEEE Electrical Insulation Magazine*, 14(3), 6-16.
- Saha, K, Hilli, D.J.T., Le, T.T. Investigations into effective methods for assessing the condition of insulation in aged transformers. *IEEE Transactions on power delivery*, 13(4), 1214-1222.
- Schäfer, M., Höhle I. A-, R. Fritsche, C. Schmeid. (2014). Use of Natural Esters in Power Transformers – Operation Experiences and State of the Art. *Stuttgarter Hochspannungs symposium*. Filderstadt.
- Sharma, B. K., Liu, Z., Adhvaryu, A., & Erhan, S. Z., (2008), One-Pot Synthesis of Chemically Modified Vegetable Oils, *J. Ag. Food Chem.* 56, 3049-3056.
- Shapiro, S. S. & Wilk, M. B (1965). An analysis of variance test for normality (complete samples). *Biometrika*, 52(4), 591-611.
- Sitinjak, S, Suhariadi, F., I., & Imsak, L. (2003). Study on the characteristics of palm oil and its derivatives as liquid insulating materials", *IEEE 7th Int'l. Conf. Properties and Applications of Dielectric Materials*, 2, 495-498.

- Tango, J.S.T., Carvalho, C.R.L., Soares, N.B. (2004). Physical and chemical characterization of avocado fruits aiming its potential for oil extraction. *Revista Brasileira de Fruticultura*, 26(1).
- Tenbohlen, S. & Koch, M., (2010). Ageing Performance and Moisture Solubility of Vegetable Oils for Power Transformers. *IEEE Transactions on Power Delivery*, 25, 825-830.
- Wilhelm, H. M., Tulio, L., Jasinski, R., & Almeida, G. (2012). Ageing markers for in-service natural ester-based insulating fluids. *IEEE Transactions on Dielectrics and Electrical Insulation*, 18, 714-719.
- Wong, M, Jackman, C. R., & Woolf. A (2018). *What is unrefined, extra virgin cold-pressed avocado oil?* Retrieved October 10,2018 from <https://www.aocs.org/stay-informed/read-inform/featured-articles/what-is-unrefined-extra-virgin-cold-pressed-avocado-oil-april-2010>.

APPENDICES

Appendix I: Test Limits for New Insulating Mineral Oil as per IEEE Std C57.106-2015.

Table AI: Test limits for new insulating mineral oil as per IEEE Std C57.106-2015.

Test and method	Limit value
Dielectric breakdown voltage	
ASTM D1816	
kV minimum	
1 mm gap	20
2 mm gap	35
Dissipation factor (power factor)	
ASTM D924	
25 °C, % maximum	0.05
100 °C, % maximum	0.30
Interfacial tension	
ASTM D971: mN/m minimum	40
Color	
ASTM D1500	
ASTM units(maximum)	0.5
Visual examination:	
ASTM D1524	Bright and clear
Neutralization number (acidity)	
ASTM D974 Mg KOH/g maximum	0.03
Water content	
ASTM D1533 Mg/kg maximum	35
Oxidation inhibitor content when specified	
ASTM D2668	
Type I oil, % maximum	0.08
Type II oil, % maximum	0.3
Corrosive sulfur	
ASTM D1275	Noncorrosive
Relative density (specific gravity)	
ASTM D1298	
15 °C maximum	0.91

Appendix II: Test limits for New Natural Ester Insulating Liquid as per IEEE Std C57.147-2018

Table AII: Test limits for new Natural Ester Insulating Liquid as per IEEE Std C57.147-2018

Test and ASTM method	Results	
	Minimum	Maximum
Flash point, ASTM D92, °C	275	—
Fire point, ASTM D92, °C	300	—
Kinematic viscosity, ASTM D445, mm ² /s (cSt)		
0 °C	—	500
40 °C		50
100 °C		15
Pour point, ASTM D97, D5949, D5950; °C	—	-10
Color, ASTM D1500	—	L1.0
Relative density ASTM D1298, at 25 °C	—	0.96
Corrosive Sulfur, ASTM D1275	—	non-corrosive
Neutralization number, ASTM D974, mgKOH/g	—	0.06
Water content, ASTM D1533, mg/kg at 20 °C	—	200
Dielectric breakdown, ASTM D1816		
kV (1 mm gap)	20	—
kV (2 mm gap)	35	
Dissipation factor, ASTM D924, %		
25 °C	—	0.20
100 °C		4.0

Appendix III: Indian Standard (IS335-1993)

Table AIII: Indian Standard-IS335-1993.

S.NO	Characteristics	Requirement IS:335-1993
1.	Appearance	The oil shall be clear and transparent and free from suspended matter or sediments
2.	Density at 29.5°C, g/cm ³	0.89 Max
3.	Kinematic Viscosity, cSt	
	At 27°C	27 Max
	At 40°C	-
4.	Interfacial Tension (at 27°C), N/m	0.04 Min
5.	Flash Point (PMCC), °C	140 Min
6.	Pour Point, °C	- 6 Max
7.	Neutralization Value	
	Total Acidity, mg KOH/gm.	0.3 Max
8.	Corrosive Sulphur	Non-Corrosive
9.	Break Down Voltage (KV)	
	Frequency of test voltage: 40Hz to 60Hz. Electrode gap=2.5mm ± 0.05mm)	30 (Min)
10.	TAN Delta (Dielectric dissipation factor at 90°C & 40 Hz to 60 Hz)	0.002 Max
11.	Specific Resistivity, ohm-cm	
	At 90°C	35 x 10 ¹² (Min)
	At 27°C.	1500 x 10 ¹² (Min)
12.	Oxidation stability	
a)	Neutralization Value after oxidation, mgKOH/g	0.4 Max
b)	Total sludge after oxidation, % by mass	0.1 Max
13.	Ageing characteristics after accelerated ageing (open beaker method with copper catalyst)	
a)	Specific Resistivity), ohm-cm	
	At 90°C	0.2 x 10 ¹² Min
	At 27°C	2.5 x 10 ¹² Min
b)	TAN Delta (Dielectric dissipation factor at 90°C & 40 Hz to 60 Hz)	0.20 Max
c)	Total Acidity, mg KOH/gm.	0.05 Max
d)	Total Sludge, % by mass	0.05 Max

Appendix IV: Breakdown Voltage (kV)**Table IV. Breakdown Voltage Raw Data.**

Tests(N)	RPAO	EVPAO	MIO	RPAO+MIO	EVPAO+MIO
1	72.460	34.500	62.96	65.560	25.220
2	72.870	34.720	63.5	65.990	25.410
3	73.290	34.970	63.9	66.210	25.500
4	73.340	35.110	64.11	66.240	25.820
5	73.520	35.600	64.38	66.470	26.240
6	73.850	35.900	64.96	66.760	26.580
7	73.960	36.210	65.12	66.890	26.610
8	74.300	36.100	65.21	67.010	26.780
9	74.340	36.270	66.27	67.120	26.830
10	74.120	36.400	66.29	67.890	26.960

Appendix V: Density**A. RPAO**

Weight of empty pycnometer=72.22g

Weight of sample +pycnometer=117.36g

Volume of pycnometer=50ml or 50cm³

$$\text{Density} = \frac{\text{Mass}}{\text{Volume}}$$

$$\text{Density at } 29.5^{\circ}\text{C} = \frac{117.36 - 72.22}{50} = 0.903\text{g/cm}^3$$

B. EVPAO

Weight of empty pycnometer=32.6640g

Weight of sample +pycnometer=79.1431g

Volume of pycnometer=50ml or 50cm³

$$\text{Density} = \frac{\text{Mass}}{\text{Volume}}$$

$$\text{Density at } 29.5^{\circ}\text{C} = \frac{79.1431 - 32.6640}{50} = 0.903\text{g/cm}^3$$

C.MIO

Weight of empty pycnometer=72.22g

Weight of sample +pycnometer=113.45g

Volume of pycnometer=50ml or 50cm³

$$\text{Density} = \frac{\text{Mass}}{\text{Volume}}$$

$$\text{Density at } 29.5^{\circ}\text{C} = \frac{113.45 - 72.22}{50} = 0.825\text{g/cm}^3$$

Appendix VI: Kinematic Viscosity, cSt

A. RPAO

1. at 27⁰C

Tube size Number =6 P/7587

Tube factor=0.96349

Time=47.39 sec

Kinematic Viscosity at 27⁰C=47.39 × 0.93649 =45.66cST

2. at 40⁰C

Tube size Number =6 P/7587

Tube factor=096349

Time=36.93 sec

Kinematic Viscosity at 27⁰C=36.93 × 0.93649

=35.58cST

B. EVPAO

1. at 27⁰C

Tube size Number =6 P/7587

Tube factor=0.96349

Time=54 sec

Kinematic Viscosity at 27⁰C=54 × 0.93649 =52.03cST

2. at 40⁰C

Tube size Number =6 P/7587

Tube factor=096349

Time=40 sec

Kinematic Viscosity at 27⁰C=54 × 0.96349=52.03cST

C.MIO

1. at 27⁰C

Tube size Number =6 P/7587

Tube factor=096349

Time=10.86 sec

Kinematic Viscosity at 27⁰C=10.86 × 0.93649 =10.46cST

2. at 40⁰C

Tube size Number =6 P/7587

Tube factor=0.96349

Time=8.46 sec

Kinematic Viscosity at 27⁰C=8.46 × 0.93649 =8.15cST

Appendix VII: Interfacial Tension

A. RPAO

Average value, mN/m, 48, 48, 48=48mN/m=0.048N/m

$$\begin{aligned} \text{Average value,} &= \frac{48 + 48 + 48}{3} = 48\text{mN/m} \\ &= 0.048\text{N/m} \end{aligned}$$

B. EVPAO

Average value, mN/m, 51, 51, 51

$$\begin{aligned} \text{Average value,} &= \frac{51 + 51 + 51}{3} = 51\text{mN/m} \\ &= 0.051\text{N/m} \end{aligned}$$

C. MIO

Average value, mN/m, 46, 46, 46.

$$\begin{aligned} \text{Average value,} &= \frac{46 + 46 + 46}{3} = 46\text{mN/m} \\ &= 0.046\text{N/m} \end{aligned}$$

Appendix VIII: Neutralization Value

A. RPAO

Weight of sample=8.55g

Volume of alc.KOH consumed in blank=0.4ml

Volume of alc.KOH consumed in sample=1.1ml

Normality of alc.KOH =0.016N

$$\begin{aligned} \text{Total Acidity, mgKOH} &= \frac{(1.1 - 0.4) \times 56.1 \times 0.016}{8.55} \\ &= 0.073\text{mgKOH/g} \end{aligned}$$

B. EVPAO

Weight of sample=9.95g

Volume of alc.KOH consumed in blank=1.1ml

Volume of alc.KOH consumed in sample=17.6ml

Normality of alc.KOH =0.016N

$$\begin{aligned} \text{Total Acidity, mgKOH} &= \frac{(17.6 - 1.1) \times 56.1 \times 0.016}{9.95} \\ &= 1.49 \text{ mgKOH/g} \end{aligned}$$

C.MIO

Weight of sample=11.09g

Volume of alc.KOH consumed in blank=0.4ml

Volume of alc.KOH consumed in sample=0.56ml

Normality of alc.KOH =0.016N

$$\begin{aligned} \text{Total Acidity, mgKOH} &= \frac{(1.3 - 0.4) \times 56.1 \times 0.016}{11.09} \\ &= 0.013 \text{ mgKOH/g} \end{aligned}$$

Appendix IX: Specific Resistivity, ohm-cm

A.RPAO

At 90°C

Instrument reading=40.8x 10²

Cell constant=629 x10⁶

Specific Resistivity (at 90⁰C), ohm-cm=40.8x10²x629x10⁶

=2.56x10¹²ohm-cm

At 27°C

Instrument reading=11.7x 10³

Cell constant=629 x10⁶

Specific Resistivity (at 27⁰C), ohm-cm=11.7x10³x629x10⁶

=7.35x10¹²ohm-cm

B. EVPAO

At 90°C

Instrument reading = 76.6×10^1

Cell constant = 629

Specific Resistivity (at 90°C), ohm-cm = $76.6 \times 10^1 \times 629 \times 10^6$

= 0.48×10^{12} ohm-cm

At 27°C

Instrument reading = 8044.8×10^1

Cell constant = 629

Specific Resistivity (at 27°C), ohm-cm = $44.8 \times 10^1 \times 629 \times 10^6$

= 0.28×10^{12} ohm-cm

C. MIO

At 90°C

Instrument reading = 76.6×10^1

Cell constant = 629

Specific Resistivity (at 90°C), ohm-cm = $76.6 \times 10^1 \times 629 \times 10^6$

= 0.48×10^{12} ohm-cm

At 27°C

Instrument reading = 14.9×10^2

Cell constant = 629

Specific Resistivity (at 27°C), ohm-cm = $76.6 \times 10^1 \times 629 \times 10^6$

= 0.94×10^{12} ohm-cm

D. RPAO+MIO

At 90°C

Instrument reading = 42.7×10^7

Cell constant=629

Specific Resistivity (at 90°C), ohm-cm=42.7x10¹x629x10⁶

=0.27x10¹²ohm-cm

E.EVPAO+MIO

At 90°C

Instrument reading=50.8x 10⁰

Cell constant=629

Specific Resistivity (at 90°C), ohm-cm=50.8x10⁰x629x10⁶

=0.32x10⁶ohm-cm

Appendix X: Water content, ppm

A.RPAO

Weight of sample=4.5526g

Sample Concentration=0.6194mg

$$\text{Water Content, ppm} = \frac{0.6194 \times 1000}{4.5526} = 136.05\text{ppm}$$

B.EVPAO

Weight of sample=4.7841g

Sample Concentration=4.4239mg

$$\text{Water Content, ppm} = \frac{4.4239 \times 1000}{4.7841} \\ = 924.71\text{ppm}$$

C.MIO

Weight of sample=4.3046g

Sample Concentration=0.3821mg

$$\text{Water Content, ppm} = \frac{0.3821 \times 1000}{4.3046} = 88.76\text{ppm}$$

Appendix XI: RPAO Oxidation stability

A. Neutralization Value after oxidation, mgKOH/g

Total acidity

Weight of sample=11.50g

Volume of alc.KOH consumed in blank=0.9ml

Volume of alc.KOH consumed in sample=1.7ml

Normality of alc.KOH =0.016N

$$\text{Total Acidity, mgKOH} = \frac{(1.7 - 0.9) \times 56.1 \times 0.016}{10.50}$$

=0.062mgKOH/g

B. Total sludge after oxidation, % by mass

Weight of sample=5.09g

Weight of empty crucible=33.8204g

Weight of crucible + residue=33.8204g

$$\text{Total Sludge, \% by mass} = \frac{(33.8204 - 33.8186)}{5.09} \times 100 = 0.035\%$$

Appendix XII: RPAO Ageing Characteristics after accelerated ageing

A. Specific Resistivity, ohm-cm

At 90°C

Instrument reading=10.5x 10²

Cell constant=629

Specific Resistivity (at 90°C), ohm-cm=10.5x10²x629x10⁶

=0.66x10¹²ohm-cm

At 27°C

Instrument reading=38.1x 10²

Cell constant=629

Specific Resistivity (at 27°C), ohm-cm=38.1x10¹x629x10⁶

=2.40x10¹²ohm-cm

B. Total acidity

Weight of sample=10.84g

Volume of alc.KOH consumed in blank=0.6ml

Volume of alc.KOH consumed in sample=1.0ml

Normality of alc.KOH =0.016N

$$\text{Total Acidity, mgKOH} = \frac{(1 - 0.6) \times 56.1 \times 0.016}{10.84}$$

=0.033mgKOH/g

C. Total sludge after oxidation, % by mass

Weight of sample=5.05g

Weight of empty crucible=63.7007g

Weight of crucible + residue=63.7030g

$$\text{Total Sludge, \% by mass} = \frac{(63.7030 - 63.7007)}{5.25} \times 100 = 0.036\%$$

Appendix XIII: EVPAO Oxidation stability

A. Neutralization Value after oxidation, mgKOH/g

Total acidity

Weight of sample=12.20g

Volume of alc.KOH consumed in blank=0.9ml

Volume of alc.KOH consumed in sample=13.6ml

Normality of alc.KOH =0.016N

$$\text{Total Acidity, mgKOH} = \frac{(13.6 - 0.9) \times 56.1 \times 0.016}{12.20}$$

=0.934mgKOH/g

B. Total sludge after oxidation, % by mass

Weight of sample=5.11g

Weight of empty crucible=60.6137g

Weight of crucible + residue=60.6137g

$$\text{Total Sludge, \% by mass} = \frac{(60.6137 - 60.6117)}{5.11} \times 100 = 0.039\%$$

Appendix XIV: EVPAO Ageing Characteristics after accelerated ageing

A. Specific Resistivity, ohm-cm

At 90°C

Instrument reading=46.1x 10¹

Cell constant=629

Specific Resistivity (at 90°C), ohm-cm=46.6x10¹x629x10⁶

=0.29x10¹²ohm-cm

At 27°C

Instrument reading=12.1x 10²

Cell constant=629

Specific Resistivity (at 27°C), ohm-cm=12.1x10¹x629x10⁶

=0.76x10¹²ohm-cm

B. Total acidity

Weight of sample=10.26g

Volume of alc.KOH consumed in blank=0.6ml

Volume of alc.KOH consumed in sample=5.6ml

Normality of alc.KOH =0.016N

$$\text{Total Acidity, mgKOH} = \frac{(5.6 - 0.6) \times 56.1 \times 0.016}{10.26}$$

=0.44mgKOH/g

C. Total sludge after oxidation, % by mass

Weight of sample=5.10g

Weight of empty crucible=60.5363g

Weight of crucible + residue=60.5398g

$$\text{Total Sludge, \% by mass} = \frac{(60.5398 - 60.5363)}{5.25} \times 100 = 0.069\%$$

Appendix XV: MIO Oxidation stability

A. Neutralization Value after oxidation, mgKOH/g

Total acidity

Weight of sample=10.35g

Volume of alc.KOH consumed in blank=0.9ml

Volume of alc.KOH consumed in sample=1.9ml

Normality of alc.KOH =0.016N

$$\text{Total Acidity, mgKOH} = \frac{(1.9 - 0.9) \times 56.1 \times 0.016}{10.35}$$

=0.087mgKOH/g

B. Total sludge after oxidation, % by mass

Weight of sample=5.11g

Weight of empty crucible=65.0453g

Weight of crucible + residue=65.0476g

$$\text{Total Sludge, \% by mass} = \frac{(65.0476 - 64.0452)}{5.11} \times 100 = 0.047\%$$

Appendix XVI: MIO Ageing Characteristics after accelerated ageing

A. Specific Resistivity, ohm-cm

At 90°C

Instrument reading=26.6x 10^l

Cell constant=629

Specific Resistivity (at 90⁰C), ohm-cm=26.6x10¹x629x10⁶

=0.16x10¹²ohm-cm

At 27⁰C

Instrument reading=10.3x 10²

Cell constant=629

Specific Resistivity (at 27⁰C), ohm-cm=10.3x10¹x629x10⁶

=0.65x10¹²ohm-cm

B. Total acidity

Weight of sample=11.99g

Volume of alc.KOH consumed in blank=0.6ml

Volume of alc.KOH consumed in sample=2.1ml

Normality of alc.KOH =0.016N

$$\text{Total Acidity, mgKOH} = \frac{(2.1 - 0.6) \times 56.1 \times 0.016}{11.99}$$

=0.087mgKOH/g

C.Total sludge after oxidation, % by mass

Weight of sample=5.25g

Weight of empty crucible=55.1249g

Weight of crucible + residue=55.1249g

$$\text{Total Sludge, \% by mass} = \frac{(55.1249 - 55.1230)}{5.25} \times 100 = 0.036\%$$